Nuclear data generation and implementation for analog Monte Carlo simulation

Camilo Cordero Ramirez

université PARIS-SACLAY

Nuclear data generation and implementation for analog Monte Carlo simulation

Génération et implémentation des données nucléaires pour la simulation Monte Carlo analogue

Thèse de doctorat de l'université Paris-Saclay

École doctorale n° 576, Particules Hadrons Énergie et Noyau: Instrumentation, Imagerie, Cosmos et Simulation (PHENIICS)
Spécialité de doctorat: structure et réactions nucléaires
Graduate School : Physique, Référent : Faculté des sciences d'Orsay

Thèse préparée au **Service d'Études des Réacteurs et de Mathématiques Appliquées** (Université Paris-Saclay, CEA), sous la direction de **Frank GUNSING**, directeur de recherche, et le co-encadrement de **Cédric JOUANNE**, ingénieur de recherche

Thèse soutenue à Paris-Saclay, le 9 décembre 2022, par

Camilo CORDERO RAMIREZ

Composition du jury

Membres du jury avec voix délibérative

Cheikh DIOP Directeur de recherche, CEA, Université Paris-Saclay	Président
Dimitri ROCHMAN Ingénieur de recherche (HDR), PSI, Villigen	Rapporteur & Examinateur
Olivier SEROT Directeur de recherche, CEA Cadarache DES	Rapporteur & Examinateur
Xavier DOLIGEZ Directeur de recherche, IN2P3, IJCLab, Orsay	Examinateur
Tatsuhiko OGAWA Ingénieur de recherche, JAEA, Tokai-Mura	Examinateur

THESE DE DOCTORAT
NNT : 2022UPASP150

université PARIS-SACLAY

ÉCOLE DOCTORALE
Particules, hadrons, énergie et noyau : instrumentation, imagerie, cosmos et simulation (PHENIICS)

Titre: Génération et implémentation des données nucléaires pour la simulation Monte Carlo analogue

Mots clés: données nucléaires, neutrons, photons, réaction, évènement

Résumé: Les données nucléaires sont en constante évolution du fait de l'accumulation de nouvelles données expérimentales, de l'augmentation de la capacité de calcul informatique, et du travail des évaluateurs qui testent la validité et cohérence des données par le biais de simulations stochastiques et déterministes. Dans le cadre de cette thèse, le focus porte sur les simulations de réactions nucléaires qui produisent plus de deux particules en voie de sortie, qui nécessitent des considérations spécifiques pour maintenir les corrélations entre ces particules et ainsi assurer la conservation de l'énergie et des moments cinétique et angulaire. Il est possible d'adapter les données nucléaires et leur exploitation pour les simulations - dites analogues - des réactions réalistes du point de vue phénoménologique (opposé au besoin historique de réduire la variance), ce qui augmente les temps de calcul mais permet d'élargir les capacités des codes de transport.

Title: Nuclear data generation and implementation for analog Monte Carlo simulation

Keywords: nuclear data, neutrons, photons, reaction, event

Abstract: Nuclear data are in constant evolution as more experimental data are gathered, computational capabilities increase, and evaluators verify their validity by means of stochastic and deterministic simulations. In the framework of this PhD thesis, the focus is on the simulation of nuclear reactions that produce more than two particles in the outgoing channel, which needs specific considerations to ensure the correlations between the particles and thus the conservation of energy and of translational and angular momenta. It is possible to adapt nuclear data and their exploitation to implement the so-called analog simulations of realistic reactions from the phenomenological point of view (as opposed to the historical need of variance reduction techniques), which increases computation time but allows the expansion of the transport codes capabilities.

Contents

List of Figures

List of Tables

Remerciements - Agradecimientos

Je tiens à remercier premièrement, principalement et chaleureusement, mon encadrant Cédric, qui est à l'origine de ce projet, qui m'a épaulé tout le long tout en me donnant une grande autonomie. Tu as été toujours à l'écoute, toujours disponible plus que les deux minutes que je demandais. Tu m'as poussé, sans pression, à faire de mon mieux. On a réussi à trouver des problèmes intéressants et on a beaucoup appris, merci.

Un très grand merci à Frank, mon directeur de thèse, pour toutes ces riches discussions sur les particules et comment il faut s'y prendre pour essayer de les copier avec un ordinateur. Merci pour avoir lu toutes les versions de ce document et pour tout ce que tu m'as appris avec les corrections.

Il est une honneur pour moi que ce document soit examiné par Dimitri Rochman et Olivier Serot, je vous prie de comprendre que la rédaction en anglais est plus fluide que si j'écrivais en français. Il est une honneur aussi d'avoir comme lecteurs Xavier Doligez, avec qui j'ai pu faire du Total Monte Carlo sur le thorium en 2018, et Tatsuhiko Ogawa, qui m'a appris à utiliser PHITS en 2019.

Je tiens également à remercier l'équipe du SERMA, qui a été pour moi indispensable à l'aboutissement de cette thèse. Particulièrement je voudrais remercier Cheikh, mon directeur de Master, mon référent de recherche fondamentale, qui m'a accompagné pendant ces 5 ans très nucléaires. Merci à Fadhel et à Andrea, mes directeurs de laboratoires, pour toujours avoir été à l'écoute, merci à Odille, Davide, Emiliano et Loïc pour vos questions et suggestions, et merci à Mireille, bien sûr. Merci à Romain pour les pauses café à 10 heures pile, à Nicolas pour me rappeler qu'il faut manger, et aux thésards pour comprendre ce qu'est être un thésard et pour les repas de midi.

Quiero agradecer a mi mamá, que me inspira, que me motiva y que me acompaña incansablemente desde siempre, la única con la que podía conversar todos los días del año, durante los largos nueve años que viví en Francia.

Agradezco a mi familia, que saben quienes son sin que les nombre, que se han esforzado por no decirme que me extrañan muy seguido y por recibirme siempre con los brazos abiertos cuando regreso a cargar baterías.

Agradezco a mis seres queridos en Francia, en orden alfabético: Alexis pour avoir changé ma vision du monde, Bartek for being there when most needed, Chifri por tanto tanto, Claire por cuidarme, Fa por los vacilones, Gil pour me comprendre, Jadzia for your inspiring activism, Jaime por tu interés en mis ideas, Jose por los molinos de viento, Lola por la música, Maca por los sanguchitos de frijol, Nico por los 24 años de amistad, Romain pour bien vouloir m'expliquer les choses, Sofi por los cocosbola, Tomás por siempre andar en las mismas que yo, Ugalde por cuidarme, Yelda pour les moments musicaux, sin quienes no hubiera valido la pena este viaje.

Résumé en français La simulation Monte Carlo de réactions nucléaires nécessite des données nucléaires sous forme de fonctions de distribution de probabilités ou de probabilités discrètes, construites à partir d'expériences visant à caractériser les intéractions entre les particules, en particulier dans le cadre de cette thèse, les intéractions neutron-noyau. La méthode Monte Carlo est basée sur la génération d'un grand nombre d'évènements aléatoires visant à explorer un espace de probabilité donné, et ainsi reproduire les comportements attendus des réactions, tels que les énergies, les angles ou la multiplicité des particules produites.

Quant à l'aspect **analogue** de la simulation Monte Carlo, celui-ci traduit le fait que les particules en voie de sortie sont simulées une par une, et elles ont toutes un poids de 1. Ceci est en contraste avec la simulation standard ou usuelle - celle qui est utilisée historiquement et de nos jours pour la simulation de réacteurs - dans laquelle une seule particule est simulée affectée d'un poids qui peut être supérieur à 1, ce qui vise à réduire le temps de calcul, tout en obtenant les mêmes résultats moyens que dans une simulation analogue. Avec l'augmentation de la puissance de calcul et le besoin de simuler plus précisément les réactions nucléaires, il devient possible d'implémenter des simulations analogues pour les cas où il est nécessaire de connaître et/ou reconnaître le comportement individuel des réactions.

Cette thèse s'inscrit dans la continuation du travail réalisé pour la simulation analogue de la réaction de fission par le CEA appelé FIFRELIN. C'est un code de décroissance nucléaire à partir duquel une bibliothèque d'évènements de fission a été générée avec la méthode Monte Carlo et contient des listes de particules produites lors de la fission; c'est-à-dire que chaque évènement de fission déclare un nombre donné de neutrons avec des énergies sortantes, ainsi que les produits de fission et les cascades gamma que l'on peut retrouver suite à la désexcitation des produits de fission. Cette base de données peut être utilisée par le code de transport neutron TRIPOLI-4®, développé par le CEA, comme source de neutrons pour la simulation de systèmes fissiles, ce qui a l'avantage d'être réaliste du point de vue phénoménologique. Un couplage de FIFRELIN avec PHITS (le Monte Carlo développé par le JAEA) a été réalisé pour implémenter un calcul de l'évolution temporelle de l'inventraire des nucléides pour en déduire la chaleur résiduelle.

La continuation du travail lié à la simulation analogue de la réaction de fission, présentée dans cette thèse, consiste à traîter d'autres réactions induites par intéractions neutroniques, telles que la diffusion inélastique, la capture radiative et la (n,2n), en exploitant les données nucléaires qui les décrivent et ainsi établir les possibilités et les limites du format des données pour la simulation analogue. Les trois réactions mentionnées produisent plus de deux particules en voie de sortie, ce qui impose un suivi de leurs corrélations pour assurer la conservation de l'énergie et des moments cinétique et angulaire. Le traîtement de ces différentes réactions commence par une analyse globale des données nucléaires associées disponibles dans le format ENDF-6, en particulier celles que l'on peut trouver dans la bibliothèque européenne JEFF-3.3. Une fois que les possibilités et les limites des données sont établies, des modifications aux données nucléaires ont été proposées quand le format le permet, et autrement, des algorithmes ont été créés et implémentés, pour rendre possible la simulation analogue de ces réactions.

Les analyses des données nucléaires se font avec l'aide du manuel des formats ENDF-6 de l'OCDE-AEN, qui permet de lire les informations par la capacité de reconnaître la structure de l'évaluation nucléaire où l'on peut trouver les informations caractérisant les intéractions neutron-noyau. Ces fichiers sont compressés pour n'être lus que par les ordinateurs. Les évaluateurs vérifient la validité et précision des données en les utilisant dans des simulations spécifiques, et proposent des ajouts ou des améliorations quand le format le permet. C'est un format qui date du début des simulations numériques, donc

il existe une urgence d'utiliser un autre plus moderne: c'est pour cela que l'OCDE-AEN propose actuellement le Generalised Nuclear Database Structure (GNDS), et permettrait d'inclure les récommendations générées au cours de cette thèse pour les trois réactions étudiées.

Premièrement, la réaction de diffusion inélastique induite par neutron amène le noyau cible dans un état d'excitation qui décroît vers son état fondamental par emission de rayons gamma. Les noyaux ayant une multitude d'états excités, la cascade gamma issue de la diffusion inélastique peut compter plusieurs transitions pour atteindre le niveau fondamental. En voie de sortie de la réaction on s'attend à avoir un neutron avec une énergie moindre que l'incidente, une énergie cinétique du noyau de recul et les énergies des gammas issus de sa décroissance. L'ordre des photons est une signature de la réaction inélastique qui peut être utilisée par un détecteur. La cinématique de la réaction est complètement décrite par la connaissance des angles de diffusion du neutron dans le référentiel du centre de masse, ce qui permet une condensation de l'information du point de vue des données nucléaires. Cependant, les données nucléaires décrivant l'emission de photons à partir du noyau excité n'est pas toujours disponible pour une simulation Monte Carlo analogue de la cascade gamma et c'est donc l'objet d'étude de cette thèse vis-à-vis de la diffusion inélastique.

Les probabilités des transitions entre les états excités du noyau peuvent être retrouvées dans la partie appelée MF=12 (nomenclature du format ENDF-6, en anglais *file* 12) du fichier d'évaluation, qui peut être divisée en 40 sections nommées MT allant de 51 à 90, chacune dédiée à la description d'un état excité donné du noyau avec ses possibles décroissances vers des états plus bas en énergie. Il est donc possible de déclarer jusqu'à 40 états excités et leurs probabilités de transition pour chaque noyau, ce qui présente une première limite du format, sachant que il existe des noyaux ayant plusieur centaines d'états, notamment les noyaux lourds.

Le format MF=12 est adapté à la simulation analogue car toute particule gamma y est décrite individuellement, ce qui rend possible le suivi des corrélations entre les photons issus de la décroissance nucléaire. Ceci n'est pas le cas du format MF=6, pour lequel il faut définir une multiplicité moyenne par état, c'est-à-dire qu'il faut connaître tous les photons qui peuvent être émis à partir d'un état excité donné, donc tous les chemins possible vers l'état fondamental. Une fois la multiplicité calculée pour un état excité donné, tous les photons qui peuvent être émis à partir de cet état sont déclarés avec une probabilité calculée avec la multiplicité. L'utilisation du MF=6 reproduit le comportement moyen par les lois statistiques, alors que l'utilisation du MF=12 produit des cascades gamma réalistes à chaque évènement, tout en produisant le même comportement moyen que le MF=6. On peut donc dire qu'il y a perte d'information dans MF=6, car il peut être construit à partir de l'information du MF=12, mais le réciproque est faux.

Les cascades gamma peuvent être simulées grâce aux informations du MF=12, alors que chaque évènement simulé avec MF=6 ne peut produire qu'un photon affecté d'une multiplicité donnée. Cependant, l'utilisation du MF=6 présente un avantage devant celle du MF=12, c'est la prise en compte du référentiel de centre de masse. L'impact de cette considération cinématique est observable dans le spectre de production de photons avec les énergies mesurées dans le référentiel du laboratoire. En effet, si le photon est émis dans la même direction que le moment cinétique du noyau excité, l'énergie mesurée dans le laboratoire est supérieure à celle du photon dans le centre de masse du noyau (l'énergie déclarée dans les données). Si l'on considère que l'emission est isotrope, on peut s'attendre à avoir un pic de production de photons centré sur l'énergie déclarée dans les données avec une largeur déterminée par l'énergie cinétique du noyau excité. C'est le boost de Lorentz. La largeur du pic dans le cas de la simulation avec MF=12 est en pratique nulle car le format ENDF-6 ne permet pas la prise en compte du centre de masse, sa largeur ne dépend

donc que de la grille énergétique donnée pour la simulation.

La largeur des pics des simulations TRIPOLI-4® ne correspond pas aux valeurs théoriques, mais correspond aux valeurs calculées en considérant le neutron diffusé comme faisant partie du centre de masse depuis lequel le photon est émis. La simulation PHITS produit la largeur des pics attendue, et cette largeur est respectée pour tous les photons d'une même cascade de façon extrêmement précise. L'étude du ^{27}Al a permis d'alerter l'équipe PHITS de l'existence d'une anomalie dans leur base de donnée, qui a été corrigée.

La considération du centre de masse pour l'émission du photon avec des énergies issues du boost de Lorentz n'est pas disponible pour la MF=12 pour une raison de format ENDF-6, ce qui peut être pris en compte pour les futures versions de données, ou même la future version du format GNDS. Tout de même, l'évolution des données concernant l'émission des photons issus de la diffusion inélastique montre le passage de MF=6 vers MF=12 dans la plupart des évaluations. Dans le cadre de cette thèse, les évaluations qui possèdent MF=6 au lieu de MF=12 ont été indentifiées et des MF=12 ont été créés à partir des données de structure de la bibliothèque RIPL-3.

Les évaluations contenant une MF=6 de la bibliothèque JEFF-3.3 ont été modifiées via le remplacement du MF=6 par MF=12 et les deux versions ont été utilisées pour deux types de simulations TRIPOLI-4®. Les deux simulations étaient initiées avec des neutrons incidents à l'énergie de plus haute probabilité de provoquer une diffusion inélastique avec le but de détecter la production de photons sur un maillage énergétique suffisament fin pour differentier les états éxcités. La différence entre les deux types de simulations est le nombre de neutrons par histoire: quand le nombre de neutrons est considérablement supérieur à 1, la simulation permet d'étudier le comportement moyen attendu sous irradiation neutronique d'un noyau; quand l'histoire consiste en un seul neutron, il est possible d'étudier le comportement individuel de la réaction.

Les simulations de plusieurs neutrons par histoire avec des évaluations contenant MF=6 ont produit des spectres cohérents par rapport à celles avec des évaluations contenant MF=12. Cette première vérification est nécessaire pour assurer que la moyenne donnée par la méthode Monte Carlo est respectée. Par ailleurs, les simulations d'un seul neutron par histoire produisent majoritairement un seul photon si l'évaluation contient MF=6. Si l'évaluation contient MF=12, TRIPOLI-4® implémente une simulation analogue de la cascade gamma, ce qui permet d'additionner les énergies et retrouver l'énergie de l'état éxcité à partir duquel la cascade gamma a commencé, pourvu que les photons encaissés dans l'histoire ne soient issus que d'un seul neutron.

Au cours de cette thèse, 22 évaluations de la bibliothèque JEFF-3.3 ont été complétées, c'est-à-dire qu'elles déclaraient plus d'états éxcités dans MF=3 que dans MF=12. De plus, les évaluations ne contenant toujours pas de MF=12 ont été identifiées et les MF=12 de 50 noyaux ont été générés à partir des données de structure de la bibliothèque RIPL-3, les données de structures de la bibliothèque ENSDF étant trop vastes, ce qui rendait difficile l'identification des nivaux de part et d'autre. Ces résultats ont été présentés aux JEFF Meetings 2019 et 2021.

Deuxièmement, la réaction de capture radiative, ou (n,γ), consiste en l'absorption d'un neutron par le noyau cible qui est de ce fait ramené dans un état d'excitation de plusieurs MeV, et généralement le noyau éxcité se retrouve une région de haute densité d'états, appelée quasi-continuum, qui empêche la différentiation des états du point de vue expérimental. La décroissance vers l'état fondamental se fait majoritairement par emission de rayons gammas, ce qui justifie l'implémentation d'une simulation Monte Carlo analogue pour reproduire le spectre gamma attendu de cette réaction. Le code Monte Carlo appelé DICEBOX, distribué par l'IAEA, a été utilisé lors de cette thèse pour simuler la décroissance de noyaux ayant absorbé un neutron d'énergie nulle.

Le fonctionnement de DICEBOX se base en la génération d'états excités (de plus haute énergie qu'une énergie critique déterminée par l'utilisateur comme séparation du quasi-continuum et les états connus) en utilisant des densités d'états qui caractérisent le quasi-continuum d'états; les intensités des transitions entre ces états sont ensuite calculées par des fonctions de force (photon strength functions) et ce processus se répète jusqu'à ce que l'énergie d'éxcitation du noyau soit inférieure à l'énergie critique. Une fois que cette énergie est atteinte, le code utilise les données de structure comme ENSDF ou RIPL pour simuler les transitions entre les états connus.

Le traitement analogue de cette réaction vis-à-vis des données nucléaires est possible seulement si l'état d'excitation atteint n'appartient pas au quasi-continuum, comme c'est expliqué dans le manuscrit pour le cas du ^{12}C. Autrement, le format ENDF-6 ne permet pas d'utiliser les données de sorte à implémenter une simulation analogue de la (n,γ). Ceci est du au fait que dans la partie dédiée à la production de photons issus d'une capture radiative des évaluations nucléaires (MF=6 MT=102), il y a des fonctions de distribution pour reproduire le spectre continu provenant des transitions dans le quasi-continuum, et les probabilités liées aux photons émis à partir des états connus, affectés d'un multiplicité donnée, le tout dépendant de l'énergie incidente du neutron.

Comme pour le cas de la diffusion inélastique, le format MF=6 n'est pas adapté à l'implémentation d'une simulation Monte Carlo analogue pour la réaction (n,γ), du fait que les données sont construites pour retrouver les spectres attendus par la simulation d'un grand nombre d'évènements, chacun produisant un seul photon. Dans une simulation analogue, chaque neutron devrait produire entre 3 et 5 photons en moyenne par évènement de capture, selon le noyau simulé.

Sachant qu'il est nécessaire de se baser sur de méthodes algébriques pour implémenter une simulation analogue de la (n,γ) comme le fait le code DICEBOX pour la génération d'états de haute énergie, et que les données nucléaires n'en sont pas adaptées, je propose un algorithme qui échantillonne un nombre donné de photons de la distribution continue du MF=6, dans le but de ne pas utiliser des fonctions de densités, et qui simule la cascade gamma une fois que les états connus sont atteints, en utilisant les données de structure de RIPL-3. Les résultats sont comparés avec ceux du code DICEBOX pour la simulation de la réaction ^{95}Mo(n,γ), comme cas de référence.

La simulation DICEBOX en question produit une distribution de multiplicité des photons asymétrique avec les évènements à quatre photons étant les plus fréquents. Le spectre gamma résultant présente des raies discrètes resortant du spectre continu, qui peuvent être associées soit aux gamma primaires, qui ramènent le noyau de son état initial vers des états connus, soit aux photons issus des transitions entre les états connus. La raie de plus haute énergie représente la transition entre l'état initial et fondamental par un seul photon et constitue aux alentours de 1% des évènements. L'ordre d'emission des photons est estudiée en fonction de la multiplicité des évènements pour observer l'évolution de la distribution d'énergie.

L'objectif de ces observations est de proposer un algorithme qui se rapproche le plus d'une simulation réaliste de la capture radiative, tout en restant avec la contrainte de n'utiliser que les données nucléaires disponibles. Celles-ci sont 1) la distribution continue du MF=6, 2) les intensités des gammas primaires que l'on peut trouver dans le dataset appelé (N,G) E=TH de la bibliothèque de structure ENSDF et 3) les probabilités de transitions entre les différents états connus de la bibliothèque RIPL-3. L'algprithme a été appelé SNGA pour Simplified Neutron Gamma Algorithm.

Si l'état initial et l'état fondamental ont une différence de spin qui permet une transition du premier vers le second, les résultats DICEBOX suggèrent que 1% des évènements devraient compter un seul photon. Ensuite, le dataset contenant les gammas primaires

pour le cas du ^{95}Mo(n,γ) suggère que 14% des réactions commencent par un gamma primaire. Ces constats ont été interprétés dans le cadre du SNGA de sorte que la condition pour commencer la décroissance par un photon échantillonné dans le MF=6 est le tirage au sort d'une valeur ξ entre 0 et 1 et qui soit supérieure à $0.15 = 0.01+0.14$. La condition pour continuer à échantillonner depuis le MF=6 est de continuer à tirer au sort $\xi > 0.15$ pourvu que la multiplicité déterminée au début de la cascade simulée n'est pas dépassée; si la cascade ne contient que des photons échantillonnés du MF=6, le dernier doit porter toute l'énergie disponible. Une fois les états connus sont atteints, la cascade est simulée selon les données de structure de RIPL-3.

Les résultats obtenus par le SNGA sont compatibles avec ceux de DICEBOX dans la mesure où la forme générale du spectre est respectée et où tous les évènements conservent l'énergie. Quand les états connus sont atteints, soit par une emission initiale de gamma primaire, soit par le passage du quasi-continuum aux états connus, il est possible d'ajouter une condition supplémentaire pour permettre une transition ou non, comme la différence de spin entre les deux états. Le cas du ^{155}Gd(n,γ) simulé par PHITS produit une distrubution de multiplicité à deux maxima, ce qui suggère une anomalie dans la simulation. Par le SNGA avec la considération de différence de spin entre les états, il a été mis en évidence que la bande rotationnelle de ce noyau était à l'origine de cette anomalie, ce qui a été communiqué à l'équipe PHITS.

La réaction (n,2n) a été traîtée comme ouverture de la thèse, dans le sens où ce qui a été appris avec la diffusion inélastique et la capture gamma servit pour simuler les cascades gammas associées à cette réaction, mais aussi établir les possibilités et les limites des données nucléaires vis-à-vis de la simulation analogue de la réaction (n,2n). Dans la bibliothèque JEFF-3.3, la seule évaluation qui contient les spectres de productions des 4 particules sortantes (les deux neutrons, le noyau de recul et les gammas) c'est le ^{19}F. La forme des spectres suggère que le méchanisme de la réaction est par diffusion inélastique du premier neutron, et le deuxième serait émis en évaporation du noyau éxcité. Cependant le spectre lié au noyau de recul semble atteindre des énergies trop hautes, de l'ordre de 3 MeV. L'algorithme N2NA, pour N2N Algorithm, implémente une simulation analogue de cette réaction en échantillonnant les énergies des particules sortantes à partir de l'évaluation et en prennant en compte l'énergie disponible pour assurer la conservation de l'énergie.

En conclusion, il est possible d'utiliser les données déclarées en MF=12 pour implémenter une simulation analogue des cascades gammas associées aux réactions de diffusion inélastique induites par neutrons, mais avec la limite de ne pas pouvoir retrouver une cinématique précise à cause des considérations de référentiel de centre de masse. Ensuite, les cascades gammas liées aux réactions de capture radiative ne peuvent pas être simulées par la méthode Monte Carlo analogue en n'utilisant que les données nucléaires disponibles dans les évaluations à cause notamment de l'existence du quasi-continuum d'états. Cependant, la déclaration analytique d'une distribution de probabilité dans l'évaluation pourrait étre utilisée pour reproduire les comportements attendus, comme pour les spectres continus de la (n,γ), de la (n,2n), ou d'autres. Ces constats peuvent être considérés comme de recommendations pour les nouveaux formats de données nucléaires comme GNDS ou futures versions de JEFF et autres bibliothèques.

1 - Introduction

In the field of Monte Carlo simulation of nuclear reactions, in particular related to particle detector simulations, the reactions are simulated using the available nuclear data that describe the expected behavior of the reactions, and using a simulation algorithm capable of generating a nuclear reaction event. This is done mainly by randomly sampling from the probability distributions that characterize the possible reactions channels, but also the program can integrate considerations to be taken into account if the reaction requires further information that cannot be stored in a distribution. These two factors are indeed at the origin of the characteristics found in the production of particles from simulated nuclear reactions. However, simulating reactions that produce more than two particles using nuclear reactor transport codes does not generally respect the correlations ensuring the conservation of energy between the emitted particles from an individual reaction. To address this issue, to be able to perform a so-called analog simulation, which consists in simulating all particles one by one (as opposed to non-analog which calculates and assigns particle weights instead of simulating all particles), one must add extra features to the transport code to take into account the specific characteristics associated with nuclear reactions that produce more than two particles. Here, the focus is on the reactions of neutron-induced inelastic scattering, neutron capture and (n,2n), all of which produce a given multiplicity of correlated particles.

The information that describes neutron-induced reactions is called evaluated nuclear data. Currently, not all nuclear evaluation files are updated to allow analog simulations, nor do all transport codes have event generation algorithms. As a result, individual multi-particle reactions are simulated with missing information and thus do not exactly reproduce the expected behaviors in the simulations.

Regarding previous studies on this topic, the CEA/SERMA work on analog simulation [2, 3, 4] focuses on the fission reaction, in which the two fission fragments emit correlated neutrons and photons. The FIFRELIN code [2] simulates the prompt component (the immediate products) of the post-fission de-excitation process, and applies statistical theories for coupled and uncoupled neutron and photon emission. As such, a database has been constructed using FIFRELIN events which gives access to realistic neutron and photon emissions from fission fragments. That is to say, a list of fission events where a neutron of a given kinetic energy generates a fission reaction which produces so-called fission fragments. These in turn emit a set of photons and neutrons with energies that depend on the fragments' excitation and kinetic energies. The construction of this database is done by the random repetition and input parameter variation of a simulation capable of producing particles according to the theoretical model that describes fission, and the available nuclear data. This allows TRIPOLI-4® [5] to use the neutron correlation of these fission events and create new neutron sources to be placed in the studied system for benchmark analysis as in ref. [3]. This development towards a more phenomenological approach - thus more time-costly - as opposed to more statistical and quick, becomes possible with faster computation and is reflected on the evolution of the nuclear data, notably in the ENDF/B-VIII.0 library [6], where one can now find a list of possible neutron multiplicities for fission events that goes up to 14 for ^{235}U, whereas before this was limited to either 2 or 3 neutrons. (Without FIFRELIN, TRIPOLI-4® can sample either 2 or 3 neutrons.)

However, this study of CEA is limited to fission reactions and could be extended to other reactions.

Another *event-by-event* fission model, called FREYA (Fission Reaction Yield Algorithm) [4], has been specifically designed for producing large numbers of fission events in a fast simulation. By employing nuclear data for fragment mass and kinetic energy distributions, using statistical evaporation models for neutron and photon emission, and conserving energy, momentum, and angular momentum throughout, FREYA is able to predict a set of correlation observables, including correlations in neutron multiplicity, energy, and angles and the energy sharing between neutrons and photons.

In addition, the IAEA has distributed the Monte Carlo code called DICEBOX [7] specific to the gamma decay of excited nuclei, as in the (n,γ) reaction, which is based on a robust theoretical model allowing the simulation of photons from the quasi-continuum of excited states in a first step, and photons of known level transitions described in the nuclear structure data, in a second step. The model used relies on photon strength functions and the excited states generated from level density models for a given nucleus, which allows to statistically reproduce the photon emission from the quasi-continuum. Once the state transition by the photon emission brings the nucleus back to a known discrete state, the gamma cascade is simulated based on the RIPL-3 [8] library. However, TRIPOLI-4® cannot use DICEBOX for each simulated reaction because it would be too costly in terms of computation time and the creation of a database of events such as the one for fission in a simplified form could be an outlook for future work.

The STEREO [9] and Nucifer [10] experiments of the CEA have detected antineutrinos from research reactors. The antineutrinos were detected indirectly, i.e. they first transform a proton into a neutron, the neutron is then absorbed by a gadolinium nucleus and this capture reaction produces detectable gamma cascades. The number of detections per day is in agreement with the theoretical predictions established by the simulations, which allowed them to conclude the indirect non-detection of the so-called right-handed antineutrino, a hypothetical particle. However, the simulations made to analyze the detector lack precision because of the incomplete nuclear data, in addition to the fact that around 300 detections per day do not give the necessary statistical confidence.

The JAEA J-PARC [11] experiment has produced gamma spectra for the neutron capture of gadolinium that are in agreement with their analogous Monte Carlo simulation using PHITS [12], validating the nuclear models and data used. In addition, Ravaux [13] has established that TRIPOLI-4® allows to correctly estimate the photon heating of the reactor, proving that the average photon behavior is respected, but not the behaviors of each photon. However, an anomaly has been found during this PhD for the simulation of ^{155}Gd in terms of its multiplicity; a ten photon decay cascade is often sampled and this should not be the case, it is expected that this number should be 4. A thorough explanation will be given in Chapter 4.

In summary, the available nuclear data and the theoretical models used are key to an accurate simulation that takes into account the correlations between all the particles produced. However, TRIPOLI-4® does not have access to all the algorithms and all the necessary nuclear data to perform an analogous simulation of experiments such as STEREO or J-PARC. The study carried out in this thesis is part of the development of the capabilities of TRIPOLI-4® to simulate particle detectors from variable-multiplicity reactions. Additionally, the new methodologies could be implemented in the new Monte

Carlo transport code of CEA called PATMOS.

This is what justifies this study. The work consists first in studying the nuclear reactions (n,n'), (n,γ) and (n,2n) from the theoretical point of view, and in identifying the missing nuclear data for the analogous treatment. Then, it consists in setting up a methodology that uses the exploitation of the nuclear data format, as well as the theoretical models of nuclear physics, so that the transport code TRIPOLI-4® can simulate all the particles produced in each nuclear reaction while ensuring the conservation of energy and their associated multiplicity.

The structure of this manuscript following the introduction is the theoretical part developed in chapter 2 concerning the physics of nuclear reactions and its required input nuclear data for Monte Carlo simulations. Then, the work performed during this PhD thesis is explained starting on chapter 3. The objective in the chapter is to determine the impact of the use of two nuclear data formats on the correlation of the photons resulting from the neutron-induced inelastic reaction (n,n'), as well as on the conservation of energy per reaction. For this purpose, the case-control study is the simulation with the unmodified nuclear data: the ENDF-6 format which contains averaged data for photon production, is a double differential cross-section in angle and in energy, thus it is suited for non-analog simulations. This type of simulation is to be compared to analog simulations based on modified nuclear data files from the JEFF-3.3 library [14] suitable for analog simulation. It is important to mention that the majority of the JEFF-3.3 evaluations are suited for analog simulation of the inelastic reaction. The creation of the files was done for the evaluation files that did not have this information, and it was done by declaring the excited states and their associated transition probabilities, extracted from the RIPL-3 library which contains all the measured excited states. The objective was then to verify the capabilities of the TRIPOLI-4® transport code to perform analog and non-analog simulations by comparing simulations using the two suitable data formats. Some recommendations will be given when using either format as they both require some considerations that depend on the studied system.

The objective explained in chapter 4 is to create an algorithm capable of using the available nuclear data and algorithms describing the process of photon emission from a nucleus after a thermal neutron capture (n_{th},γ), with the goal of producing events that respect photon correlations and energy conservation. For this purpose, the (n,γ) simulations of DICEBOX allowed us to verify the capability of the algorithm to produce the expected photon spectrum. At this stage we only studied the production of photons, knowing that these are the only particles emitted. However, we know that there are other reactions, in particular the (n,2n) reaction, which certainly produces a multitude of photons on the way out but also two neutrons which must be transported with precise energies (and angles). Hence we have adapted the photon production algorithm to the (n,2n) reaction, for which there is no reference code.

The following PhD work is on particle interaction simulations in the framework of nuclear physics. In particular, interactions between neutrons, as well as photons, with nuclei. The focus of this study is on neutron induced reactions that yield more than one particle as byproducts, carried out with the analog Monte Carlo method to ensure particle correlation and energy conservation even by event. Before entering in the technical aspect of this type of neutronic simulations, it is in place, from my perspective, to make a scientific and historical digression to praise the tremendous human effort of ingenuity and creativity

behind both simulations and nuclear physics, not only because these fields arise from our necessity to understand natural phenomena, but also because they have contributed greatly to build an important part of the current structure of society.

Modern day simulations are the result of an exponential development in computational capacities. The word computer is part of the every day vocabulary but its original meaning is a machine that calculates, that computes repetitive algebraic tasks and allows the users to focus on more difficult problems that require creativity and critical thinking. Humans create machines that allow them to focus on better techniques and thus create better machines, and so on. Computational simulations are used in virtually all branches of science to assess the validity of theoretical or parameterized models proposed by the respective experts by means of comparing the simulation results to experimental data. In the case of this manuscript, the simulation technique used is called analog Monte Carlo method, which relies on the beforehand knowledge of the statistical and individual behaviors of particles related to nuclear physics, and also on pseudo-random number generation to imitate the natural randomness of nuclear reactions. The use of these tools provides an exact answer to how particles can be transported within a given medium and, according to the law of large numbers, a sufficiently vast repetition of random transport events elucidates all the possible characteristics of nuclear reactions along the particle path. An important aspect in this work is how the input nuclear data format given to the algorithm influences the outcomes of the simulation.

Nuclear physics are also the result of an exponential development, but in this case it is in our deep understanding of Nature, in contrast to our capability of inventing new physical tools like computational simulations. Nuclear physics is a branch of science that has its firsts seeds in the human quest of understanding what matter is. The Greek philosopher Democritus (460-370 BCE) proposed the idea of the atom: the element of Nature that is not composed of smaller elements, as dividing matter in smaller pieces should end at some point, he thought quite logically. This idea was *proven wrong* by his contemporaries who were certain that Nature abhors voids, and according to Democritus, atoms would somehow bound off each-other in an otherwise empty space.

Fast forward a couple of millennia: the advent of statistical mechanics in Maxwell and Boltzmann's kinetic theory of gases, in addition to electrodynamics and the periodicity of Mendeleev's table, the realization was unavoidable that matter is made of molecules, in turn made of atoms. Presumably, the question of the void is more subtle than just empty space because the concepts of emptiness and of space require very specific and very complex re-definitions, mainly because of quantum mechanical and relativistic considerations. What was then called, and still is called, an atom, is not indivisible: Joseph Thomson discovered what constitutes the "shell" of the atom, the electron, in 1897. It is a negatively charged (currently believed to be indivisible) particle which would later allow the understanding of the periodicity of elements, and the origin of electric, magnetic, chemical, and a multitude of other fascinating phenomena. Ernest Rutherford discovered the atomic nucleus in 1911, a positively charged, massive center of the atom, from which the name nuclear physics is coined. James Chadwick discovered the neutron in 1932, a neutral particle that is key for fusion and fission, and for the stability of nuclei as it "dilutes" their inner positive charge, allowing cohesion in spite of the electric repulsion of protons. It also explains why there is a proportionality of 2:1 ration between the mass:charge ratio of light nuclei.

The newly discovered structure of the atom in the first few decades of the twentieth

century went hand in hand with the theoretical predictions of quantum mechanics and special relativity, two revolutionary theories at the time that have evolved into today's so-called Standard Model (SM) of particle physics, the most accurate description of matter currently available, in other words, our best answer to the question that Democritus and so many others tried to tackle. The SM is based on the idea that what is fundamental in Nature is the existence of quantum fields. Particles, as we can define them in this most modern way, are the quantized excitations of their corresponding fields, thus generating the wavelike behavior observed under some specific conditions. Another important cognitive leap provided by this theory is the central role of interactions: the concept of force becomes an emergent property of interactions, as opposed to an *a priori* existing unexplained property of Nature. For instance, two electrons interact via the exchange of photons, a transfer of energy that changes their direction in space-time, a claim that can be translated in very precise mathematical formulation, or equivalently with a Feynman diagram, and this was previously described as the force of electric repulsion between particles of same charge, using the vectorial quantity called Lorentz force.

In a similar sense as the periodic table of elements groups different atoms due to their chemical properties, the SM groups its components according to the interactions. The SM describes three fundamental interactions which explain a vast range of physical phenomena, and requires the Higgs mechanism for the intrinsic mass of the massive particles to be non zero. One of the SM fundamental interactions is the electromagnetic interaction, mediated by photons (mediators of the interactions are bosons, defined as integer spin particles in Bose-Einstein statistics, meaning that they can condensate and share the same energetic state) and with an intermediary magnitude compared to other interactions. The magnitude is measured in terms of a dimensionless coupling constant that can be thought of as a strength of interaction, which in the case of the electromagnetic interaction is called the fine-structure constant and its asymptotic value is approximately $1/137$ at zero energy and increases logarithmically to about $1/127$ at 90 GeV.

The interaction with the strongest magnitude and shortest range (only applies in distances on the order of 10^{-15} meters) is called strong interaction, and its mediator particle is called gluon because it glues quarks and nucleons (protons and neutrons) together. Quarks, electrons and neutrinos are fermions (described by Fermi statistics as half-integer spin particles, meaning that they cannot share the same energetic state) and all are currently believed to be indivisible. Neutrinos have the lowest intrinsic mass among the fermions, a property discovered through their *flavor oscillations*: if they evolve (oscillate) in time, it would mean they have mass. Massless particles travel at the speed of light. Neutrinos interact via the weak interaction through $W\pm$ and Z bosons to participate in nuclear decay processes, for instance neutron decay into proton involves the emission of a W^- that decays into an electron and an antineutrino.

Neutrinos were proposed by Wolfgang Pauli to explain the continuous beta decay (electron emission from radioactive sources) spectrum (as opposed to the expected discrete spectrum like in alpha decay) could only be explained by the existence of an almost massless neutral (if it was charged, its detection would be much easier) particle that would account for the missing energy. It is with experiments that have unexpected results that science leaps forward, and the same goes for the rest of the nuclear theory, for example in experiments that showed that protons and neutrons were actually composed of a multitude of quarks. Nuclear reactions at high energies have uncovered much of modern physics

today. The cohesion of quarks and nucleons via gluons is described in quantum chromodynamics and it inspired the mathematics of String Theory, a proposition to unify gravity and quantum mechanics that appears very far away from testable predictions. This is to say that the underlying mechanisms of nuclear physics are still quite mysterious, which leaves plenty of space for new discoveries. The fact that nucleons are made of a quarks and gluons does not seem to help in understanding all nuclear processes. Otherwise, we would have already understood many things: asymmetric fission, magic numbers... Is nuclear matter a Fermi gas or a liquid drop or a solid lattice or a quark-gluon plasma?

Even though the SM is the most accurate theory in history to describe Nature, it does not include gravity, it does not show explicitly why there are three flavors to each of the fermions, it does not explain the matter/anti-matter asymmetry observed in the early universe, it does not suggest the existence of dark matter, even less of dark energy, and most importantly for this work, it does not give a comprehensive view of what is the best approach to nuclear physics. This is to say that nuclear models stagnated around half a century ago, and there is no consensus available from the analysis of SM results in what the state of matter of the nucleus really is. Indeed the liquid drop model uses the idea that nuclear matter is like a liquid (surface tension for example) to explain the cohesive magnitudes between the nucleons, however it is the Fermi gas model that explains the excited states of the nucleus and it is also possible to think of solid states, as crystal lattices, to explain other phenomena such as asymmetric fission. Hopefully, the study of neutron stars might shed some light on how to improve our understanding of nuclear physics. Recent neutron star findings suggest nuclear matter has a *spaghetti and lasagna* [15] structure more than solid, gas, liquid or plasma.

In the context of nuclear energy research and development, crucial for ensuring the proper functioning of the most energy dense source of power currently available to humanity, this PhD work aims to improve the simulations of nuclear reactions by updating the data that characterize nuclei interactions with neutrons, called nuclear evaluations or evaluated nuclear data, specifically applied to the domain of detector and instrumentation simulations. The need of such work has been set by the Commissariat à l'Énerige Atomique et aux énergies alternatives (CEA), where I have been given the opportunity to work alongside great researchers in the Service d'Etudes de Réacteurs et de Mathématiques Appliquées (SERMA).

CEA is the French atomic energy commission, created in 1945 with the joint initiative of Charles de Gaulle, Frédéric Joliot-Curie and Raoul Dautry, mainly to house scientific research in the nuclear domain. Today it has more than 16000 employees and an annual budget of 4 billion euros. In 2010 it was decided that alternative energies research should also be performed, in accordance with the challenge of producing electricity with minimum CO_2 emissions, and without nuclear reactors. There are ten centers in France, each specialized in a particular branch, for instance in Cadarache where the experimental reactors are located. Other domains are defense, technologies of digital information and communication, material sciences as well as biology and health. The center in Saclay is specialized, among others, in neutronic and thermo-hydraulic simulations. Codes such as APOLLO-3® for deterministic calculations of neutron transport, as well as TRIPOLI-4® for the probabilistic approach (used for this investigation) are developed in SERMA. There is a strong collaboration between this research organization and French industry: Énergie de France and Framatome play major roles in what is investigated in the center.

The transport code TRIPOLI-4® is based on the Monte Carlo method, so the resolution of particle transport problems is exact when the complete domain of possibilities of a given particle experiment is explored thoroughly. This will be further discussed in dedicated paragraphs. The exact treatment of physical phenomena regarding nuclear reactions and subsequent emission of multiple particles justifies the utilization of such a computational tool for the investigation of the impact of the nuclear data format on the accuracy of simulations. In other words, the fact that the Monte Carlo method is based on randomness and on the probability distributions of particle behavior makes TRIPOLI-4® an excellent way to test physical models against experimental data collected by detectors.

The objective of improving the capability of the code to simulate reactions and/or detections, not only for reactor physics, but also more broadly for nuclear physics, is inscribed in the objectives of SERMA, ultimately for the development of the new Monte Carlo code PATMOS/TRIPOLI-5. An example of possible simulation is that of the Sterile Reactor Oscillation (STEREO) experiment performed in CEA. It is intended to indirectly look for the existence of the sterile antineutrino, by detecting non-sterile antineutrinos and checking if the counts coincide with the calculated amount. Additionally, the antineutrino detection creates another verification tool for the fuel usage in reactors around the world and this type of experiment develops detection techniques. The current status of the STEREO experiment is that no deviation has been found between theory and experimental data, meaning that the evidence for the sterile antineutrino has not been found yet. However, the experiment relies on the capture in gadolinium of the neutron produced by the transformation of the proton, and the nuclear data of the neutron capture reaction of gadolinium can be improved, which is a main focus of this PhD thesis.

The sterile antineutrino is a hypothetical particle proposed in the framework of the SM (and is a candidate for dark matter) and cannot be directly detected precisely because of its sterile nature, meaning that it does not interact via the weak interaction. Antineutrinos that do interact weakly, have been detected directly in the sense that they transform protons into neutrons through inverse beta reaction: the interaction of the incoming antineutrino and one up quark in the target proton is mediated by a W+ boson and the resulting particles are a positron and a neutron, in turn detected.

The resulting positrons annihilate with surrounding electrons, emitting two photons that can be detected. Neutrons can be absorbed in gadolinium nuclei and the mass excess is released in a gamma cascade that can also be detected. Because these two phenomena have specific values of particle multiplicity and energy, the detection of a precise sequence of photons can be considered the signature of an antineutrino-proton interaction.

In fact, this weak interaction can only happen if the antineutrino has a right handed chirality, so the hypothetical sterile antineutrino is known to have a left handed chirality. The mechanism of oscillation between right-handed and left-handed chirality, which is a vectorial product of the intrinsic spin and the momentum independent of the frame of reference, is precisely the interaction of massive particles with the Higgs field. This interaction of particles and the Higgs field impedes them from going at the speed of light, thus there is a time dependence, which explains the intrinsic mass of the particles, also independent of the frame of reference. Thus, all massive particles must have both right and left-handed versions of themselves and all have been detected, except for sterile antineutrinos because they are removed from the only interaction that allows their direct detection. That is why it is crucial to have the most accurate physical models, backed by the most precise data,

to compare it to the experiments and potentially find some new entity that broadens our understanding of Nature.

The analog simulation applies to experiments that need particle-by-particle treatment, for example the neutron capture event in a given isotope has the signature of the emission of a multitude of photons with defined energies, an electromagnetic cascade, produced in the decay of the excited states of the residual nucleus after capture. If these kinds of signatures are detected in the experiments, their associated frequencies or intensities can be compared to those provided by the simulation, thus allowing to conclude on the validity of the predictions. In contrast, for reactor simulations, with the objective of saving time and memory, non-analog methods are used to replicate photon spectra to ensure energy conservation.

This manuscript will first give an overview of the state of the art models applied to nuclear reaction simulations and the necessary data for its input, followed by the propositions to improve those simulations, mainly regarding the inelastic reaction and the capture reaction.

Notations

The shorthand notation for a nucleus X with atomic number Z (number of protons) and with mass number A (number of protons + neutrons) is:

$$^{A}_{Z}X$$

Isotopes are nuclei that have same Z and different A.

All the energies in this work are given in electron-Volts (eV), which is the measure of the amount of kinetic energy gained by a single electron accelerating from rest through an electric potential difference of one volt in vacuum. Also:

- 1 meV = 10^{-3} eV
- 1 keV = 10^{3} eV
- 1 MeV = 10^{6} eV

All the masses in this work are given in MeV/c^2, and the mass of the neutron m_n, of the proton m_p and the atomic mass unit u are:

- $m_n = 939.565$ MeV/c^2
- $m_p = 938.272$ MeV/c^2
- $u = 931.494$ MeV/c^2

In the evaluated nuclear data, isotope mass is given as a multiple of m_n, but outside of the nuclear data and nuclear reactor framework, isotope masses are usually given as a multiple of u.

In this work, the words *gamma* and *photon* are used interchangeably, as gamma rays refer to photons emitted from nuclei, and all this work concerns nuclear processes. The same is true for *state* and *level*: they both refer to excitation energies that can be reached when a nucleus absorbs the necessary amount of energy.

2 - State of the Art

2.1 Nuclear physics

2.1.1 Quantum mechanical considerations

Although neutrons may be referred to as particles, as they have inner structure it is more exact to say that they are composite particles, whereas fundamental particles are indivisible by definition and by measurement. Indeed, neutrons are composed of three constituent quarks: two down quarks (d) and one up quark (u), and also a myriad of quark/anti-quark pairs, all interacting with each other via gluons and photons in such a way that the neutron is provided with net zero color charge and net zero electromagnetic charge, and with a rest mass of 939.5654 MeV/c^2. The down quark of the neutron can spontaneously decay into an up quark, turning the neutron into a proton, making the lifetime of a free neutron approximately 880 seconds.

Nevertheless, in the framework of this study one can refer to neutrons as particles, as the energies of the investigated nuclear reactions are insufficient to peer inside the neutron to consider it composed of smaller elements, and because the discrete nature of its interactions allows a point-like computational treatment. Indeed, neutrons simulated with a maximum energy of 20 MeV (or 20% of the speed of light c) have a de Broglie wavelength of 6.4 fermi (10^{-15}m) so they can only "see" other nucleons as a whole, which are the size of a few fermi, and not their smaller inner structure. Also, in the case of reactor and detector simulations, neutrons are fast enough to interact with the medium before even having time to decay, so neutron decay in not considered in the simulations. The propagation of neutrons in a medium can be simulated with the Monte Carlo method to obtain a solution for the transport equation in the formalism set by L. Boltzmann, further discussed in section 2.3. For reactor physics, relativistic and quantum mechanical considerations are already taken into account in the input nuclear data, thus no major corrective calculations are performed during reactor simulations.

However, this work focuses on specific nuclear reactions, so one must be more careful than in reactor simulations and provide corrections when necessary. Indeed, the very nature of nuclear reactions can only be understood from the quantum mechanical formalism where waves represent the particles involved in the reactions and the post-reaction observables can be calculated as the result of the said waves interactions, according to the Schrödinger equation for non-relativistic interactions, or the Dirac equation otherwise. The most important quantum mechanical phenomenon in this work is the existence of discrete energy states within the nucleus that are populated by its available nucleons. This fact is analogous to the excited states of the electronic orbitals in atoms, which can be determined exactly for hydrogen-like atoms using the Schrödinger equation. In the case of the nucleus, there are two sets of energy states, as neutrons and protons can yield different sets of energies for their respective nucleonic orbitals or shells. If the nucleus is provided with external energy, nucleons can populate more energetic shells. This is analogous to the photoelectric effect if the nucleon is ejected from the nucleus.

The solution of the Schrödinger equation using the Woods-Saxon potential describes approximately the interactions of nucleons within a nucleus, which generates the so-called nuclear shell model and the energy states can be estimated. Similarly to how H_2 is in

a lower lying state than 2 free hydrogen atoms, nuclei with an even number of protons and an even number of neutrons (even-even) tend to have higher binding energies, which implies that proton and neutron separation energies (the minimum energy to separate one proton or neutron from the nucleus) are also higher. This is true also for odd-odd nuclei. This is due to the fact that nucleons are fermions, so two of them can share the same shell by having opposite spin orientations. This in turn generates the concept of the so-called magic numbers, which refer to specific nuclei of 2 (deuteron), 8 ($^{16}_{8}O_8$ is said to be doubly magic), 20, 28, 50, 82, etc, nucleons, with particularly high binding energies. However, the observed *large* magic numbers have not been predicted exactly by any of the theoretical models, only the first ones can be estimated quite accurately.

The main reactions studied in the framework of this PhD involve photon interactions with nuclei, mainly the emission of photons from excited states. The characteristics of such interactions can be obtained by defining the Hamiltonian for a proton that interacts with its neighbor nucleons and with an electromagnetic (EM) field that corresponds to the photon in question. According to [16], the Hamiltonian for the proton of reduced mass m is

$$H = \frac{1}{2m}(\vec{p_n} - e\vec{A})^2 - g_s\frac{eh}{4\pi m}\vec{s}\cdot\vec{B} + V(r) \tag{2.1}$$

where the subscript n on $\vec{p_n}$ signifies that this is the momentum of the proton due to its interaction with the nuclear force alone, e is the fundamental electric charge, $\vec{A}$ is the EM vector potential, g_s is the spin g-factor, h is the Planck constant, $\vec{s}$ is the spin vector, $\vec{B}$ is the magnetic field and $V(r)$ is the nuclear potential due to the strong interaction alone. If this expression is expanded, the total Hamiltonian can be divided in two: one for the interaction of the proton with all other nucleons due solely to the strong interaction, and one that can be called perturbation potential H_{pert} that gives rise to photon interactions. The Fermi Golden rule [16] says that the probability for a transition from one excited state $|\Psi_i\rangle$ to another $|\Psi_f\rangle$ by means of photon interaction is proportional to the square of the matrix element $\|\langle\Psi_f|\|H_{pert}\|\|\Psi_i\rangle\|^2$. It can be recognized that the vector potential $\vec{A}$ must carry out the creation and annihilation operators for the photon. Thus photon emission corresponds to

$$\vec{A} = \vec{A_0}^{\dagger}e^{-i(k\cdot r-\omega t)} \tag{2.2}$$

where $\omega = c|\vec{k}|$ and $|\vec{k}| = 2\pi/\lambda$, λ being the wavelength of the photon. The operator $\vec{A_0}e^{i(k\cdot r-\omega t)}$ corresponds to the absorption of a photon. This symmetry indicates that the absorption of a photon brings the nucleus to an equivalent state to that of a nucleus being excited by an inelastic collision.

The Maxwell equations for electrodynamics, expressed with the vector potential $\vec{A}$ in the absence of sources, gives rise to the constraint for $\vec{A}$ that

$$\triangle\vec{A} + \frac{\omega^2}{c^2}\vec{A} = \vec{0} \tag{2.3}$$

where $\triangle$ is the Laplace operator. This is called the vector Helmholtz equation and its solutions can be found in terms of the solutions to its scalar version

$$\triangle a + \frac{\omega^2}{c^2}a = 0 \tag{2.4}$$

which in turn has a solution of the form

$$a_{LM} = j_L(kr)Y_{LM}(\theta, \phi) \tag{2.5}$$

where L = 0, 1, 2,... and |M| ≤ L. The solutions for a are products of radial functions (j_L) and angular spherical harmonic functions (Y_{LM}) that determine the allowed transitions according to the spin-parity of their energy states. This constitutes the basics of nucleon-photon interaction which establishes a theoretical framework to estimate the probabilities of nucleons to reach higher or lower energy states.

2.1.2 Classical and relativistic kinematics of a particle

The simulation of nuclear reactions requires a set of input general information, which needs to be as accurate as possible, and the objective is to produce a given number of output observables. The outcome of the reaction can be for example the energies of the outgoing particles produced by the reaction. The special theory of relativity provides a theoretical framework for describing nuclear reactions, notably by identifying the mass-energy equivalence, and also by considering the effects of changing the reference frame while keeping the speed of light constant. These considerations imply that the classical way (in the framework of Newtonian mechanics) of calculating outcomes such as the outgoing particle energies becomes more subtle. With regards to the kinematics of nuclear reactions, in order to quantify the impact of relativistic corrections to classical quantities, one has to consider the energetic interval where the particles evolve, to get their velocity v, and assess the impact on the physical system in question using the Lorentz factor γ where

$$\gamma = \frac{1}{\sqrt{1 - \frac{v^2}{c^2}}} = \frac{1}{\sqrt{1 - \beta^2}} \tag{2.6}$$

and $\beta = \frac{v}{c}$.

In the computational experiments typically performed during this work, the maximum neutron kinetic energies are lower than 20 MeV, and this value amounts to the extreme case of β=0.2 (a 20 MeV neutron travels at 20% the speed of light). At this velocity the Lorentz factor is 1.02 and the energy measurements in the laboratory frame of reference start to show deviations on the order of a few percent. In addition, photons are relativistic by nature as they are massless, and electron emission in nuclear reactions is highly energetic, so one must perform all the quantitative analyses of neutron-induced reactions using special relativity. The graph shown in Figure 2.1 shows the variation of the Lorentz factor as a function of neutron kinetic energy, and it should be noted that under 100 MeV, γ varies on the order of a few percent, and below 1 MeV, it is even less. The Lorentz factor is crucial for switching reference frames, which allows to perform kinematics analyses of nuclear reactions by expressing the values of interest for the reaction in the center-of-mass (CM) frame.

By convention, the notations for a binary nuclear reaction that consists of a projectile A, a target B, a detected product of the reaction C, and other residual products D are

$$A + B \rightarrow C + D$$

or equivalently

$$B(A, C)D$$

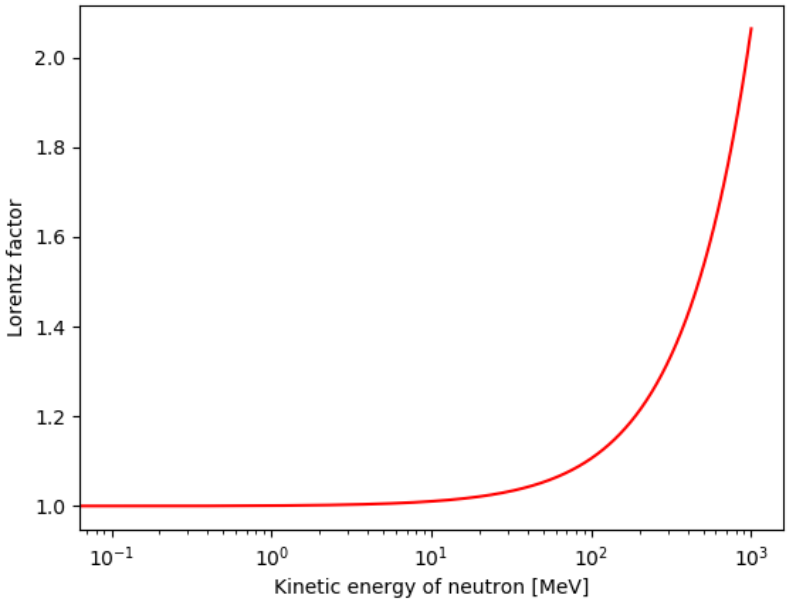

Figure 2.1: Lorentz factor as a function of incident neutron energy.

If one wants to refer to the generic reaction, the notation is (A, C). In the laboratory frame of reference (LAB), one considers that the target is at rest, the kinetic energy of the projectile is T_A and its mass is m_A. The total energy of the projectile E_A in the LAB frame is then

$$E_A = T_A + M_A \tag{2.7}$$

where $M_A = m_A \times c^2$.

From the Einstein energy relation and equation 2.7, the momentum of the projectile p_A is given by

$$P_A = \sqrt{E_A^2 - M_A^2} = \sqrt{T_A^2 + 2M_A T_A} \tag{2.8}$$

where $P_A = p_A \times c$.

One can also define the so-called center-of-mass (CM) frame of reference in which the total momentum of the system vanishes. Energy and momentum of the projectile given in the CM frame have indices c, and the Lorentz transformations to go from one reference frame to the other are:

$$\begin{aligned} E_{Ac} &= \gamma[E_A - \beta p_A] \\ E_A &= \gamma[E_{Ac} + \beta p_{Ac}] \end{aligned} \tag{2.9}$$

and

$$\begin{aligned} p_{Ac} &= \gamma[p_A - \beta E_A] \\ p_A &= \gamma[p_{Ac} + \beta E_{Ac}] \end{aligned} \tag{2.10}$$

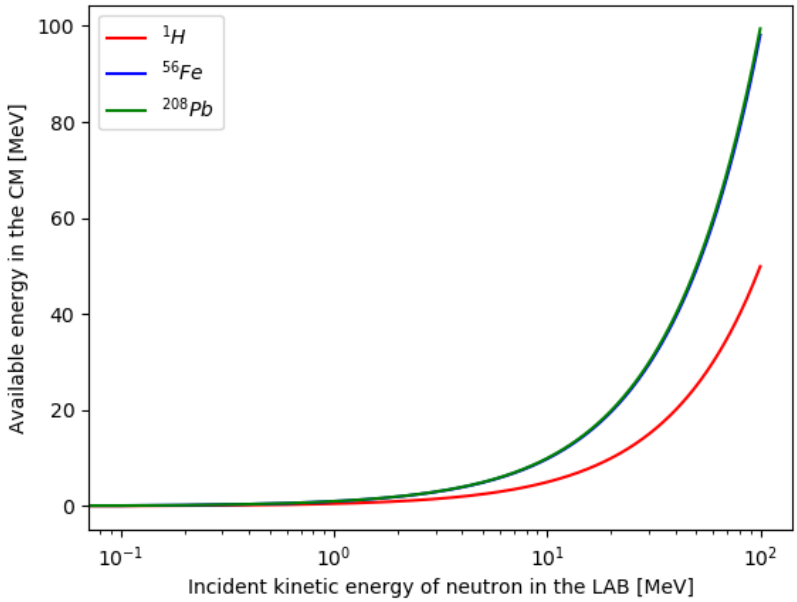

Figure 2.2: Available energy in the CM frame as a function of incident neutron energy in the LAB frame.

Knowing that

$$\beta = \frac{\sum P}{\sum E} = \frac{P_A}{E_A + E_B} = \frac{\sqrt{T_A^2 + 2M_A T_A}}{T_A + M_A + M_B} \tag{2.11}$$

and considering the classical approximation of $T_A << M_A$, one obtains $\beta \to \frac{\sqrt{2M_A T_A}}{M_A + M_B} \to 0$, so the first order expansion of γ is

$$\gamma = 1 + \frac{1}{2}\beta^2 \tag{2.12}$$

which allows to find a first order approximation of E_{Ac} using equations 2.7 then 2.9:

$$E_{Ac} = T_{Ac} + M_A = (1 + \frac{M_A T_A}{(M_A + M_B)^2})[M_A + T_A - \frac{2M_A T_A}{M_A + M_B}] \tag{2.13}$$

and the approximation of $T_A << M_A$ yields

$$T_{Ac} = \frac{T_A M_B^2}{(M_A + M_B)^2} \tag{2.14}$$

Taking the analogous steps one finds for the kinetic energy of the target B in the CM frame

$$T_{Bc} = \frac{M_A M_B}{(M_A + M_B)^2} T_A \tag{2.15}$$

The sum of these two energies determines whether a given reaction can happen or not. Each reaction has a so-called reaction Q-value, a threshold energy below which the

reaction cannot occur. If $T_{Ac}+T_{Bc} > Q$ then the transport code opens the possibility of the reaction channel associated to a given Q-value. The graph shown in Figure 2.2 illustrates the evolution of available energy in the CM frame as a function of incident neutron kinetic energy in the LAB frame, according to the mass of the target (here are shown the cases of ^{1}H,^{56}Fe and ^{208}Pb). For the heavier nuclei, it can be observed that the available energy in the CM frame start to be non zero above 1 MeV of incident neutron energy (in the LAB), whereas the lighter nuclei require more than 10 MeV to start having non zero available energy. For a given reaction, if its Q-value is positive, one can draw a horizontal line at $E_{av} = Q$ and the abscissa value of the crossing of the horizontal line and the curve is the threshold energy for the reaction in the LAB frame.

2.1.3 Reactions

Elastic scattering

Neutron elastic scattering (n, n') occurs when the total kinetic energy in the center of mass frame is conserved in the process of a neutron collision with a target nucleus. It is a two-body reaction that is analog by nature. Similarly to the analytical procedure taken for equations 2.12 to 2.14, and knowing that $p_{Ac} = p_{Cc}$ and $m_A = m_C$, where A represents the incoming neutron n, and C represents the outgoing neutron n', one finds

$$T_C = \frac{T_A}{(M_A + M_B)^2}[M_B^2 + M_A^2 + 2M_A M_B \mu_{Cc}] \tag{2.16}$$

where $\mu_{Cc} = cos(\theta_c)$ is the deviation of the outgoing neutron with angle θ_c in the CM frame as shown in Figure 2.3. The only unknown in equation 2.16 is μ_{Cc}, as T_A and the masses are set before the simulation. This in turn means that the simulation of this reaction only requires angular data, which usually is in the form of a probability distribution.

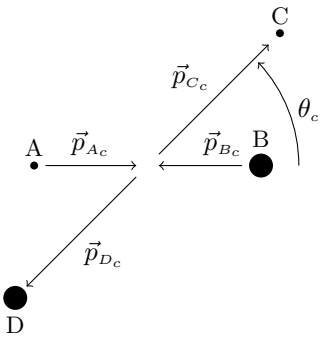

Figure 2.3: Elastic scattering represented in the center of mass frame, where $A = C$ and $B = D$.

Inelastic scattering

In the neutron-induced inelastic scattering reaction $(n, n'\gamma)$, the produced photons, or γ rays, can be emitted by a nucleus B when the neutron n transfers a part of its kinetic energy

to B, bringing B (which before the collision is considered at rest in the LAB frame and in its ground state) to an excited state B^*, and the kinetic energy of the outgoing neutron is different than the incident energy. Then, for B^* to return to its ground state, an integer number i of photons can be emitted with a total energy up to the available energy that was provided by n. In the framework of the Nuclear Shell model, the projectile n transfers energy to the nucleons, which in turn momentarily populate higher shell levels (or excited states) before they emit photons to decay into lower energies. This two-body reaction can be expressed formally by the following two processes:

$$\begin{aligned} n + B &\rightarrow n' + B^* \\ n' + B^* &\rightarrow n' + B + i\gamma \end{aligned} \tag{2.17}$$

where n' is the scattered neutron.

The energies of the neutrons produced in reactors are in the range of the MeV and are thus capable of bringing the vast majority of heavy nuclei to their excited states after inelastic collisions. Shortly thereafter, the process of nuclear decay produces photons with energies that depend on probabilities of emission, and the interaction of those photons with their surrounding medium yields important energetic transfers, hence the interest of having a precise characterization of their decay scheme in the first place for reactor simulations, and in the second place for particle coincidence in detector simulations.

The reaction described in 2.17 obeys the following relations (according to the notation of section 2.1.1, the scattered neutron n' corresponds to C, and the residual excited nucleus B^* corresponds to D)

$$\begin{aligned} p_{Cc} &= p_{Dc} \\ \sqrt{2M_C T_{Cc}} &= \sqrt{2M_D T_{Dc}} \\ T_{Dc} &= \frac{M_C}{M_D} T_{Cc} \end{aligned} \tag{2.18}$$

The available energy in the CM frame is

$$T_{Ac} + T_{Bc} = \frac{M_B T_A}{M_A + M_B} \tag{2.19}$$

where A corresponds to n and B to X. The conservation of energy gives

$$T_{Cc} + T_{Dc} = Q + T_{Ac} + T_{Bc} \tag{2.20}$$

where Q is the reaction threshold, which corresponds to the excitation energy E_{exc} of B^* for the inelastic reaction. Indeed, $Q_{inl} = M_D - M_B$, thus $M_D = M_B + Q$. Plugging 2.18 and 2.19 in 2.20 gives

$$\begin{aligned} T_{Cc}[1 + \frac{M_C}{M_D}] &= Q + \frac{M_B T_A}{M_A + M_B} \\ T_{Cc} &= \frac{(M_B + E_{exc})[E_{exc}(M_A + M_B) + M_B T_A]}{(M_A + M_B)(M_B + E_{exc} + M_C)} \end{aligned} \tag{2.21}$$

Equation 2.9 and approximation 2.12 yield

$$
\begin{aligned}
T_C &= T_{Cc} + \frac{1}{2}\beta^2 M_C + \beta p_{Cc}\mu_{Cc} \\
&= T_{Cc} + \frac{M_A T_A M_C}{(M_A + M_B)^2} + \frac{\sqrt{2M_A T_A}\sqrt{2M_C T_{Cc}}}{(M_A + M_B)^2}\mu_{Cc}
\end{aligned}
\tag{2.22}
$$

According to equations 2.21 and 2.22, in order to determine the outgoing energy of the neutron n' in the LAB frame (end-result given by TRIPOLI-4®), the input data required is the reaction Q-value and the deviation μ_{Cc}. These values can be stored as a constant in the case of Q, and μ_{Cc} as a distribution. Once $T_{n'}$ is calculated from its CM value by a Lorentz transformation, the remaining energy goes to the recoil nucleus B^* and, according to the structure data of the decay schemes, the electromagnetic cascade brings B^* to its ground state.

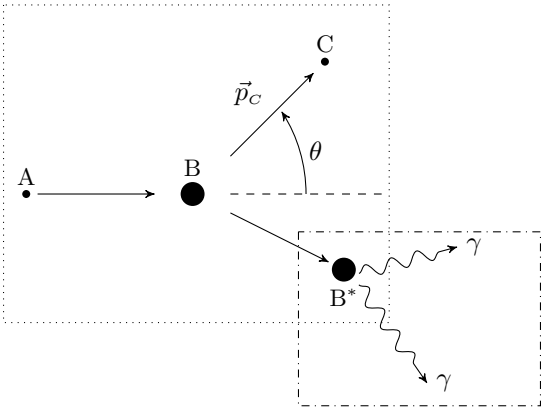

Figure 2.4: Inelastic scattering represented in the laboratory frame where B* is the nucleus B in an excited state.

The gamma decay process that follows the inelastic reaction takes place in the moving frame of the recoil nucleus $B^* = D^*$ as shown in Figure 2.4, where the moving frame of the recoil nucleus is represented as a dotted-dashed rectangle. The emitted photons carry specific amounts of energy as they are produced from discrete state transitions within the excited nucleus. The gamma energies $E_{\gamma c}$ are stored in decay scheme libraries and can be considered as the measured energies in the CM frame of the nucleus that emits them. The energy measured on the LAB frame depends on the velocity of the recoil β_r as follows:

$$
\begin{aligned}
\beta_r &= \frac{P_{D^*}}{E_{D^*}} \\
E_\gamma &= \gamma_r E_{\gamma c}(1 + \beta_r \mu_{\gamma c})
\end{aligned}
\tag{2.23}
$$

Generally, the emission of gammas from an excited nucleus is declared as isotropic in the nuclear data evaluation, which means $\mu_{\gamma c}$ is uniformly distributed in [-1;1] (however, the anisotropies can also be declared). In terms of the photon production spectrum, instead of having Dirac-like peaks of emission at the energies of emission $E_{\gamma c}$, one should observe

Gaussian-like peaks (if isotropic) spread over an energy interval that depends on β_r. Indeed, the lighter the target, the faster the recoil nucleus will be scattered. This phenomenon is called Lorentz boost as it boosts the energy of the photon when it is emitted in the direction of motion of the excited recoil nucleus ($\mu_{\gamma c} > 0$). It is a phenomenon analogous to the Doppler effect, illustrated with Figure 2.5.

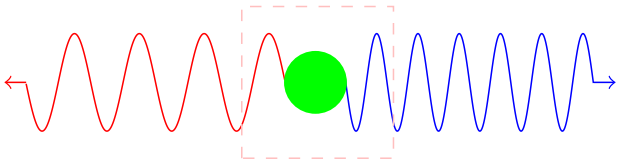

Figure 2.5: Lorentz boost: photons are blue- or red-shifted according to the emission angle. The particle that emits the photons is in green and its center of mass frame is the dashed square moving to the right.

One source of bias for the calculations of equations 2.23 in the simulation is to keep β of the reaction system (scattered neutron + excited recoil nucleus) instead of β_r (which only accounts for the motion of the excited recoil nucleus). This will be further discussed in Chapter 3.

Neutron Capture

In (n, γ) reactions, also called neutron capture, a neutron is absorbed by a target nucleus and the mass difference introduced by the absorption results in the emission of gammas via an electromagnetic cascade. This work is focused on thermal neutrons inducing the neutron capture reaction because otherwise there are several hundred resonances on total neutron cross section in the range of several hundred eV [17] to take into account that would greatly impact the simulation. Additionally, Light Water Reactors function on the principle of *thermalizing* the neutrons (decreasing their energy from MeV to meV) as the cross sections for fission increase drastically at thermal energies, which is also the case for the capture reaction.

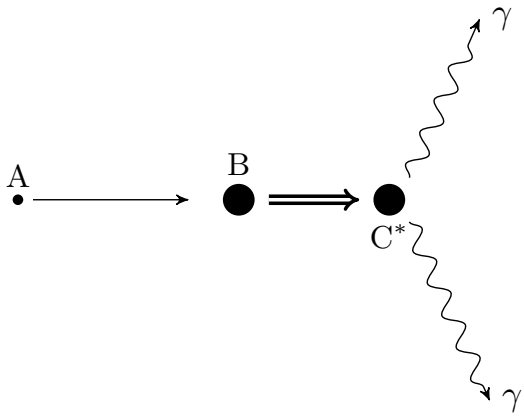

Figure 2.6: Neutron capture reaction represented in the laboratory frame where C* is the result of B absorbing a neutron and reaching an excited state of C.

The (n, γ) reaction yields several gammas in a particular order that should account for most of the available energy. Thus, for the verification of this reaction one has to check the gamma multiplicity and the total energy of the cascade as well as the order of gamma emission. Examples of expected multiplicities and available energy are, according to nuclear data at 10^{-5} eV: $^{56}\mathrm{Fe}(n, \gamma)$ produces on average 2.3 photons that should carry 7.45 MeV, $^{155}\mathrm{Gd}(n, \gamma)$ produces 3.9 photons with 8.54 MeV and $^{238}\mathrm{U}(n, \gamma)$ produces 2.8 photons with 4.8 MeV.

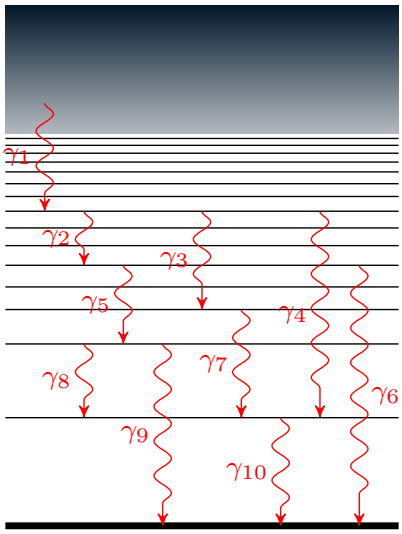

Cascade 1 : $\gamma_1 + \gamma_2 + \gamma_5 + \gamma_8 + \gamma_{10}$
Cascade 2 : $\gamma_1 + \gamma_2 + \gamma_5 + \gamma_9$
Cascade 3 : $\gamma_1 + \gamma_3 + \gamma_7 + \gamma_{10}$
Cascade 4 : $\gamma_1 + \gamma_4 + \gamma_{10}$
Cascade 5 : $\gamma_1 + \gamma_2 + \gamma_6$

Figure 2.7: Possible decays starting from the continuum of states.

When nuclei reach several MeV of excitation energy, the energy levels cannot be differentiated experimentally, so they are considered as a continuum of states. On Figure 2.7, the continuum of states is presented as a diffuse-gray rectangle from which photons can be produced and reach discrete energy states presented as lines. Photons emitted from the continuum can either bring the nucleus to its ground state, in which case one photon carries all the available energy; or they can bring the nucleus to a lower excitation energy but staying in the continuum, in which case the photon carries relatively low energy; or they can bring the nucleus to a discrete level, in which case a normal electromagnetic cascade ensues, as is the case shown in Figure 2.7 where γ_1 comes from the continuum and 5 possible cascades are shown.

The studied aspect of the reactions in this work is the production of gammas, in particular the correlation between their energies of emission. Considering all the possibilities

that the existence of the continuum introduces, it becomes impossible to store all the correlations. To tackle this issue, one has to implement statistical decay tools in order to correctly simulate this reaction. Indeed, the information regarding photon emission from (n, γ) can be found in the nuclear data in the format of energy and angle distributions, as well as expected multiplicities, as functions of incident neutron energy. However, this information represents an averaged expected behavior for the emitted particles, so their correlations are not embedded in the data, thus the energy conservation can only arise as a mean value corrected by well chosen particle weights, and thus the conservation of energy does not emerge from each reaction event (as it should if the event was *realistic*). This data format is not appropriate for analog simulations by construction (as it relies on particle weights, for example if the cascade should produce 5 photons, the chosen photon from the distribution has a weight of 5) so one must rely on photon strength functions and level density functions to estimate which energy should be attributed to the emission from the continuum, and as the nucleus reaches discrete levels, one follows the decay scheme for the isotope in question.

An alternative method is to use a format in which discrete emissions can be stored, with the possibility of also declaring a continuous multiplicity, in turn capable of storing a continuous emission spectrum as a function of the incident neutron energy.

(n,2n)

In (n,2n) reactions, a high energy neutron separates one neutron from the target nucleus. The different mechanisms of this process will be discussed in Chapter 5. In the outgoing channels there must be 2 neutrons, a recoil nucleus with A-1 nucleons and possibly a number of gammas (if the recoil nucleus is in an excited state). Thus (without considering gammas) (n,2n) is a three-body reaction in the outgoing channel. The reaction presents a threshold energy, the so-called neutron separation energy S_n, so the kinetic energy of the incoming neutron must be significantly higher than S_n. To verify the accuracy of the simulation we have studied the possible gamma, neutron and recoil spectra that are expected, considering all the energy correlations to ensure that the total energy is conserved.

The information concerning the four (n,2n)-reaction-products (*i.e.* n, n', recoil, gammas) is stored as energy (mostly evaporation spectrum) and angle distributions for particles emitted post-reaction. In general, one can only find in the (n,2n)-dedicated section of the evaluated nuclear data one distribution with multiplicity of 2 for the two outgoing neutrons, which implies that both neutrons are treated equally regarding the kinematics. This aspect does not allow a correct energetic balance needed for analog simulations, but does allow to find an average behavior using a Monte Carlo code to explore a large number of events.

In most evaluations we can seldom find the energy distributions for all the particles involved, so in this work we focused on the ^{19}F nucleus because its evaluated file of the European library version 3.3 (JEFF-3.3 [14]) has the four relevant distributions. There are several options for analyzing this reaction, here we consider that the incoming neutron scatters in-elastically off the target with an almost uniform distribution, then it has been measured experimentally that the excited nucleus of the reaction emits the second neutron in an evaporation spectrum. The recoil nucleus can remain in an excited state, which explains the importance of having a gamma distribution in the file, as they can account for the rest of available energy, if any is left.

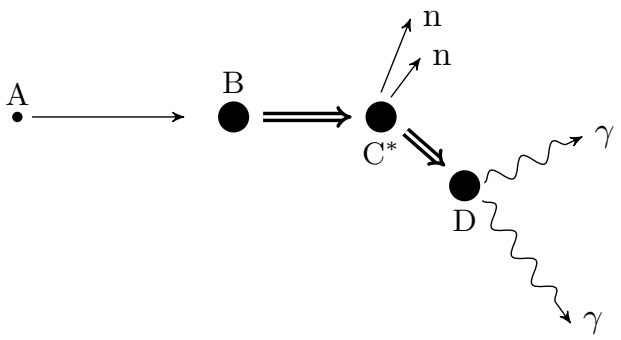

Figure 2.8: $(n, 2n)$ reaction represented in the laboratory frame.

Photonuclear

Photonuclear reactions (γ, z) consist of a photon collision with a nucleus which can provoke a myriad of outcomes that depend on the incident photon energy E_γ. The outcome z can be a number i of neutrons if $E_\gamma > S_{i\times n}$; if $z = f$ it is called photo-fission, a reaction that has been added recently to the nuclear libraries (the Japanese library has (γ,f) since 2004); if $z = \alpha$ it means $E_\gamma > S_\alpha$, and so on. The kinematics analysis of this reaction is analogous to the previous ones considering

$$\beta = \frac{E_\gamma}{M_B + E_\gamma} \tag{2.24}$$

Internal conversion

The reactions previously discussed (with the exception of elastic scattering) have in common that the target nucleus is brought to an excited state and the latter decays to reach its ground state. The so-called internal conversion is a competing process with respect to photon emission. This process consists in the ejection of one (or several) of the inner shell electrons by the electromagnetic interaction of the excited nucleus with the electronic orbitals. Depending on a number of factors such as available energy or amount of angular momentum of the excited nucleus, this process can be the preferred decay channel for example if the excited state reached has an high angular momentum, and electrons are better suited for such a decay compared to photons. In any case, for the sake of phenomenological precision, the ENDF-6 format allows the declaration of these probabilities in the photon production data by setting a specification flag called LG=2 to impose that all transitions in the photon production data must declare one probability of photon emission and one probability of electron emission.

2.2 Evaluated nuclear data

Nuclear data, *i.e.* all measures that have been collected to describe neutron-, photon-, and charged-particle-induced reactions on a vast number of isotopes, can be grouped

in a computer-oriented system that serves as an input for simulation codes that should reproduce the behavior of the studied isotopes. The first attempt to create such a library took place in the Lawrence Livermore National Laboratory in the 1950's, the so-called Evaluated Nuclear Data Files (ENDF) [18]. It is called evaluated because the data is in constant improvement, as users of the library either require new data, or find anomalies within the data. The format used in this library is called ENDF-6 format [19], and is the international standard format, used by the Nuclear Energy Agency (NEA) library called Joint Evaluated Fission and Fusion File (JEFF)[14], the main library used during this PhD work.

It is impossible to store every possible reaction outcome in a data file, so other libraries have been created to be complementary to the evaluated data files. In the case of this work, the relevant libraries are the Evaluated Nuclear Structure Data Files (ENSDF)[20], which stores, among others, the information regarding nuclear excited states (energies, transition probabilities, spin-parities), and its European counterpart: the Reference Input Parameter Library (RIPL)[8], the main structure library used during this PhD work.

2.2.1 Brief history of nuclear data libraries

Since its creation, the Evaluated Nuclear Data Library has seen a succession of forms and formats [18]. In its earliest form it was a series of internal memos containing tabulations of cross sections and angular distributions for a few isotopes to be used in neutronics calculations. It was soon found that some type of mechanization should be undertaken both for efficiency and for convenience. Thus, in rapid succession, the library went through stages of punched card and punched paper-tape, and then to the first magnetic-tape BCD card image form. Of course, once the library was in one computer-readable form, it could be translated with relative ease to another computer-readable form. Ten different particles are presently defined: neutrons, photons, electrons, protons, alphas, etc, and more can be added. In the beginning, nuclear data was available mostly for elements instead of isotopes, and this has been evolving progressively. Indeed, today the libraries are divided only by isotopes.

In the most recent libraries, such as ENDF/B-VIII, JENDL-5 (from Japan), JEFF-3.3, TENDL-21 (created using TALYS and optical models), one can find more isotopes than before and each isotope also contains more data. For example, JEFF-2.2 contains 310 isotopes (of which 14 are natural) JEFF-3.1 contains 381 isotopes (of which 6 are natural), whereas JEFF-3.3 contains 562 isotopes as free gas and no natural isotopes. The same goes for ENDF/B: version VI.4 contains 322 isotopes (of which 16 are natural), version VII.0 contains 393 (of which 3 are natural) and version VIII has 556 isotopes and 0 natural. Also, complementary data has been progressively added to the evaluations : for example data concerning the (n,2n) reaction, previously had only one dedicated section (MT=16) and now there exists the possibility to dedicate sections to describe production of 2 neutrons with residual energy in the n^{th} state, $n \in [0:14]$ (MT=875 to 890 for discrete representation and MT=891 corresponds to 2 neutrons produced in the continuum).

ENSDF on the other hand is maintained by the National Nuclear Data Center (NNDC) on behalf of the international Nuclear Structure and Decay Data Network sponsored by the International Atomic Energy Agency, Vienna. Data for $A = 5$ to 44 are extracted from the evaluations published in Nuclear Physics; for $A > 45$ the file is used to produce the Nuclear Data Sheets[21].

2.2.2 ENDF & JEFF

Regarding the structure of the libraries, particularly the ENDF-6 data format, the hierarchy to organize nuclear data goes from nucleus, to files, to sections and finally to records. These have their specific code names: MAT, MF, MT, MR respectively. MAT is set by the atomic number Z of the nucleus it represents, followed by a number that indicates which isotope and isomer it is, and natural elements have MAT numbers Z00. For example, the MAT number for hydrogen is 125 because Z=1 and 25 defines the lightest stable isotope found in nature. MAT=126 and 127 would be the two lowest meta-stable states of hydrogen and MAT=128 is deuteron. Other examples are MAT=9222 for ^{233}U, MAT=9225 for ^{234}U and MAT=9228 for ^{235}U.

A **file**, in the ENDF nomenclature, is a block of data in an evaluation that describes a certain data type. To name a few types, MF=3 corresponds to reaction cross sections, MF=4 to angular distributions, MF=5 to energy distributions, and MF=6 to product energy-angle distributions. MF=12 corresponds to photon production yield data, MF=13 to photon production cross sections, MF=14 to photon angular distributions, and MF=15 to continuous photon energy spectra. Within a given file, one finds different **sections** dedicated to specific reactions. For example MT=18 of MF=3 corresponds to the fission cross section, MT=16 of MF=5 to energy distribution for neutrons emitted from (n,2n), MT=102 of MF=6 to photon production distributions from (n,γ) and, MT=51...90 of MF=12 to the energies and transition probabilities of the first 40 exited states.

In particular MF=6, any reaction is defined by giving the production cross section for each reaction product in barns/steradian assuming azimuthal symmetry:

$$\sigma_i(\mu, E, E') = \sigma(E) y_i(E) f_i(\mu, E, E')/2\pi \tag{2.25}$$

where i denotes one particular product, E is the incident energy, E' is the energy of the product emitted with cosine μ, $\sigma(E)$ is the interaction cross section found in MF=3, y_i is the product yield or multiplicity, and f_i is the normalized distribution with units (eV.unit-cosine) where

$$\int dE' \int d\mu f_i(\mu, E, E') = 1 \tag{2.26}$$

This representation ignores most correlations between products and most sequential reactions; that is, the distributions given here are those, which would be seen by an observer outside of a "black box" looking at one particle at a time. The process being described may be a combination of several different reactions, and the product distributions may be described using several different representations.

However, the replacement of the system of codes built off this format has been recognised as an important initiative. In 2013, the NEA Working Party on International Nuclear Data Evaluation Co-operation (WPEC) launched a project to review the requirements for an international replacement of the ENDF-6 format. The recommendations prompted the creation of a new Expert Group on a Generalised Nuclear Data Structure (GNDS) in 2016 that has used these requirements as the framework for a new format specification. Following rigorous international review, version 1.9 was unanimously approved as the first official published format. This is extremely interesting for the topic of this PhD as the analog simulation requires more accurate and detailed data than what is currently available. An example of this being the capacity to take into consideration center-of-mass corrections

in photon production stored in MF=12, which is currently unavailable as will be further discussed in the chapter of inelastic scattering.

The work presented here is based on the analysis of the JEFF library as the CEA is a contributing member of its revision and improvement.

2.2.3 ENSDF & RIPL

The Evaluated Nuclear Structure Data File (ENSDF) is a library that contains nuclear structure and decay data for all the known nuclides. The evaluation effort of expert critical review of all available experimental data is coordinated by the National Nuclear Data Center at the Brookhaven National Laboratory, who are also responsible for its publication. Each type of experiment is thus presented as a separate data set. The fact that all known experimental data is used to deduce nuclear structure information to be included in the library, makes ENSDF extremely vast and should thus be used as a reference encyclopedia-like library for specific utilization, as opposed to attempting to rely strictly on all its information, as will be discussed further in this work. As of the most recent update on September 9, 2022, the ENSDF database contains 19569 data sets for 3409 nuclides.

In the ENSDF data, the users can find:

1. Nuclear level properties (observation source, energy, half-life, decay modes, spin and parity)

2. Gamma ray energies, intensities, multipolarities, mixing ratios and conversion coefficients

3. Nuclear radiation energy and intensity as well as radiation-specific data for different radiation types (gammas, alphas, betas and neutrons)

The Reference Input Parameter Library (RIPL) has been created and updated by the International Atomic Energy Agency (IAEA) since 1993 to make available the necessary numerical input for advanced modelling codes that perform calculations of nuclear reactions. The final RIPL coordinated research project (RIPL-3) was released in January 2009, and is the nuclear structure data most adapted to the work of this PhD. The information found in this library is extremely important for theoreticians involved in the development and use of nuclear reaction modelling (ALICE, EMPIRE, GNASH, UNF, TALYS) both for theoretical research and nuclear data evaluations.

The seven segments that evaluators can find included in the RIPL-3 library are:

1. MASSES contains ground-state properties of nuclei for about 9000 nuclei, including three theoretical predictions of masses and the evaluated experimental masses of Audi *et al.* (2003).

2. DISCRETE LEVELS contains 118 datasets (Z from 0 to 117) with all known level schemes, electromagnetic and γ-ray decay probabilities available from ENSDF in April 2014.

3. NEUTRON RESONANCES contains average resonance parameters prepared on the basis of the evaluations performed by Ignatyuk and Mughabghab.

4. OPTICAL MODEL contains 495 sets of phenomenological optical model parameters defined in a wide energy range. When there are insufficient experimental data, the evaluator has to resort to either global parameterizations or microscopic approaches. Radial density distributions to be used as input for microscopic calculations are stored in the MASSES segment.

5. LEVEL DENSITIES contains phenomenological parameterizations based on the modified Fermi gas and superfluid models and microscopic calculations which are based on a realistic microscopic single-particle level scheme. Partial level densities formulae are also recommended. All tabulated total level densities are consistent with both the recommended average neutron resonance parameters and discrete levels.

6. GAMMA contains parameters that quantify giant resonances, experimental γ-ray strength functions and methods for calculating gamma emission in statistical model codes. The experimental GDR parameters are represented by Lorentzian fits to the photo-absorption cross sections for 102 nuclides ranging from ^{51}V to ^{239}Pu.

7. FISSION includes global prescriptions for fission barriers and nuclear level densities at fission saddle points based on microscopic HFB calculations constrained by experimental fission cross sections.

In the framework of this work, the segment DISCRETE LEVELS of the RIPL library was used to obtain the information concerning the excited states of the studied nuclides. The information found in this library was found to be more coherent with the JEFF library, in terms of the energy value and even existence of excited states - compared to ENSDF.

2.3 Monte Carlo Simulation

The Monte Carlo method consists in formulating a game of chance or a stochastic process $f(x)$ which produces a random variable x. In the case of interest in this work, x would be a nuclear event, and $f(x)dx$ the probability of x happening, with $\int_\Omega f(x)dx = 1$. If the sought after solution of an equation can be written as the expected value $E[x]$, then an approximation to $E[x]$ can be obtained by sampling the distribution $f(x)$. The primary source of error is due to the fact that only a finite sample can be simulated in practice: the degree of accuracy of the Monte Carlo method depends on the sample size. Under mild hypotheses, the empirical average sampled from the distribution converges to the sought expected value (*i.e.*, is an unbiased estimator), and the statistical error decreases as $\frac{1}{\sqrt{N}}$, N being the size of the sample [22]. The method is, essentially, a statistical approach to the study of integro-differential equations that occur in various branches of the natural sciences [23]. The field of nuclear physics in particular focuses on the spatial and temporal evolution of particles within a given medium, and the behavior of neutrons specifically is described by the solutions of the Boltzmann integro-differential equation where neutron radiation is considered as a diluted gas of diffusing particles with reproduction and death, also called history. The birth of the particle consists of assigning specific values of the phase space $(\vec{r}, E, \vec{\Omega}, t)$ to the new particle, sampling a path length and according to what the particle does in the new coordinates of the phase space (collision, absorption, leakage), determining weather the particle dies or not. If this process is done *event-by-event*, then

the simulation is called *natural* or *analog*, as the physical phenomenon is not altered. This requires very precise nuclear data and very large number of histories.

In the domain of focus of this work, variance reduction methods are not treated because, by construction, the analog simulation is more time consuming than its non-analog counterpart. Indeed, in the analog simulation one has to keep track of all parameters of all particles (all particle weights =1), whereas the non-analog simulation relies on averaged quantities and particle weights can be more than 1.

Non-analog simulation is by construction a simulation bias for variance reduction and consists in changing the probability distribution function (pdf) $f(x)$ into another pdf $f^*(x)$ such that the expectation value is unchanged:

$$E[x] = \int_D y f(y) dy = \int_D y \frac{f(y)}{f^*(y)} f^*(y) dy \tag{2.27}$$

This means that the simulation with $f^*(x)$ will produce a particle weight W^* such that

$$W^* = W \frac{f(x)}{f^*(x)} \tag{2.28}$$

where W is the analog weight and W^* is the non-analog weight associated with $f^*(x)$ such that $E[x]$ unchanged. The way to choose $f^*(x)$ is to solve the adjoint equation of the studied system.

2.3.1 Solving neutron transport equations

The Boltzmann equation for the transport of neutrons is

$$\frac{1}{v}\frac{\partial \psi}{\partial t}(\vec{r}, E, \vec{\Omega}, t) + \left[\vec{\Omega} \cdot \vec{\nabla} + \Sigma_{tot}(\vec{r}, E, t)\right]\psi(\vec{r}, E, \vec{\Omega}, t) = \int_{4\pi} d\Omega' \int_0^\infty dE' \Sigma_s(\vec{r}, E' \to E, \vec{\Omega}' \to \vec{\Omega}, t)\psi(\vec{r}, E', \vec{\Omega}', t) + S(\vec{r}, E, \vec{\Omega}, t) \tag{2.29}$$

where ψ is the angular flux of neutrons which characterizes the population of neutrons at position $\vec{r}$, energy E, direction $\vec{\Omega} = \frac{\vec{v}}{\|\vec{v}\|}$, at time t. The solution is strongly influenced by macroscopic cross sections denoted Σ_i where i is the reaction type; s=scattering, a=absorption, tot=total. This value is obtained by adding for each isotope k their microscopic cross section $\sigma_k(E, \vec{\Omega})$ (contained in the evaluation) multiplied by the atomic density $N_k(\vec{r}, t)$ (number of atoms per cm^3) of the medium where the neutrons are being transported.

$$\Sigma_i = \sum_k \sigma_{i,k}(E) N_k(\vec{r}, t) \tag{2.30}$$

The integro-differential equation 2.29 takes into account all the possible factors that have an influence on the variation in neutron population of a region of space, with a specific energy and direction. For reactors operating at nominal power or other systems at steady state, $\partial_t = 0$ simplifies the problem drastically, because if ψ is a constant function of time, the dimensionality of the problem is reduced from 7D to 6D and some dependencies between the variables are eliminated.

The leakage of neutrons out of the phase space is accounted for with the streaming operator $\vec{\Omega} \cdot \vec{\nabla}\psi$ and those disappearing due to reactions are in $\Sigma_{tot}\psi$.

On the right hand side of the equation are the source terms, mainly neutrons that scatter (Σ_s) into the phase space of interest (before the scattering they had energy E' and after, the neutron energy becomes E, the same goes for the direction $\vec{\Omega}$), or that are produced externally by the source S, where the fission term can be included.

The previous description of particle transport qualifies it as a Markovian process, *i.e.* all effects have a cause. In the particular case of neutronics, the algorithm of the process can be summarized as follows: the emission of the neutron provokes a random sampling of its track length. The outcome can lead the neutron to cross a boundary: on one hand, a reflection or a change of media can occur (in this case another track length is to be chosen), on the other hand, the neutron is leaked out and its history is over. Another possibility for the neutron is an interaction that could induce a scattering (thus new angle, energy and track length to be sampled) or an absorption (like neutron capture for example). These are the random events that allow multiplication factors or photon production to evolve during the simulations.

Coming back to the nuclear data contained in the evaluations, in particular the point-wise cross-sections σ_i : they are defined as probabilities of neutron-target interactions used for continuous energy calculations. The denomination of [microscopic] *cross sections* comes from the fact that they are given in cm^2, as if the neutron was a dart and the target a dartboard : the smaller the dartboard surface, the more difficult it is to aim. As per equation 2.30, σ_i determine the macroscopic cross-section Σ_i, given in cm^{-1}, to represent the inverse of the mean free path (or track length) of the neutron in a given medium.

A simplified description of what the transport code has to solve is the angle-integrated transport equation with no time dependence, with monokinetic neutrons in infinite homogeneous medium:

$$\begin{aligned} \int_{4\pi} \psi(\vec{r}, E, \vec{\Omega}) d\vec{\Omega} &= \Phi(\vec{r}, E) \\ \Sigma_t \Phi = \Sigma_s \Phi + S \Rightarrow \Phi &= \frac{S}{\Sigma_t - \Sigma_s} = \frac{S}{\Sigma_a} \end{aligned} \tag{2.31}$$

Indeed, the interactions of this work are initiated by monokinetic neutrons (there is an energy cut-off set in the simulations as soon as the neutron collides) onto one single type of nucleus in addition to the fact that S is set as an isotropic and monokinetic point-source inside a 50 cm radius sphere of a given isotope. Thus, it is possible to consider an infinite homogeneous medium as geometrical dimensions of the simulated systems are larger than the mean free path. Finally, the coefficient Σ_a^{-1} is calculated with the data in the evaluations for establishing the game of chance, then the interaction to consider for each neutron can be sampled, as previously explained. Equation 2.31 is an analytical solution for the Boltzmann equation under strong constraints, and is compatible with the Monte Carlo analytical solution (considering infinite sampling) which is based on the principle that the collision density $\Sigma_t \Phi$ can be obtained as a geometrical series that describes $n \to \infty$ consecutive scattering events:

$$\Sigma_t \Phi = S \sum_{n=0}^{\infty} (\frac{\Sigma_s}{\Sigma_t})^n = \frac{\Sigma_t}{\Sigma_t - \Sigma_s} S \tag{2.32}$$

Another crucial aspect of the Monte Carlo method is the definition of how the available data is interpolated. Generally, it is a statistical interpolation, meaning that if distributions

of produced particles are given at 1 MeV and at 1.5 MeV (incident neutron energies) and the incident energy is 1.3 MeV:

1. A pseudo-random number ζ between 0 and 1 is sampled
2. Calculation of $\xi = \frac{1.3-1}{1.5-1} = 0.6$
3. If $\zeta \leq \xi$ the distribution of 1.5 MeV is chosen, and if $\zeta > \xi$ the distribution of 1 MeV is chosen
4. The sampling is done in the chosen distribution

2.3.2 Monte Carlo of CEA : TRIPOLI-4®

TRIPOLI-4® is a continuous-energy Monte Carlo transport code used for reactor physics evolution (particles in multiplying media, for critical or sub-critical systems, with or without fixed sources, under steady-state conditions), shielding (particle propagation over long distances with many orders of magnitude of flux attenuation), criticality safety and nuclear instrumentation. It relies on the stochastic behavior of particles as its mean for simulating physical systems and estimating macroscopic quantities. In this sense it can be considered as a reference simulation, as there are no approximations compared to a deterministic approach, so the results of the latter should always be compared to those of the former. However, it requires very good statistics, which in turn makes it very time-consuming. The code currently simulates the transport of neutrons, photons, electrons, and positrons.

It differs from earlier versions in that it has been completely rewritten in more recent programming languages (C and C++), with more complete descriptions of geometrical elements (surface-based and/or combinatorial geometries) and more precise representations of basic nuclear data (point-wise representation of cross-sections, although the code also allows multi-group homogenized cross-sections).

The basic workings of the particle simulation process consist in assigning a random value for its path length s: the path between the moment it is emitted and when it disappears. In this way its so-called history is constructed, which will be guided through the phase space $(\vec{r}, E, \vec{\Omega})$ determined by the geometry and composition of the system. In a homogeneous medium, the probability density function for the propagation of neutrons is

$$f(s) = \Sigma_{tot}(E) e^{-\Sigma_{tot}(E)s} \tag{2.33}$$

which multiplies Σ_{tot}, the probability of interaction between the neutron and its target at energy E, by the probability $e^{-\Sigma_{tot}(E)s}$ of traveling a distance s without collision. A random number ξ is uniformly selected between 0 and 1 to determine the path length s as follows

$$s = -\frac{1}{\Sigma_{tot}} \ln(1 - \xi) \tag{2.34}$$

Convergence of results can only be reached when enough points of the phase space have been explored. In other words, neutrons have to interact many times with the medium, which also means that the number of histories N has to be such that the standard deviation, which is proportional to $\frac{1}{\sqrt{N}}$, is of the order of a few pcm ($=10^{-5}$), as required for

reactor simulations. Another aspect to bare in mind is that the outgoing channel of some interactions has more than one particle, and typically the way to acknowledge such events is by giving a *weight* to each history, depending on the number of particles that need to be dealt with.

The current nuclear evaluations present averaged quantities, for example $\nu = 2.45$ neutrons emitted after a fission event. This means that one neutron history is simulated provoking a fission event, and all the parameters of the neutron produced by the fission are multiplied by 2.45. After a sufficiently large number of simulated histories, this shortcut is actually representative of reality as the phase space is explored thoroughly. This aspect is fundamentally different in the analog simulation where the weight is always exactly 1, so there is no longer a need of relying in large number of histories to find the expected values of a particular interaction, in addition to having accurate events that allow correlation of particles and energy conservation. However, for a same variance compared to the non-analog simulation the cost of the former is more calculation time.

The **ANALOG** option in TRIPOLI-4® enables to perform a fully analog simulation regarding collisions and transport between collisions. It cannot be used with criticality calculations and only **NEUTRON** or **PHOTON** are allowed as particle type for this option but both cannot be used together since analog photon production induced by neutron interactions is not available yet. However, when the evaluation contains MF=12, photon transport is already analog in the case of inelastic scattering, hence the **ANALOG** option does not need to be added. What is expected from this alternative way of simulating particles is that every event that induces inelastic scattering should conserve energy and explicitly show particle correlation, contrary to non-analog simulations where the electromagnetic shower is accounted for by assigning a non integer weight to the photon histories.

2.3.3 Monte Carlo of JAEA : PHITS

The Particle and Heavy-ion Transport code System (PHITS) [12] developed by the Japanese Atomic Energy Agency is a Monte Carlo code used in the framework of this thesis for studying the impact of the nuclear data files by means of measuring the accuracy of nuclear reaction simulations. Particularly in the domain of secondary particle emissions - meaning particles that were not present in the initial state of the system and are found in the exit channel of various types of reactions - PHITS is used here to analyse the characteristics of the reaction processes and outcomes. The resulting emitted particles require additional considerations in terms of energy conservation, angular distributions and correlations. A better handling of these considerations is necessary to improve the accuracy of nuclear physics simulations, in particular those that need event-by-event analysis.

PHITS is chosen for our analyses to make use of its new theoretical model to simulate gamma de-excitation of excited nuclei called EBITEM (ENSDF-Based Isomeric Transition and isomEr production Model)[1]. It is developed based on the Evaluated Nuclear Structure Data File (ENSDF), supplementary evaluated data tables, and theories. In the model, reaction products after nucleon evaporation are de-excited by using theoretical calculations if the excitation energy is higher than 3 MeV and the mass number is greater than 40 atomic mass units (A>40). Otherwise, the nuclei are de-excited based on the scheme provided in the ENSDF. Thus by tracking nuclear de-excitation, production of prompt gamma-rays and isomers can be simulated. A description of this algorithm can be found on Figure 2.9.

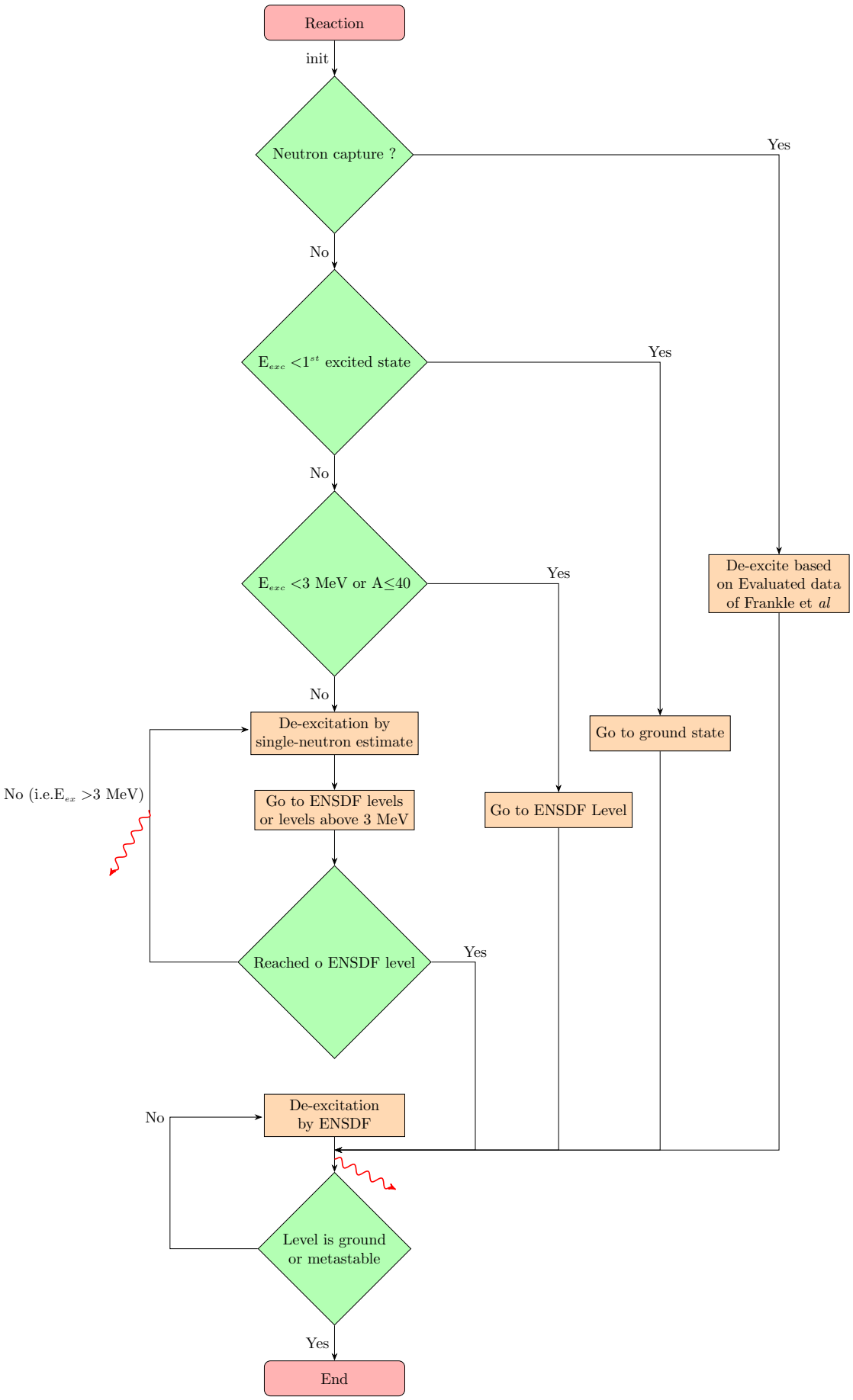

Figure 2.9: Algorithm of EBITEM. E_{ex} and A denote the excitation energy and mass number, respectively. Flow chart taken from ref. [1].

The model is applicable for neutron capture products and spallation products of 1071 nuclear species from lithium to berkelium and works as an event generator that explicitly tracks the transition between excitation levels. For both neutron capture reactions and spallation reactions, production of isomers and prompt gamma-rays are reproduced with reasonable accuracy by using EBITEM. Although some of the gamma-ray peaks not included in ENSDF are not reproduced, the peaks and continua of gamma-ray spectra are well predicted. The possibility to activate the event generator mode is what makes it possible to ensure all the PHITS simulations of interest in this work are analog.

Prior to the implementation of EBITEM, PHITS adopted a combination of a very simple nuclear de-excitation model and an event generator model [24]. An alternative method is to transport particles based on evaluated nuclear data instead of using event generators. The disadvantage of the nuclear-data-based method is that correlations between particles are not considered, thereby energy and momentum conservation in each event are not satisfied. Moreover, production of isomers was not considered because meta-stable states are generally below excitation energies of 1000 keV and no theoretical models are valid to precisely predict level structures in this energy range.

The methodology created for PHITS to handle nuclear data is to store all possible information not found in the evaluations regarding the isotopes within the source code. For example, in the list of PHITS compilation files, one can find *gammod3.f* where the energies in keV of the excited states are stored in vectors such as

$$\text{elevel13027} = (/0., 843.76, 1014.56, 2212.01, 2734.9, 2982.,...$$

which corresponds to the first few excited states of ^{27}Al, and this particular vector contains 245 entries, taken from ENSDF, compared to the maximum of 40 excited states that can be declared in the evaluated data. Moreover, in *gammod4.f* are stored the number of possible decays per excited state in the vector called *ndch*, and also the energies of the transitions in vector *egam*. In *gammod5.f* one finds vector *nlev* which indicates the arrival state post photon emission, and in *gammod6.f* are stored the vectors *brat* containing the branching ratios (or probabilities) of the gamma emission. Naturally, the size of *elevel* and *ndch* are the same because each of the entries of *ndch* describes each of the entries of *elevel*. The same goes for vectors *egam*, *nlev* and *brat*: they form a bijection that follows the order of the entries. The combination of these vectors contains sufficient information to create a game of chance that reproduces the gamma cascades using a Monte Carlo algorithm.

In terms of the evaluated data, it is also stored within the code in the ACE format. The default nuclear library of PHITS is of course JENDL-4.0, however it is possible to add an ACE file created from another library. This was done for this work to estimate the impact of data modifications.

3 - Implementation of analog and non-analog inelastic neutron scattering simulations in TRIPOLI-4® using excited nuclear states and transition probabilities as input data

3.1 Brief description of the neutron-induced inelastic scattering and its associated nuclear data

The objective of this chapter is to establish the impact of two nuclear data representations (or formats), that will be named hereafter MF=6 (concerning non-analog simulations) and MF=12 (concerning analog simulations) on the simulation of photons emitted from inelastic neutron scattering events, particularly with regards to the conservation of energy per reaction and the order of emission that can be expected in a given gamma cascade. In the non-analog case, the input data requires the declaration of a particle weight, or photon yield, that will be associated to the photon sampled from the declared transition probabilities. In the analog case, the input data must declare all the known transition probabilities associated to each excited state, allowing the transport code to implement a game of chance that reproduces the gamma cascade by going through the sections until the ground state is reached.

The ENDF-6 format [19] allows the declaration of up to 40 excited states for both MF=6 and MF=12, and the information regarding each excited state can be stored in sections MT=51 to MT=90, ordered in increasing energy. In MF=6, each section declares all the possible photon energies that could potentially be emitted during an electromagnetic cascade that starts from the energy state of the section in question. However, only one photon energy is sampled for the inelastic neutron scattering event simulated by the transport code, and the photon yield Y_γ affected to the section - which in general is a non-integer value - artificially increments the counter of the simulated photon energy by Y_γ. As a large number of events are simulated, the average energy of the simulated photons equals the available energy of the reaction. In MF=12 on the other hand, each section contains only the excited states that can be reached by decay of the excited state of the section in question, and the associated transition probabilities. In this way, every photon that is sampled per section has a weight of exactly one, and a realistic cascade is simulated at each reaction event, which implies that energy is conserved for each neutron interaction. However, contrary to MF=6, MF=12 does not allow center of mass frame considerations by construction of the format, and these corrections become noticeable for nuclei with low mass, so both data representations present the shortcomings of either no correlations between photons (MF=6), or imprecise kinematical results (MF=12).

This chapter starts with a short overview of the possible decay channels that can be simulated in the case of neutron interactions capable of bringing nuclei to their excited states, then a summary of the available data concerning the neutron inelastic scattering is given. Then, a particular focus on the case of ^{27}Al(n,n'γ) is presented to illustrate the main differences of analog and non-analog Monte Carlo simulations implemented with the transport code of the CEA, TRIPOLI-4® [5], followed by a comparison of the analog

simulation implemented with the transport code of the JAEA, PHITS [12], with a focus on the kinematics of the reaction. The chapter concludes with the report of the created MF=12 of this PhD and the perspectives for further improvement of analog simulation capabilities.

3.2 Decay of an excited state

When a nucleus is in an excited state, there are several options to dissipate its available energy. It can be through the emission of a photon, an electron, emission of neutron if the excitation energy is higher than the neutron separation energy $E_{exc} > S_n$ (for ^{19}F S_n=10.43 MeV), emission of proton if $E_{exc} > S_p$, alpha emission if $E_{exc} > S_\alpha$, etc. ^{12}C can even decompose in 3 α particles if $E_{exc} > 7$ MeV.

For the inelastic reaction there is always an outgoing neutron and most of the time, photons are emitted from the recoil excited nucleus, the competing process being internal conversion. Photon transitions are labeled E1, E2, M1, M2 (the solutions of equation 2.5) according to the type of decay they bring to the excited nucleus. E stands for electric transition, M stands for magnetic transition, and 1 and 2 are the angular momenta J carried by the photon, which correspond to $\Delta J = |J_f - J_i|$ of the final and initial states. For electric transitions, parity $\pi(E, \Delta J) = \pi_f \pi_i = (-1)^{\Delta J}$ and for the magnetic transitions $\pi(M, \Delta J) = \pi_f \pi_i = (-1)^{\Delta J+1}$. Thus, parity does not change for E-even or M-odd transitions, while it changes for E-odd or M-even transitions.

Photons have extremely low chance of bringing an excited state to a lower one if the difference in angular momentum of the two states is zero, or if it is larger than or equal to 3, and in such cases, other decay modes such as internal conversion are favored.

3.3 Evaluated data for inelastic reactions

Inelastic scattering is a particularly important reaction to take into account when modeling nuclear systems. It is a threshold reaction which, depending on the nuclei, can start above a few keV for the heaviest nuclei and a few hundreds of keV for the lightest nuclei. These reactions are characterized by a transfer of the kinetic energy of the incident neutron into excitation energy of the target nucleus. The latter is then in an excited state. One can thus consider it is a two-body reaction on the outgoing channel: scattered neutron and excited nucleus. As previously mentioned, the knowledge of the kinematics of the scattered neutron in the CM reference frame allows to reconstruct the kinematics of the recoil nucleus and the neutron in the LAB reference frame. In the first ENDF/B and JEFF libraries, the evaluations contained these angular distributions, however, there was not systematically the decay data of the excited states by photon or electron emission.

In the context of inelastic scattering that brings a given nucleus to a discrete state, the most complete description with respect to the ENDF-6 format is the use of MF=12 which allows to define the different probabilities of the emission of the first photon from the excitation state reached. The ensuing transitions are systematically towards lower energy states compared to the initial state reached. These can be the ground state or excited states of lower energy. Additionally, in MF=12 there can also be information on the alternative channel in competition with photon emission: parameters LO=2 with LG=2 make it possible to introduce conversion electrons, which are electrons in low-lying

electronic orbitals that can be knocked-out by the excitation energy of the nucleus. It is also possible to declare primary photons using the flag LP=2 where the photon energy EG'_k is given by

$$EG'_k = EG_k + \frac{AWR}{AWR+1}E_n \tag{3.1}$$

where EG_k is the γ energy of transition k and AWR is the mass of the nucleus in neutron mass units.

One caveat of MF=12 is that there is no indication of the reference frame in which these photons are emitted, so CM considerations for photon emission are not possible yet using this file.

Another method is to use MF=6, which allows to describe all the products of a reaction and also take into account the possible CM frame corrections. In the case of interest here, there is a dedicated section for the neutron, another for photons and one for the recoil nucleus (not always). The MF=6 format allows to choose the reference frame in which the particles are emitted. For this reason, it is possible in the case of the choice of the LAB frame to give the energy distribution of neutrons. In the case of photons, information is given on the photon yield as a function of the incident neutron energy. Then, for a series of incident energies, one finds energy distributions, possibly coupled to emission anisotropies. These energy distributions are themselves split between a discrete spectrum (associated with a probability for each line) and a continuous distribution with probability densities. The sum of the discrete probabilities and the integration of the continuous spectrum is normalized to 1. The interest of the double discrete and continuous description allows a good management of the discrete lines which could be *drowned* in a continuous spectrum when the spectrum has to be interpolated between two energies. This point will be further explained later. In the case of scattering towards discrete states, only discrete lines are declared with a sum of discrete probabilities normalized to 1. This information does not allow to define a temporal order in the emission of photons and does not allow to reconstruct a decay pattern.

As an illustration of the representation of the aforementioned data, here are presented the steps taken for the example of ^{27}Al. First, according to ENSDF data, the first three excited states of the nucleus are represented schematically on Figure 3.1.

The horizontal lines represent the energy states, on the left-hand side are their spin-parities, on the right-hand side are their energies (in keV) and average lifetimes. The vertical arrows correspond to photon emissions, and point to the state the nucleus would decay into if that photon was emitted. Above the arrows are indicated the energies (in keV), the types (E or M) and the intensities of the transitions to lower-lying states. The second excited state at 1014.56 keV, declares two possibilities: either the decay brings the nucleus into its ground state, or into the first excited state. The most probable event is the decay into the ground state, which is why the intensity is set to 100. The other possibility is the decay into the first state with a probability of $\frac{3.05}{3.05+100.0} = 0.02959728$, followed by the decay of the first excited state into the ground state. This data regarding the second excited state can be stored in MF=12, MT=52, of JEFF-3.3, as shown on Figure 3.2.

The previous text can be read from the top left to the bottom right as follows: the nucleus has Z=13 protons, A=27 nucleons, which for all isotopes is stored via Z×1000+A, then the nucleus is 26.74975 times more massive than the neutron, the 2 indicates that the file is to be understood as a transition probability array, the 1 that all transitions are

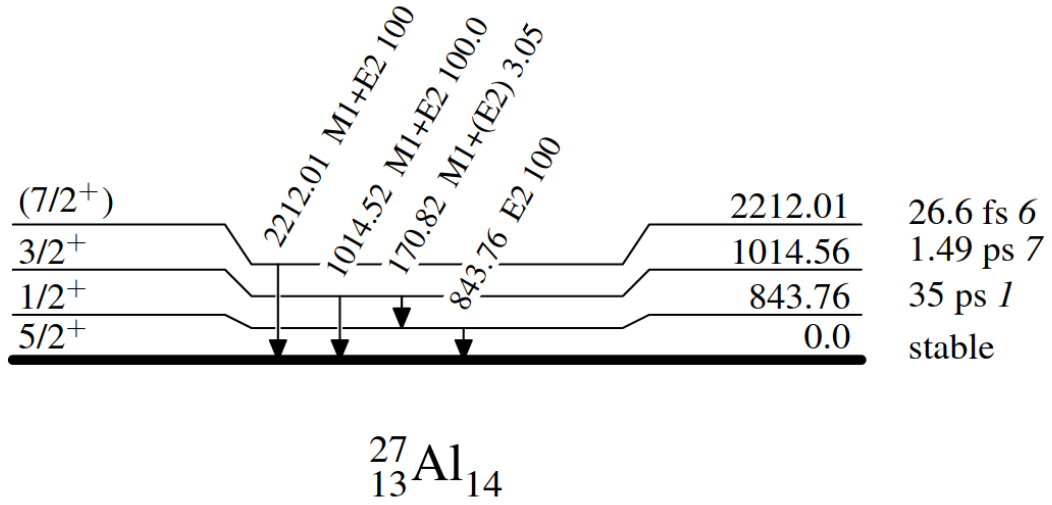

Figure 3.1: First three excited states of ^{27}Al according to ENSDF.

```
13027.0000 26.7497500          2          1          2          0132512 52    1
1.014450+6 0.000000+0          0          0          4          2132512 52    2
8.437500+5 2.959728-2 0.000000+0 9.704027-1                      132512 52    3
                                                                 132512  099999
```

Figure 3.2: Section MT=52 of file MF=12 of ^{27}Al from the JEFF-3.3 library.

γ emissions (and not other competing processes like conversion electrons), the 2 is the number of levels below the present one (including the ground state), and the 0 is there by default. 1325 is the MAT code for ^{27}Al, 12 refers to MF=12, and 52 to the second excited state, MT=52. 1, 2, 3 on the right column are the line numbers. On line 2 is written the level energy of 1.01445×10^6eV and on the third line it can be read that there is a transition into the 8.4375×10^5eV level with a transition probability of 2.959728% (which corresponds to the probability found in ENSDF) and another transition to the ground state with 97.04027%. If this information is coupled to angular data stored in MF=4 and 14, it is possible to perform a full analog simulation of the decay of the excited state.

MF=6 on the other hand can be built from the information of MF=4, 12 and 14, but it is not adapted to analog simulations because information is condensed in the MF=6 format, in other words, information would be lost if MF=12 was translated into MF=6. The information on the second excited state of ^{27}Al stored in MF=6, MT=52, of JEFF-3.2, is shown on Figure 3.3.

The value on line 48, second column, indicates to the transport code that this level yields a multiplicity of 1.029 photons:

$$1.029 = 1 \times 0.97 + 2 \times 0.029$$

This comes from the fact that 97% of the decays go to the ground state, so 1 photon, and in the remaining 2.9% of events, 2 photons are produced. As a result, file MF=6 allows in 3% of cases the emission of one 843 keV photon with a weight of 1.029 that comes from the second excited level without first the emission of the 171 keV photon that would be necessary prior to the 843 keV photon. The correlations within the cascades are thus lost.

```
1.302700+4 2.674975+1          0          4          1          21325 6 52   43
         2          2                                                1325 6 52   44
1.052374+6 1.000000+0 1.500000+8 1.000000+0                         1325 6 52   45
0.000000+0 0.000000+0          0          1          1          21325 6 52   46
         2          2                                                1325 6 52   47
1.052374+6 1.029000+0 1.500000+8 1.029000+0                         1325 6 52   48
0.000000+0 0.000000+0          1          2          1          21325 6 52   49
         2          2                                                1325 6 52   50
0.000000+0 1.052374+6          3          0          6          31325 6 52   51
1.014450+6 9.436346-1 8.437500+5 2.818270-2 1.707000+5 2.818270-21325 6 52   52
0.000000+0 1.500000+8          3          0          6          31325 6 52   53
1.014450+6 9.436346-1 8.437500+5 2.818270-2 1.707000+5 2.818270-21325 6 52   54
0.000000+0 0.000000+0          0          0          0          01325 6  099999
```

Figure 3.3: Section MT=52 of file MF=6 of ^{27}Al from the JEFF-3.3 library.

The information in MF=6 can be constructed using MF=12. Indeed, in MF=6 it is indicated on line 54, second column, that 94% of decays point to the ground state (the first column indicates the photon energy), and the 94% value can be obtained using the multiplicity of the state and the probabilities of emission:

$$0.94 = 0.97/1.029$$

This result in term *forces* the other two emissions to *share* the remaining 6%, because if the 171 keV photon is emitted, the 843 keV needs to be emitted as well (this would correspond to a *realistic* two-step decay). The fact that MF=6 can be built using MF=12 applies to all isotopes, and this redundancy means that an evaluation with MF=12 cannot have MF=6.

3.3.1 MF=12 creation for evaluations that only have MF=6

Each excited state of the nucleus has a probability of being reached through neutron inelastic scattering, and so each state has an associated probability distribution function (pdf) that depends on the energy of the incoming neutron, as shown for the ^{27}Al example on Figure 3.4, where the end at 20 MeV is artificial. The functions are discretized and stored in MF=3, where the pdf of the excited states can each be found from section MT=51, for the first state, to MT=90 for the 40^{th} state. MT=91 is reserved for the continuum inelastic scattering, which accumulates the possible gamma emissions coming from states of higher energy than the 40^{th} state, in addition to the continuum, where states are so energetically close that experiments cannot tell them apart; therefore density functions in #states.MeV^{-1} are used. It can be observed in Figure 3.4 that the inelastic cross sections have a threshold energy, a maximum of probability a few keV above the state energy for the center-of-mass considerations, and that MT=4 is the sum of the cross sections MT=51→91. The MT=4 probability distribution function is normalized to 1 according to the neutron incident energy so that the sampling of a pseudo-random number can determine which state is reached. Then, once the neutron has brought the target to an excited state, there is an electromagnetic shower that follows, where the emission of the photons is determined by transition probabilities.

The cascades can be stored in files MF=6 or MF=12 and have to be consistent with MF=3. This is to say that if MF=3 stops at the fifth state, or MT=55, the information in MF=6 or MF=12 also ends at MT=55, in addition to the necessity that all excited state

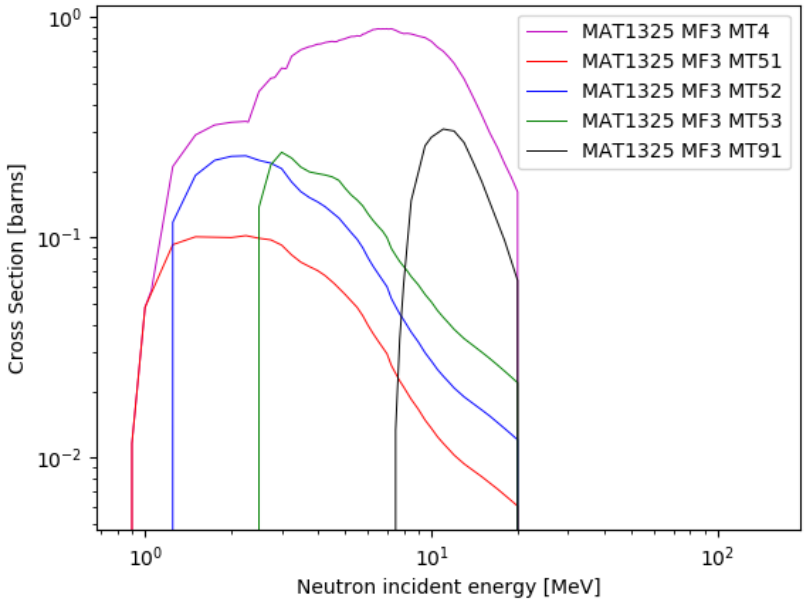

Figure 3.4: Neutron inelastic scattering cross section of ^{27}Al from the JEFF-3.3 library.

energies must match exactly between MF=6 (or MF=12) and MF=3. Another constraint is that for all the intermediate decays there must be a one-to-one correspondence with the levels of MF=3, meaning that emitted photons that do not bring the nucleus back to the ground state need to bring the nucleus to a level defined in MF=3.

If the focus is on the energetic levels themselves and their associated probabilities of photon emission, MF=12 is more suited than MF=6 for storing the complete decay scheme. This is because MF=12 provides the information required to construct the averaged gamma emission probabilities in MF=6. The reverse is false because MF=6 contains averaged quantities (mean number of photons produced per state) and indicates the possibility of decays to all intermediate levels, contrary to MF=12 where all levels and probabilities are explicitly there to enable an analog treatment of (n,n'γ) and the correlations are established as the scheme for all levels is respected. The information for photon cascades can be found in the RIPL-3 library, a database that contains the energetic structure of the nuclei, the energy of the excited states and all the possible photons that can be emitted. This nuclear structure data is transcribed in the framework of this thesis for the JEFF library in the ENDF-6 format of MF=12 to implement analog simulations of inelastic scattering.

Once the steps of writing a MF=12 are complete, it is assumed that the photons are emitted isotropically, as the angular dependence of photon emission with respect to the angle of incidence of the neutron should be small or null. In any case, an evaluation file with MF=12 must also contain MF=14, in which the data indicates to the transport code the angle of the outgoing photons (isotropic in the case of interest here). Yet again, MF=14 must be divided in the same number of sections as MF=3 and MF=12, so that there is always a one-to-one state correspondence.

The procedure undertaken by TRIPOLI-4® in the case of an inelastic reaction event

is the following:

1. Determine the excited state reached according to the MF=3 probabilities,
2. Read the section in MF=12 that corresponds to the current state to sample a γ transition,
3. If the ground state is not reached, repeat step 2.

In the case of MF=6, if the transport code initiates an inelastic reaction simulation, the excited state will be also determined by the MF=3 probabilities but the difference is that the MF=6 section that describes the state will result in the emission of only one photon: in terms of the outcome, the energy bin that corresponds to the photon will be lit and the standard deviation associated to the energy bin will decrease according to the multiplicity declared in the MF=6 section.

3.3.2 Heterogeneity of data between ENDF and JEFF

It was observed in the course of the PhD that the data found in ENDF and ENSDF, mainly the precision in the value of the state energy and even its existence, is not fully compatible with that of JEFF. Indeed, the libraries of the United States and Europe are bound to differ slightly as they are constructed from the experimental data gathered by their respective laboratories. Additionally, a data library such as ENSDF is constructed by following a critical review of all available experimental data, thus adopting a maximum amount of data, which is bound to differ significantly with respect to any limited data set, for example the declared excited states of a given evaluation file in the JEFF library.

In the beginning of this study, the construction of MF=12 for the JEFF library from the ENSDF data was attempted and proved to be more challenging than with the RIPL library. Another difficulty for the experimentalists and the data evaluators are the excited states and transitions associated to and from them, that are expected to occur as suggested by the experiments and nevertheless the detection of such transitions is indicated as uncertain in the data. The existence or not of a single transition can create or dismiss a number of possible decay schemes.

3.3.3 Simulation of photon emission from nuclear state transition

In the beginning of the PhD, the evaluation of ^{27}Al - a nucleus extensively studied in material irradiation experiments, which should result in very coherent data between ENSDF and JEFF - was used as the control case, by means of checking if the method for writing MF=12 produces the same file as that of the JEFF-3.3 evaluation. The comparison between the reference file in JEFF and the file that was written extracting data from ENSDF yields small differences in the values of the transition probabilities, as well as some discrepancies regarding the number of photons that may be produced per excited level. Regardless, the overall result produced using ENSDF was considered in accordance with the information provided by JEFF when small corrections are brought. Nevertheless, for the other studied isotopes the use of the RIPL-3 database is more suited to the JEFF data.

Methodology

The simulations implemented in TRIPOLI-4® for studying the impact of the data format (MF=6 versus MF=12) on the outcome of the inelastic reaction on the control case of

^{27}Al consisted each of one single 5 MeV neutron per batch (TRIPOLI-4® accumulates the measurements set by the user in each batch), emitted isotropically from the center of an aluminium sphere of 50 cm radius. The batch - in this case identified with the neutron history - starts with the emission of one neutron at the origin, and ends when its kinetic energy goes below the E_{inf} imposed by the user, which in this case is 4.99 MeV to ensure that the neutron interacts only once per batch. During this process, photon energies are measured by means of detecting their emission in a given energy bin (hence the energy grid must be tailored to each nucleus so to distinguish between its levels). This can be done with the TRIPOLI-4® response **PRODUCTION PHOTON FROM NEUTRON SECONDARY_SPECTRUM** and the creation of a .xml output file allows to have explicit information of each batch.

Once the photon production spectra of both MF=6 and MF=12 simulations are verified to be coherent, in order to observe the photon correlations that should appear from the decay of the excited state to the ground state, one can produce a histogram that shows the number of times a given energy was the result of the sum of all photon energies produced from one neutron history. If one batch indicates the production of more than one photon, the sum of the energies should correspond to the energy of the excited state from which the photon cascade started. This in turn implies that the multiplicity of photons is another aspect that allows the comparison between the simulations; it is expected that MF=6 produces one photon per batch, and MF=12 should produce more than one photon on average considering all batches (one neutron can produce a single photon that brings the excited nucleus directly to the ground state, in which case the photon yield is one for both MF=6 and MF=12).

Results

The MF=12 written for this verification process from the ENSDF library being the same as the MF=12 found in the JEFF-3.3 evaluation, the two TRIPOLI-4® simulations (using either MF=6 or MF=12) yield the same production spectrum in terms of presence of photons (the lit bins in both output files are the same) but not in terms of the intensities as shown on Figure 3.5. However, it was calculated that the integration over the energy range of both spectra is the same (due to the width of the peaks of MF=6), *i.e.* total energy is conserved on average in both cases, so one can consider that the two spectra are coherent, yet not identical.

With regards to the correlation between the emitted photons, one can observe in the histogram of Figure 3.6 that a given number of neutron histories produced 1.72 MeV of total photon energy within the MF=6 simulations (the presence of this photon can be seen in Figure 3.5 on both MF=6 and MF=12 simulations). However, the peak of 1.72 MeV is absent in the MF=12 case on Figure 3.6. This is because the 1.72 MeV photons are only produced in the decay from the fourth excited state at 2.735 MeV, to the second state at 1.015 MeV. Then, state 2 decays to the ground-state in two possible ways, producing a total photon energy of 1.015 MeV in both of them. Thus, the transition 4→2 of 1.72 MeV is accumulated in the 2.735 MeV channel in the case of MF=12 in Figure 3.6 because of the *inevitability* of the transitions 4→2→0 or 4→2→1→0. One can conclude that the use of MF=12 produce *realistic* photon cascade events from neutron inelastic scattering.

With regards to the photon multiplicity, it was found that the average number of photons produced per batch using MF=12 is 1.28, whereas MF=6 yields 1.00, as reported

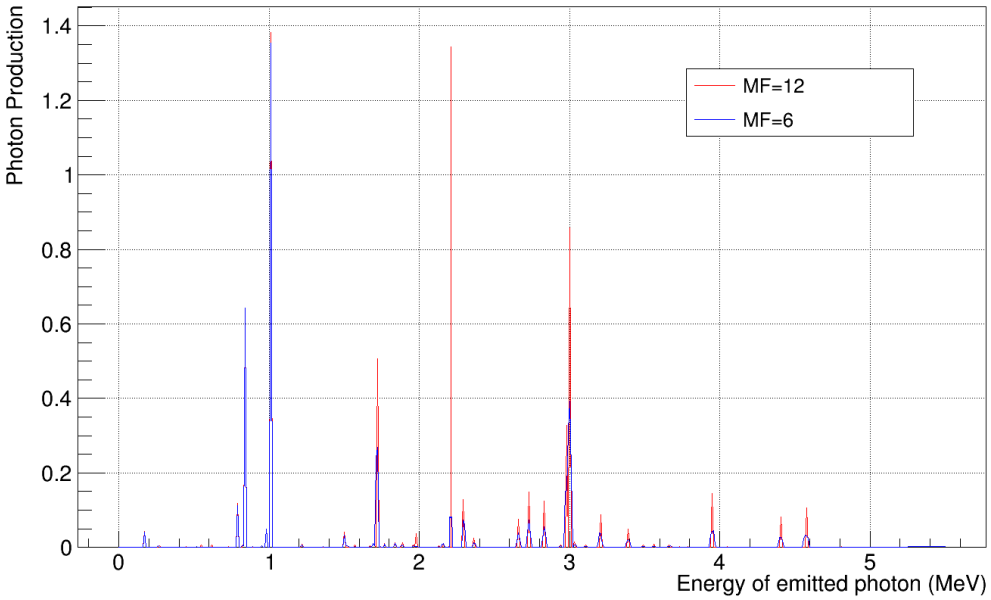

Figure 3.5: Photon production spectrum from TRIPOLI-4® simulations of neutron inelastic scattering onto a ^{27}Al target.

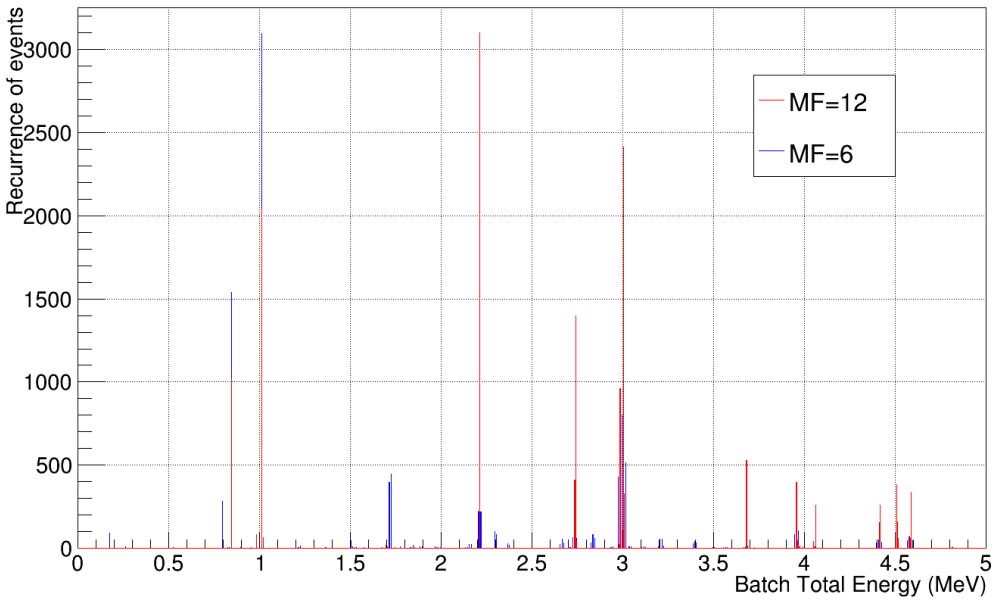

Figure 3.6: Histogram of photon production from neutron inelastic collisions onto a ^{27}Al target. Batch Total Energy is the accumulated energy of photons produced by one neutron in one batch.

on Table 3.1. The quantities obtained for both simulations are as expected: the objective of MF=12 is to enable the code to transport various individual photons that would physically

Average γ production in ^{27}Al(n,n'γ) events	
MF=12	1.28
MF=6	1.00

Table 3.1: Photon multiplicity in inelastic scattering simulations implemented in TRIPOLI-4®

be produced in an event of inelastic scattering, as opposed to MF=6 which produces *only one* particle (in the sense of only one energy bin per batch with a non-zero value) to be emitted with a calculated weight to reach the conservation of total energy as explained previously for variance reduction techniques. However, for simulating experiments that rely on counting photons such as detectors, or more generally in event-by-event analysis of particle interactions, there are corrections that need to be brought to the evaluations as well as to the transport codes to achieve the most realistic simulation possible. Indeed, MF=12 allows the simulation of the cascades but does not simulate the expected spread of energies that appears in the MF=6 case, which accounts for the Lorentz boost, i.e. if the photon is emitted in the same orientation as the momentum of the nucleus that emits the photon, in the LAB frame the photon will appear as more energetic than the transition energy. The transition energy is the energy of the photon in the center of mass of the nucleus that emits it.

Further analysis

An important aspect to notice in Figure 3.5 is the difference in width, or *spread* of the peaks, between MF=6 and MF=12. A zoom of the previous spectrum around the emission peak that corresponds to the third excited state of ^{27}Al at 2.21 MeV is shown on Figure 3.7 as an illustration. It can be observed that the case of MF=6, there is a spread around the state energy as this data format takes into consideration the Lorentz boost, as the data is given in the CM frame, as opposed to that of MF=12 which is given in the laboratory system. The third excited state of ^{27}Al decays 100% to the ground state, which simplifies the kinematical analysis.

For the calculation of the kinematical limits of photon emission around the energy of an excited state (shown as vertical lines in Figure 3.7), one defines the total energy in the CM of the system *Excited nucleus* Al* (without including the neutron) as

$$E_c = E_{Al^*c} = M_{Al} + e = M_{Al*} \tag{3.2}$$

where e is the excitation energy and c indicates that the value is given in the CM system.

Knowing that the TRIPOLI-4® output energies are by default given in the laboratory system, the sought after photon (γ) energies can be computed as follows

$$E_\gamma = \gamma_{Al^*} E_{\gamma c}(1 + \beta_{Al*} \cos\theta_c) \tag{3.3}$$

where $E_{\gamma c}$ is the energy of the photon emitted in the CM of ^{27}Al*, it is the energy declared in the structure data, and $\gamma_{Al^*} = (1 - \beta_{Al*})^{-1/2}$.

Equation 3.3, on account of the cosine function, *forces* the energy of photons to have a maximum value when the angle of emission is in the same orientation as $\vec{P}_{Al^*c}$ and a

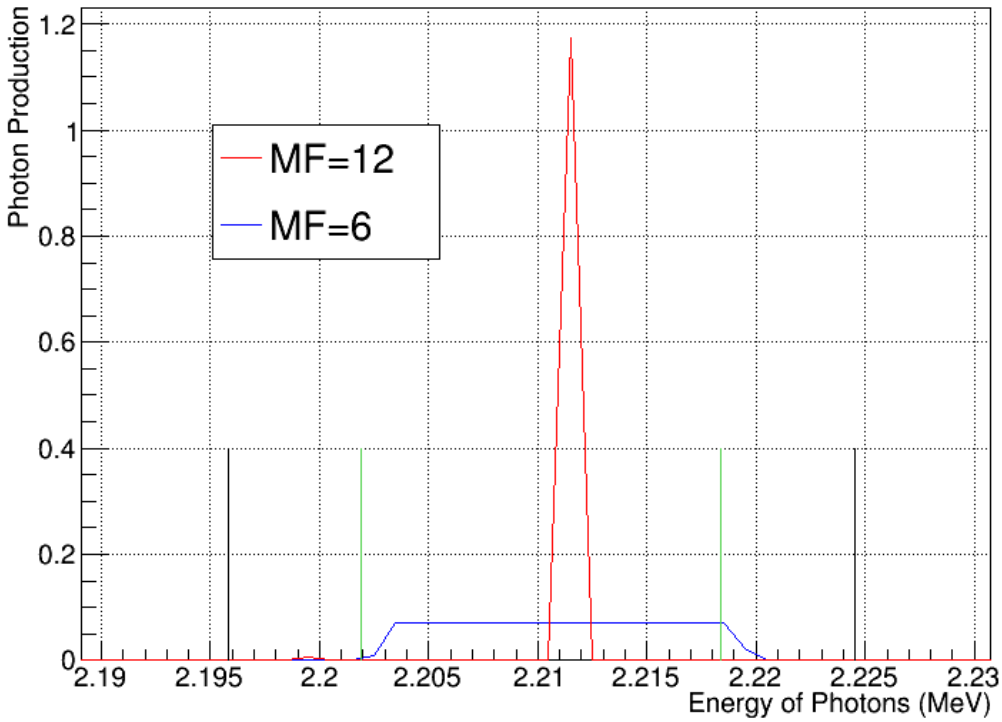

Figure 3.7: Photon production from the third excited state of ^{27}Al which decays to the ground state.

minimum value for emission in the opposite direction. These values are indeed measured in the laboratory frame with homogeneous intensity due to the declared isotropy of emission angles in the data.

The quantitative analysis is as follows: the conservation of energy of the two steps in expression (6) for the case of aluminum can be written in the laboratory system:

$$E_{tot} = T_n + M_n + M_{Al} = T'_n + M_n + M_{Al^*} + T_{Al^*} \tag{3.4}$$

where $T_n = T'_n + T_{Al*} + e$ and $M_{Al*} = M_{Al} + e$.
The speed β of the systems n+Al and n'+Al* is given by

$$\beta = \frac{\sum P}{\sum E} = \frac{P_n}{E_{tot}} = \frac{\sqrt{T_n^2 + 2M_nT_n}}{T_n + M_n + M_{Al}} \tag{3.5}$$

The total energy in the CM is then

$$E_c = \frac{E_{tot}}{\gamma} = E_{tot}\sqrt{1-\beta^2} \tag{3.6}$$

which gives the energy of the outgoing particles in the CM

$$E_{n'c} = \frac{E_c^2 - M_{Al*}^2 + M_n^2}{2E_c} \tag{3.7}$$

$$E_{Al^*c} = \frac{E_c^2 + M_{Al*}^2 - M_n^2}{2E_c} \tag{3.8}$$

and the momenta in the CM

$$P_{n'c} = \sqrt{E_{n'c}^2 - M_n^2} \tag{3.9}$$

$$P_{Al^*c} = \sqrt{E_{Al^*c}^2 - M_{Al*}^2} \tag{3.10}$$

Then, the Lorentz transformation

$$\begin{pmatrix} E_{Al^*} \\ P_{Al^*} \end{pmatrix} = \begin{pmatrix} \gamma & \beta\gamma \\ \beta\gamma & \gamma \end{pmatrix} \begin{pmatrix} E_{Al^*c} \\ P_{Al^*c} \end{pmatrix} \tag{3.11}$$

allows the calculation of the speed of ^{27}Al* in the laboratory system through the following relation

$$\beta_{Al*} = \frac{P_{Al*}}{E_{Al*}}. \tag{3.12}$$

As such, all the values needed for calculating E_γ in equation 3.3 having being computed and using the JEFF-3.3 value of $e = 2.2111$ MeV as the energy of the third excited state of ^{27}Al, the numerical application yields:

$$2.1969 \text{ MeV } < E_\gamma < 2.2254 \text{ MeV} \tag{3.13}$$

These kinematical limits are shown as black vertical lines in Figure 3.7 and it can be seen that the spread of possible values for the photon energies that is too wide to explain the observed spread of the results using the MF=6 format.

If the calculations for photon energy in the LAB are performed considering that the CM of the system (^{27}Al*) is the same as the CM of the system (^{27}Al* + neutron), *i.e.* instead of using β_{Al*}, β is used as follows

$$E_\gamma = \gamma E_{\gamma c}(1 + \beta \cos\theta_c) \tag{3.14}$$

then the extreme values of the photon energy are

$$2.2029 \text{ MeV } < E_\gamma < 2.2193 \text{ MeV} \tag{3.15}$$

represented as green vertical lines in Figure 3.7, which suggests that the code does not shift the CM to the excited nucleus, but rather keeps the information of CM of the system (neutron + aluminium).

The handling of photon production with respect to the reference frame is further checked with the transport code of the U.S.A. Monte Carlo N-Particle (MCNP). Its results do not present any noticeable spread regardless of the evaluation used, which could imply that the center of mass effects are not taken into consideration in the code during the simulation of this particular reaction. Indeed, using the MF=6 in ENDF/B-VII.1 or the MF=12 in JENDL-4.0, production of photons from the third excited state in MCNP simulations takes into account only the state energy, and not the Doppler effect introduced by the center of mass; an equivalent situation to that of the TRIPOLI-4® simulations

that relied on MF=12. The two peaks are shifted from each-other because JENDL defined this level at 2.21 MeV and ENDF at 2.2111 MeV. This disagreement between results and theory opens the door to bring the necessary corrections into the transport codes, to both consider the correct reference system **and** keep the correlations within the cascades.

3.4 Inelastic neutron scattering simulation using PHITS

The Monte Carlo code PHITS is specialized in nuclear reaction simulations and was thoroughly used for comparison of reaction outcomes. In this section, the studied observable is the emission of the 2.21 MeV photon produced in neutron inelastic scattering on ^{27}Al using PHITS version 3.17. An anomaly was found in that the photon was not simulated, because the nucleus was de-excited using theoretical calculations instead of the structure data (as it is supposed to because the EBITEM criteria are not fulfilled as A<40 and $E_{ex} < 3$MeV), in addition to the fact that the calculated excitation energy was lower than the state energy declared in the source code data (in the elevel13027 vector stored in the source code as explained in section 2.3.3). Thus, instead of emitting one photon from the third state with a correct Lorentz boost, one photon was emitted from a non-defined state slightly lower than the third state that brought the nucleus to the second state and then the decay scheme was followed. The anomaly was corrected in the source code, and after recompilation, the photon was correctly simulated, and the anomaly was reported to the PHITS team.

The set of PHITS parameters that correctly reproduces the physics of the emission of the 2.21 MeV photon from ^{27}Al is the Event Generator Mode (EGM) with the Time (or Production) tally, and JENDL4.0 is used by default. As previously shown, TRIPOLI-4® appears to choose an imprecise center of mass for its kinematic corrections when using MF=6, with the additional bias of not having the correlations between the photons. In EGM simulation, which is in fact the analog mode for the simulation of nuclear reactions, PHITS is capable of producing the spread of values around the 2.21 MeV peak and the limits of the spread correspond more accurately to those calculated when considering the CM of only the (^{27}Al*) system, as shown on Figure 3.8, as opposed to the CM of the system (neutron + ^{27}Al*) in the case of TRIPOLI-4®.

It can be observed on Figure 3.8 that the kinematical limits of the emission spectrum correspond well to the calculated values. It can be concluded that PHITS not only simulates the gamma decay cascade, which conserves total energy and momentum for every neutron history, but also each photon emission is corrected, by means of calculation, to account for the expected spread caused by the Lorentz boost. Also, when using the JEFF-3.3 data, the spectrum presents a tail which is not observed when using the JENDL-4.0 data which is due to the declaration of a 2.19 MeV transition that is not present in the JENDL-4.0 data.

To go further with the kinematical analysis, two modified evaluation files were created in the ACE format (as required by PHITS). The modifications consisted in increasing drastically the probabilities of reaching the third state on one hand, and doing the same for the eleventh state on the other hand. By doing so, the MF=3 with enhanced probability of reaching the 2.21 MeV state (MT=53) would produce mainly the 2.21 MeV photon (because it is the only possible transition) and the MF=3 with the enhanced probability of reaching the eleventh state (MT=61) of energy 4.51 MeV would produce mainly a 2.3

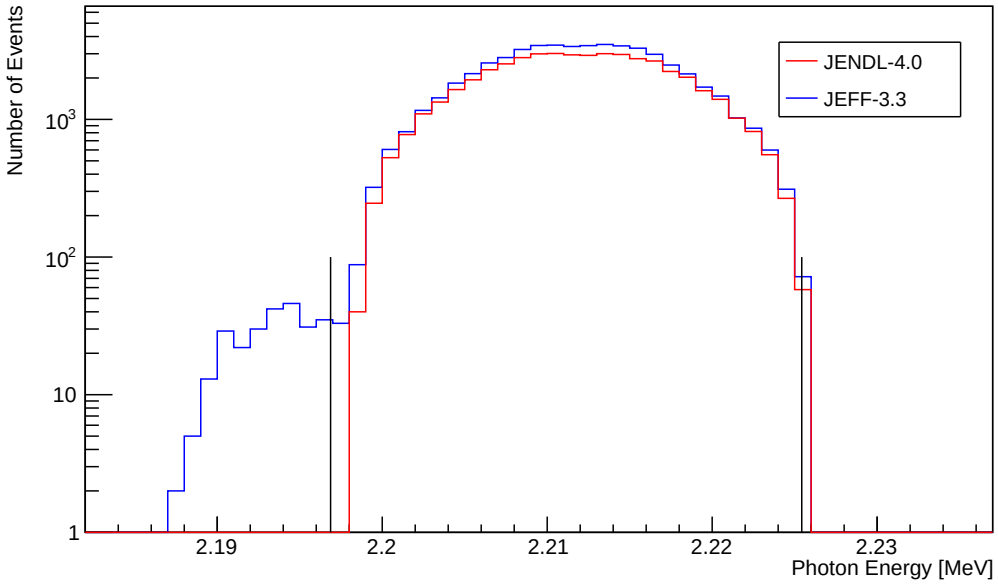

Figure 3.8: Zoom on the 2.21 MeV emission peak simulated by PHITS with the JENDL-4.0 and JEFF-3.3 data. The calculated limits using the (^{27}Al*) CM system are indicated by vertical black lines.

MeV photon (this transition has a 62% probability of happening) that brings the excited nucleus to its third excited state (MT=53), which in turn decays to the ground state. There should be a difference (in terms of Lorentz boost) between the 2.21 MeV photon emitted directly from the third state, compared to that emitted after the decay 11→3, as the available energy in the center of mass of the excited ^{27}Al* decreased with the first emission. Indeed, this difference can be observed in Figure 3.9.

The calculation for the kinematical limits of the 2.3 MeV photon from the eleventh state and the 2.21 MeV photon from the third state is the same as the previous calculations. The 2.21 MeV photon emitted after the decay of the eleventh state to the third state is slightly different, as the available energy in the CM of ^{27}Al* is reduced by the first photon emission. The total energy in the CM of ^{27}Al* after the emission of the 2.3 MeV photon is

$$E_{Al^*c} = \frac{(M_{Al} + 4.51)^2 + (M_{Al} + 2.21)^2}{2(M_{Al} + 4.51)} \tag{3.16}$$

and determines the extreme values that can be measured in the LAB frame according to the extreme emission angle ($\cos\theta_c = \pm 1$) as follows

$$\begin{aligned} E_{Al^*,min} &= \gamma_{Al^*} E_{Al^*c}[1 - \beta_{Al^*}\beta_{Al^*c}] \\ E_{Al^*,max} &= \gamma_{Al^*} E_{Al^*c}[1 + \beta_{Al^*}\beta_{Al^*c}] \end{aligned} \tag{3.17}$$

where

$$\beta_{Al^*c} = \sqrt{1 - \frac{(M_{Al} + 2.21)^2}{E^2_{Al^*c}}} \tag{3.18}$$

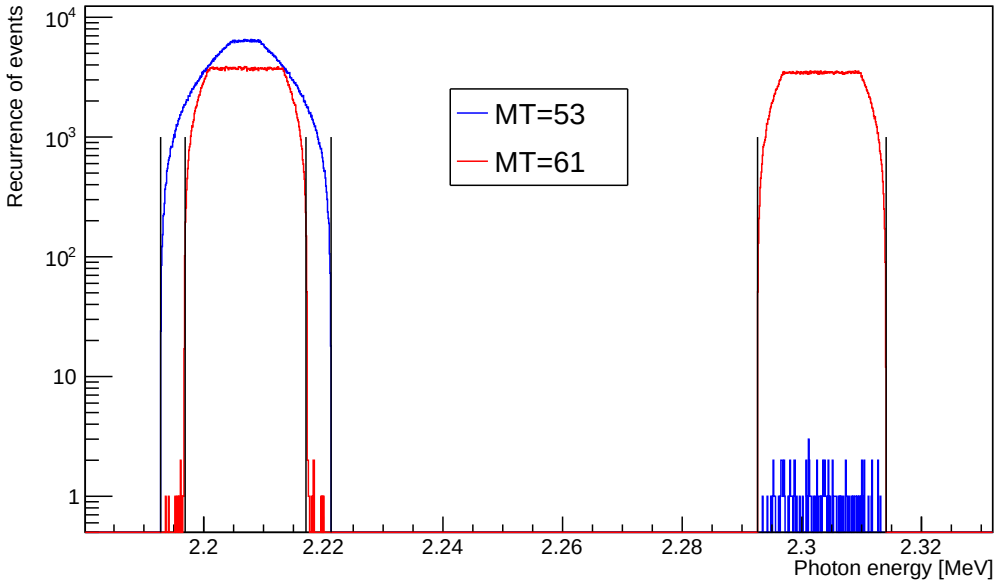

Figure 3.9: PHITS simulations with enhanced probabilities of reaching either the 3^{rd} or the 11^{th} excited state of ^{27}Al. The calculated kinematical limits are indicated by vertical black lines.

and γ_{Al^*}, β_{Al^*}, are the values calculated with equation 3.12.

Since the interest here is to have the extreme values of photon emission, the situation where this is possible is when there is minimum loss of energy in the ^{27}Al* frame, *i.e.* the value of interest is $E_{Al^*,min}$. With this in mind, one calculates the following quantities:

$$\begin{aligned} \beta_{Al,min} &= \sqrt{1 - \frac{(M_{Al} + 2.21)^2}{E^2_{Al^*,min}}} \\ \gamma_{Al,min} &= \frac{1}{\sqrt{1 - \beta^2_{Al,min}}} \end{aligned} \tag{3.19}$$

in order to obtain the sought after extreme values of photon emission

$$\begin{aligned} E_{\gamma,min} &= \gamma_{Al,min} E_\gamma [1 - \beta_{Al,min}] \\ E_{\gamma,max} &= \gamma_{Al,min} E_\gamma [1 + \beta_{Al,min}] \end{aligned} \tag{3.20}$$

where E_γ=2.21 MeV. For the numerical application it was necessary to use E_γ=2.207 MeV as this is the value used by PHITS and the values of possible photon emission energy in the LAB frame are

$$2.1969 \text{ MeV} < E_\gamma < 2.2171 \text{ MeV} \tag{3.21}$$

which correspond outstandingly well with the PHITS simulation, as shown in Figure 3.9.

3.5 Potential and effective contributions to the JEFF library

One of the main motivations of this work is to complete nuclear data to allow the users of simulation codes to implement ever more precise tests of nuclear systems such as detectors, nuclear medicine, mineral exploration, astrophysical studies, and of course nuclear reactors. This tendency can be appreciated when looking at the evolution of the nuclear libraries, in particular here the JEFF library. For example, the JEFF-3.2 evaluation of ^{27}Al contains MF=6, whereas its JEFF-3.3 evaluation contains MF=12.

As previously mentioned, the evolution from JEFF-3.2 to JEFF-3.3 not only increased the number of available nuclides from 472 to 562, but also, in relevance with this chapter, the number of evaluation files that contain MF=12 for the description of nuclear excited states increased from 239 to 422. Currently there are still 68 evaluation files of the JEFF-3.3 library that contain MF=6 for the excited states, which means that it is possible to implement a simulation analysis such as the one previously explained for the case of ^{27}Al. That is to say, it is possible to retrieve the structure data from the RIPL-3 library and convert the information into the ENDF-6 format to replace the corresponding information stored in MF=6 and compare photon production spectra using both sets of evaluations by means of analog Monte Carlo simulation, particularly with TRIPOLI-4® implementation. Additionally, it was found that 22 evaluation files of the JEFF-3.3 library contain incomplete MF=12, in the sense that the number of declared excited states in MF=3 was higher than the number of declared excited states in MF=12. The missing sections of MF=12 were written in the ENDF-6 format by extracting the information from the RIPL-3 structure data, and sent to the JEFF community. Table 3.2 reports the added data. To verify the accuracy of the method used, the complete MF=12 were created for each case and compared to the existing data; it was concluded that there was coherence between the structure data of RIPL-3 transformed into MF=12 and the corresponding sections of MF=12 found in JEFF-3.3.

Prior to the completion of the MF=12 that did not contain the same number of sections as in MF=3, the focus was on finding the evaluation files that only contain MF=6 (related to the excited states) in the JEFF-3.3 library and on creating MF=12 for them. As previously stated, there are 68 cases that can be worked on and it was possible to create 50 MF=12, as the information required is not available for all of them (structural and/or angular). Table 3.3 reports the created data. All the written data were tested by means of TRIPOLI-4® simulations that used either MF=6 or MF=12, where the photon production spectra resulted in the same shape for both MF=6 and MF=12 formats. All simulations to test the coherence of photon production were implemented so that the mean number of collisions per neutron history was close to 10^{-1}, the example of ^{58}Fe is shown on Figure 3.10. Additionally, the incident energy and cut-off energy were set where the neutron capture cross section is at minimum, typically 10 MeV and 5 MeV respectively for the heaviest isotopes. These measures are to ensure that most of the neutron interactions result in inelastic scattering. With 10^5 neutrons per batch and 10^3 batches, the relative errors in photon production measurements approximate 1%. The energy binning was chosen to be able to distinguish the excited states and the maximum energy is slightly higher than the last energy level of the evaluation. The simulation time is 5 to 10% higher for MF=12 simulations as the photon transport is done one by one. This depends highly on the complexity of the decay schemes.

Isotope	Added MT	Isotope	Added MT
^{27}Mg	79-80	^{100}Ru	80
^{26}Al	75-78	^{134}Cs	78-80
^{31}P	71-80	^{150}Sm	78-80
^{32}P	78-80	^{151}Sm	75-80
^{32}S	69-78	^{153}Gd	78-80
^{33}S	73-80	^{160}Dy	80
^{34}S	67-80	^{165}Dy	79-80
^{35}S	71-79	^{168}Er	79-80
^{38}Ar	71-80	^{189}Os	80
^{73}As	80	^{200}Hg	75-80
^{77}Se	75-80	^{237}Np	80-81

Table 3.2: List of evaluation files with mismatching number of MT between MF=3 and MF=12 that were completed

Tested and verified evaluation files				
^{35}Cl	^{54}Fe	^{57}Fe	^{58}Fe	^{58m}Co
^{62m}Co	^{94m}Nb	^{100}Mo	^{99}Tc	^{106m}Ag
^{127m}Te	^{129m}Te	^{131m}Te	^{135}Cs	^{142}Ce
^{144}Ce	^{152}Eu	^{152m}Eu	^{159}Tb	^{166m}Ho
^{180m}Ta	^{204}Pb	^{205}Pb	^{225}Ac	^{226}Ac
^{227}Ac	^{227}Th	^{228}Th	^{229}Th	^{233}Th
^{234}Th	^{232}U	^{235}Np	^{239}Np	^{236}Pu
^{238}Pu	^{241}Pu	^{246}Pu	^{242m}Am	^{243}Am
^{244}Am	^{244m}Am	^{247}Bk	^{249}Bk	^{250}Bk
^{249}Cf	^{250}Cf	^{253}Cf	^{253}Es	^{254}Es

Table 3.3: List of evaluation files for which complete MF=12 were written

For each isotope there is another set of simulations that consists of one neutron per batch. In this way all photons scored per batch correspond to only one neutron interaction (as the neutron cut-off energy is set close to the incident energy), and the sum of energies should correspond to an energy state. The sum of energies is then fed into histograms where the excited state energies are indicated by vertical lines and the peaks of the histogram should coincide with the vertical lines. This was the case for all simulations that used MF=12. It was observed that the lower energy peaks are higher with MF=6 than with MF=12 and that the higher energy states are only represented by MF=12 simulations, as can be seen on Figure 3.11. This is because in general the probability of one photon emission that brings the excited nucleus back to ground state decreases as the state energy increases, as it is more likely to go through intermediate states. In order for MF=6 simulations to show peaks at higher energies requires a high probability to decay to the ground state, whereas MF=12 simulations will naturally appear at each excited state energy.

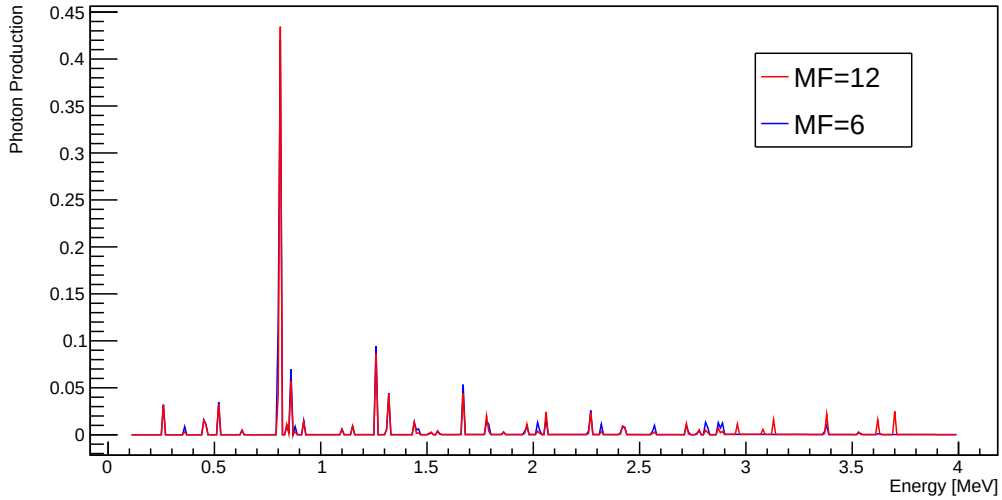

Figure 3.10: Photon production spectrum of ^{58}Fe analog (MF=12) and non-analog (MF=6) simulations.

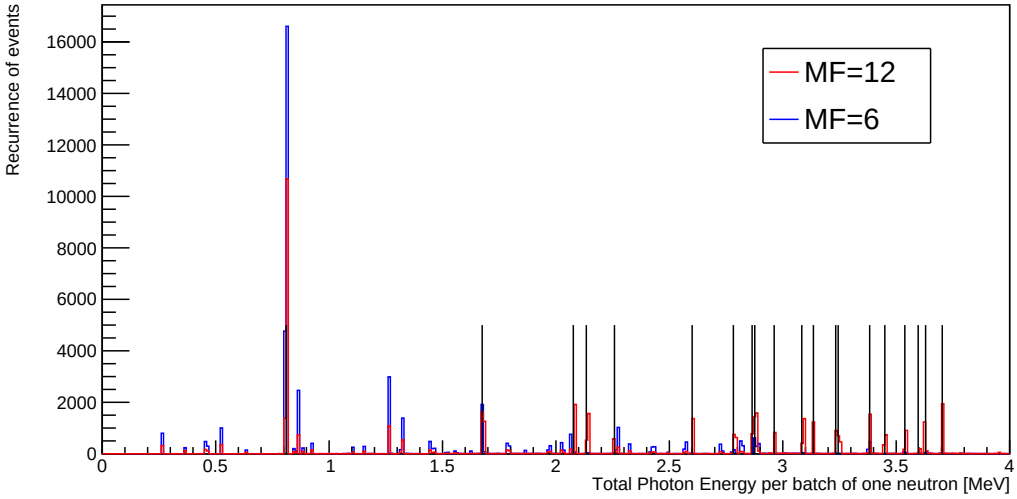

Figure 3.11: Histogram of sum of photon energies per neutron interaction with ^{58}Fe in analog (MF=12) and non-analog (MF=6) simulations, vertical black lines indicate ^{58}Fe excited state energies.

4 - Identification of nuclear structure parameters for analog simulation of neutron capture reactions

4.1 Brief description of the neutron capture reaction and its associated nuclear data

The objective of this chapter is to describe the different stages of the neutron capture reaction, in order to establish an algorithm that can rely on nuclear structure data, and potentially analytical models as well. The algorithm is an analog Monte Carlo simulation of all the possible γ-decay cascades that result from neutron capture events, thus ensuring that the produced photons conserve total energy in each event.

In this chapter the neutron capture reaction is discussed from the experimental and theoretical points of view. It is important to mention that only thermal capture is considered, as the energy of the incoming neutron can have a strong impact on the gamma spectra of the reaction due to fluctuations of the intensity of the primary transitions, when considering different initials states (resonances), as explained by C. E. Porter and R. G. Thomas in ref. [17]. However, the neutron energy chosen for the simulations is 10^{-5} eV, which results in an excitation energy just above the neutron binding energy S_n. This energy is the lowest energy defined in the evaluation libraries and is artificially low so that in practice it can be considered the zero-energy case.

In terms of the ENDF-6 format used in this analysis, the energy and angle distributions that characterize the (n,γ) reaction can be found in the evaluation files in section MT=102 of file MF=6 (but one can also find related data with the combinations MF=12+MF=15 or MF=13+MF=15). The MF=6 MT=102 data is divided in two parts: when the declared energies are in decreasing order, each energy ϵ_i represents a gamma transition from the well defined (or known) excited states, and its associated probability p_i is defined so that

$$\sum_i p_i = y_d \tag{4.1}$$

with y_d the expected proportion of gamma emissions from well known states, if the distribution is sampled once per neutron capture. Moreover, when the declared energies E_i are in increasing order, the probability densities of emission P_i are defined such that

$$\begin{gathered} \sum_i (E_{i+1} - E_i) P_i = y_c \\ y_d + y_c = 1 \end{gathered} \tag{4.2}$$

which is intended to reproduce the gamma emissions from the quasi-continuum of states by sampling an energy in the interval [E_i;E_{i+1}]. The case of MF=6 MT=102 of JEFF-3.3 for ^{155}Gd is shown on Figure 4.1 to illustrate the separation of the data in the distribution. It can be noticed that the discrete peaks of emission are absent from the energy range of about 2 MeV up to 4 MeV. This aspect will be further discussed in this chapter. It should also be noted that the contribution of the continuous spectrum is higher than the discrete peaks, and it was calculated that $y_d \approx 0.25$ and that $y_c \approx 0.75$, which implies that the main decay mode for this nuclide is through gamma emissions from the quasi-continuum of states.

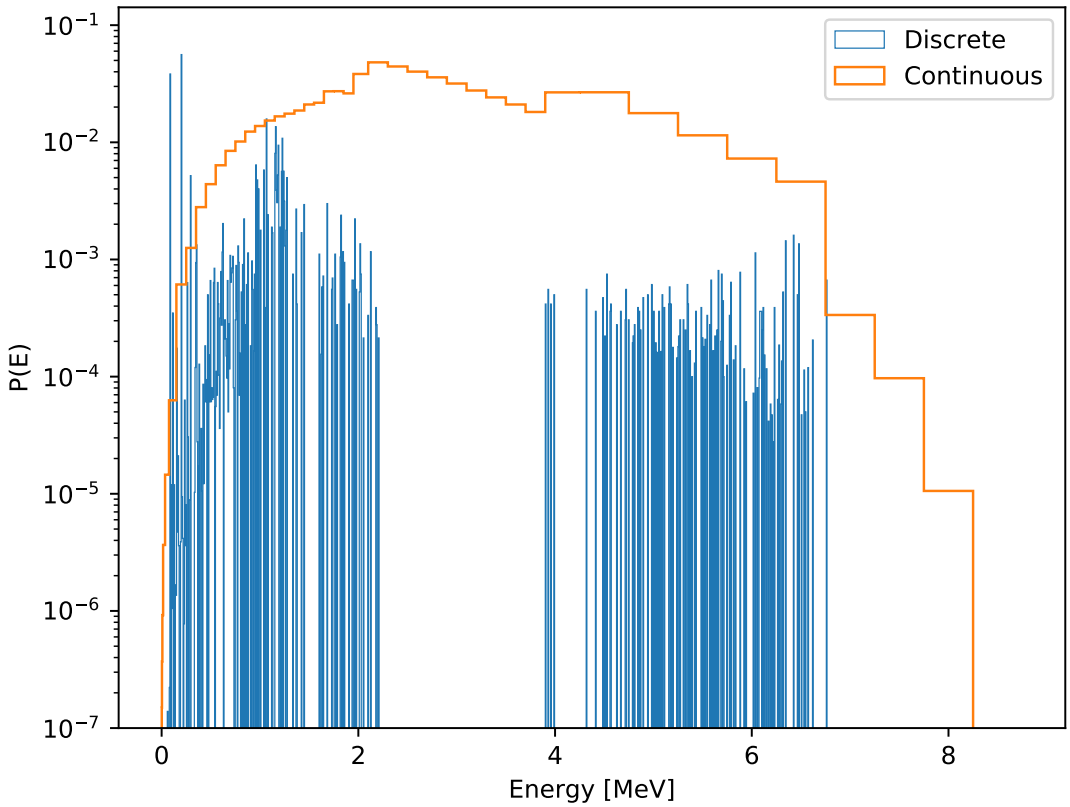

Figure 4.1: Graphic representation of the data stored in MF=6 MT=102 of JEFF-3.3 for ^{155}Gd where $\int P(E)dE = 1$.

It should be noted that all photons are discrete, and that the separation of the data previously mentioned comes from the fact that at high excitation energies the density of levels becomes very high, and the spacing between levels (=states) becomes comparable to the width of the states. The radiation width of a state is inversely proportional to its lifetime. If there are several states to decay to, each branching has its own partial radiation width. This is the same as a branching ratio. (It is not exact to use the term "continuous photon", to distinguish from the well defined gamma transitions: the "discrete photons", however useful the terms may be.) This is of particular importance in the (n,γ) reaction because when a given nucleus absorbs a neutron, it can reach several MeV of excitation energy, where the so-called quasi-continuum of states is found. In this sense, experiments can only go so far in determining where the states lie in, and it becomes necessary to develop numerical methods if one wants to characterize such nuclear systems. On the other hand, the so-called well defined (or known) states are those that can be experimentally distinguished because they are sufficiently separated in energy, these coincide with the excited states that were dealt with in the previous chapter.

This chapter starts with describing the analog simulation of the (n,γ) reaction without reaching quasi-continuum states, followed by an analysis of simulations implemented with the DICEBOX code [7] distributed by IAEA, as it is considered in this PhD the reference simulation for the capture reaction. An overview of the theoretical models used by DICEBOX is then given to suggest clues on how to simplify the reaction simulation using

a C++ code which only relies on the available structure and neutron data. The simplified neutron capture algorithm is then used for studying the decay scheme stored in the ENSDF dataset ^{155}Gd(n,γ) as it was found from PHITS [12] analog simulations that the existence of a rotational band in the final state after neutron capture can bring anomalies in terms of gamma multiplicity and gamma production spectrum because of how the data are constructed. The chapter concludes with the requirements for the future nuclear data formats.

4.2 Analog simulation of the neutron capture reaction

The neutron capture reaction has a high probability of occurrence with low energy neutrons (on the order of the meV). When the reaction takes place, the compound nucleus post neutron capture reaches a high energy state (on the order of the MeV), which can also be understood by the fact that the cohesion of nucleons within the nucleus is ruled by the strong interaction. The mass of the nucleus is a first parameter to take into consideration to describe the (n,γ) reaction. To determine the limits between low mass, intermediary mass and high mass, one can set arbitrary quantities of nucleons. For example, below A=20 can be considered low mass and above A=150 can be considered high mass. Inversely, low mass nuclei have excited states that start at a few MeV whereas high mass nuclei have excited states that start at a few keV.

In this section of the chapter the focus is on the possibility of implementing simplified analog simulations for the case of neutron capture on low mass targets, particularly the case of ^{12}C. When the reaction

$$n +^{12} C \rightarrow^{13} C^{*} \tag{4.3}$$

takes place, the minimal excitation energy of ^{13}C is 4.95 MeV. The decay scheme of ^{13}C is presented in Figure 4.2 where the red transitions correspond to the possible primary decays (the first emitted photon from the excitation state, after which the cascade is known in this case) that reaction 4.3 can produce. It must be stressed that the fact that the Q-value of reaction 4.3 lies between known discrete states, is what allows an analog simulation of this reaction, as opposed to other situations where the excitation energy is much higher and the nucleus reaches the quasi-continuum of states, where states not clearly separated by the experiments intended to determine the energy of excited states.

It can be observed on Figure 4.2 that there are 4 possible photons (in red) that can be emitted from the 4.95 MeV excitation state, after which there are 6 other possible decays towards the ground state. The energy of the photons in red can change if the incident energy of the neutron increases, because of the conservation of energy and momentum. This type of consideration is taken into account in the evaluated file by using the flag LP=2 within MF=12 where the photon energy E_γ is calculated as follows

$$E_\gamma = E_{\gamma_0} + \frac{AWR}{AWR+1} E_n \tag{4.4}$$

E_{γ_0} is the transition energy to a given state of ^{13}C excited by neutron capture of ^{12}C with zero incident energy, AWR is the mass of the target in units of neutron mass and E_n is the incident energy of the neutron in the LAB frame. Transition probabilities in black depend on the incident energy of the neutron, in the sense that the levels can be fed

differently according to the excitation energy reached. This will be discussed further after providing the concrete data for the example of $^{12}C(n,\gamma)^{13}C$.

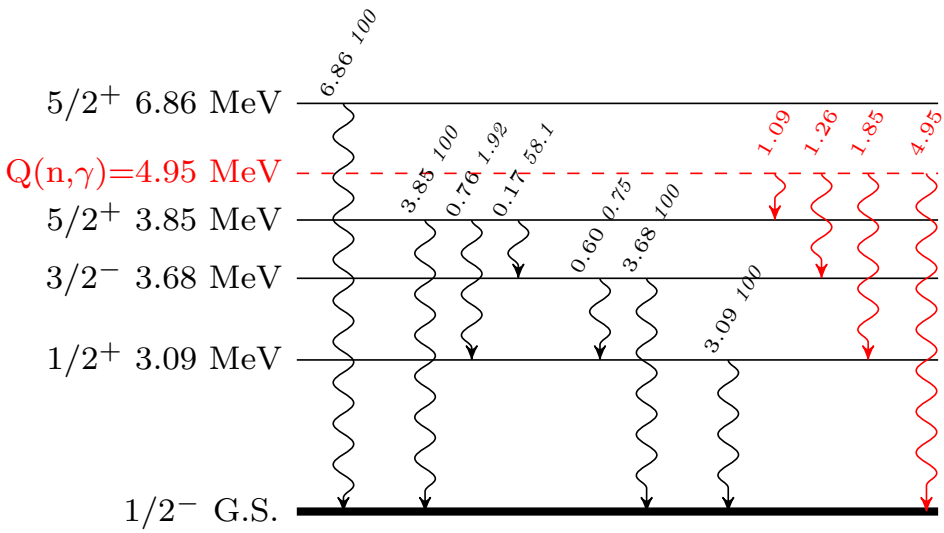

Figure 4.2: Decay scheme of ^{13}C, red transitions correspond to the possible primary decays due to a neutron capture of ^{12}C.

The EGAF data [25] for the possible photon emissions of reaction 4.3 are :

- 4.95 MeV : 67.47%
- 3.68 MeV : 32.14%
- 3.09 MeV : 0.43%
- 1.86 MeV : 0.16%
- 1.26 MeV : 32.36%
- 0.60 MeV : 0.24%

The declared PGAA Firestone [26] intensities are :

- 4.95 MeV : 0.0026
- 3.68 MeV : 0.00122
- 3.09 MeV : 1.65 10^{-5}
- 1.86 MeV : 6.2 10^{-6}
- 1.26 MeV : 0.00124

- 0.60 MeV : 9.5 10^{-6}

The declared PGAA Budapest [27] intensities are :

- 4.95 MeV : 0.0027
- 3.68 MeV : 0.00117
- 3.09 MeV : 1.47 10^{-5}
- 1.86 MeV : 7.6 10^{-6}
- 1.26 MeV : 0.00123
- 0.60 MeV : 1.08 10^{-5}

JENDL-5 declares a multiplicity of 1.32 for thermal neutrons for the discrete spectrum that accounts for the fact that if the state at 3.68 MeV is reached by the 1.26 MeV transition then the probabilities of emission must be the same:

- 4.95 MeV : 68%
- 3.68 MeV : 32%
- 1.26 MeV : 32%

and for an incident energy of 200 keV (this energy corresponds to E_n in equation 4.4 and the energies of the photons from the red transitions will be corrected accordingly), the multiplicity declared in JENDL-5 is 1.97 with the following spectrum :

- 4.95 MeV : 8%
- 3.85 MeV : 8.13%
- 3.68 MeV : 7.7%
- 3.09 MeV : 76%
- 1.86 MeV : 76%
- 1.26 MeV : 3%
- 1.09 MeV : 13%
- 0.77 MeV : 0.16%
- 0.59 MeV : 0.16%
- 0.17 MeV : 4.7%

The last listed data corresponds directly with the scheme presented in Figure 4.2 as all the 4+6 photons are present. Additionally, the data in ENDF/B-VIII and JEFF-4.0T1 also declare a multiplicity of 1.32 and are identical to the JENDL-5 thermal data. The ratios are calculated by considering first that the percentages in red should add to 100%. Indeed:

$$8 + 76 + 3 + 13 = 100 \tag{4.5}$$

Then, to obtain the branching ratio of the 3.85 MeV emission, reached 13% of cases from the initial state at 4.95 MeV, one needs to refer to the scheme presented in Figure 4.2, where the probability of decaying to the ground state from the state at 3.85 MeV is:

$$\frac{100}{100 + 1.92 + 58.1} = 0.625 \tag{4.6}$$

To get the probability of emitting the 3.85 MeV photon from the initial state at 4.95 MeV, the two aforementioned probabilities are multiplied:

$$0.13 * 0.625 = 0.08125 \tag{4.7}$$

which corresponds to the declared probability of emission for the 3.85 MeV transition. The same calculation can be done for all transitions, and the sum of percentages gives the multiplicity:

$$8 + 8.13 + 7.7 + 76 + 76 + 3 + 13 + 0.16 + 0.16 + 4.7 = 196.85 \tag{4.8}$$

To conclude, in order to implement an analog simulation of the ^{12}C(n,γ)^{13}C reaction, the required information concerns the transition ratios of the 1.09 MeV, 1.26 MeV, 1.86 MeV and 4.95 MeV photons, as the decay scheme of the three lower lying states is already defined and stored in the structure data. The flag LP=2 allowing such procedure results in a more realistic simulation of the reaction, knowing that it is adapted to a reduced number of nuclides. However, the question remains of how to access the structure data. Indeed, the decay scheme can be stored in the structure data evaluation of ^{13}C, but the data of the *red* photons should be stored in the reaction evaluation of ^{12}C + neutron, and the ENDF-6 data format is not adapted to this type of manipulation. A similar conclusion is obtained in the previous chapter, regarding the difficulty of taking into consideration the Lorentz boost in MF=12 for the inelastic reaction. The fact that the ENDF-6 format introduces artificial limitations is one of the motivations for creating a modern nuclear database structure called GNDS (General Nuclear Database Structure) for which an expert group was tasked to define the GNDS specifications such as the ones explained in this work.

4.3 Gamma transitions from the quasi-continuum to the discrete states

The neutron capture reaction is a multi-stage process in which a number of photons is emitted from the nucleus that absorbed the neutron. Because the compound nucleus is in an excited state that reaches several MeV, its excited levels are so close to each other that one can consider them as a quasi-continuum of states, and this effect starts to appear at lower energies for heavier nuclei. As photons are emitted from the quasi-continuum, the excited nucleus reaches lower energy states that are considered discrete if their separation is experimentally identifiable. There is no consensus for determining exactly at which *critical* energy E_{crit} the quasi-continuum ends and the discrete states begin, either by calculation or by experimentation, so the usual decision is to set an E_{crit} that suits best a given nucleus.

In order to describe as accurately as possible the continuum of states, nuclear level densities (NLD) can be identified from experiments and parametrized as continuous functions,

measured in MeV^{-1}. Then, NLD can be coupled to the so-called photon strength functions (PSF) as per equations 4.9 and 4.10. PSF are measured in MeV^{-3}, and their objective is to foster some emission energy ranges more than others. Indeed, at high energy states, in the quasi-continuum domain, the emission of photons can bring the excited nucleus to a level of the quasi-continuum, which implies that the energy of the photon is generally on the order of the keV. Conversely, if the energy of the photon is of the order of the MeV, it most probably means that the emission brings the nucleus to the discrete domain. Tomoyuki Tanaka *et al.* propose in [28] that for the modeling of the quasi-continuum part they compute the probability $P(E_a, E_b)$ for E1 transitions with $E_\gamma = E_a - E_b$ in terms of the transmission coefficient $T_{E1}(E_\gamma)$ and the number of levels $\rho(E_b)\delta E_b$ as

$$P(E_a, E_b) = \frac{dP}{dE}(E_a, E_b)\delta E = \frac{\rho(E_b)T_{E1}(E_\gamma)}{\int_0^{E_a} \rho(E'_b)T_{E1}(E'_\gamma)}\delta E \tag{4.9}$$

where $E'_\gamma = E_a - E'_b$, $\rho(E_b)$ is the NLD and δE is a finite energy step in the computations. $T_{E1}(E_\gamma)$ depends on the PSF $f_{E1}(E_\gamma)$, in turn a function of cross section σ_i, width Γ_i, and energy E_i of the resonances (index i refers to the resonances). The transmission coefficient is written as

$$\begin{aligned} T_{E1}(E_\gamma) &= 2\pi E_\gamma^3 f_{E1}(E_\gamma) \\ f_{E1}(E_\gamma) &= \frac{1}{3(\pi\hbar c)^2} \sum_i \frac{\sigma_i E_\gamma \Gamma_i^2}{(E_\gamma^2 - E_i^2)^2 + E_\gamma^2 \Gamma_i^2} \end{aligned} \tag{4.10}$$

where values of E_i, σ_i and Γ_i can be found in [29]. This is one of the possible choices to define the NLD and PSF to exploit, and T. Tanaka *et al.* chose to use four resonances, all E1-type, so the sum in equation 4.10 goes from i=1 to i=4.

To conclude on the theoretical model used in DICEBOX, it refers to a PSF of the form $f^{(XL)}$ which for the PSF in equation 4.10 requires that $X = E$ and $L = 1$. The summary of the parameters necessary for starting a DICEBOX simulation are:

- Setting general information (Z, A, S_n, E_{exc} and initial spin/parity)
- Declaring the known levels and transitions, sourced from ENSDF or RIPL-3
- Defining the *critical* energy E_{crit} for the minimum energy for generating states
- Defining the known and modeled primary gamma intensities, the normalisation is often unknown
- Choosing the models and parameters for NLD and PSF
- Setting the parameters for conversion electrons (optional), found in BRICC [30], depends only of Z

It is highly encouraged to perform multiple-batch simulations as opposed to one-batch simulations with the equivalent number of (n,γ) events, as for each batch, new levels and transition intensities from NDLs and PSFs are generated, which makes the simulation outcomes more statistically representative of the reaction process. The fact that new levels are generated is possible due to the arbitrary nature of the determination of the simulation parameters and does not affect the validity of the produced spectrum.

4.4 Analysis of the DICEBOX (n,γ) simulations

DICEBOX is based on the analog Monte Carlo method, and consists in generating different probability densities to best reproduce the gamma cascades associated to the (n,γ) reaction. The focus in this section is the example of the ^{95}Mo(n,γ) reaction. DICEBOX simulations of 10 batches of 10^5 thermal neutrons were implemented and resulted in the multiplicity distribution shown in Figure 4.3, where the mode of the distribution is at 4-photon events. The average number of photons of the simulation is 4.34, where the yield declared in MF=6, MT=102 of the JEFF-3.3 library is 4.53. The shape of the distribution depends on the complexity of the decay scheme associated to the simulated nucleus, but it can be expected for a majority of nuclides that after the gamma emission(s) from the quasi-continuum, the well known levels to be reached, and most cascades consist of around 2 to 7 transitions towards the ground state. That is to say that the overall shape of the multiplicity in Figure 4.3 should be a general case for any (n,γ) simulation, but with a mode, mean and standard deviation depending on the nucleus. Nevertheless, two exceptions will be discussed later in this chapter.

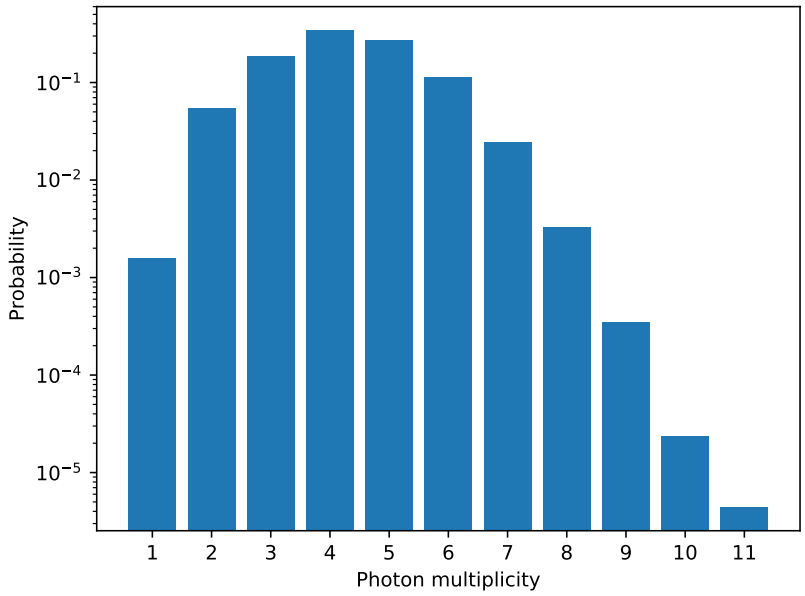

Figure 4.3: DICEBOX photon multiplicity distribution for ^{95}Mo(n,γ).

The 7-photon (n,γ) events simulated by DICEBOX yielded sufficient statistical significance to identify a clear shape of the spectrum for each of the 7 simulated photons, as can be seen on Figure 4.4. The different spectra suggest that the energy distribution attributed to a given photon strongly depends on the available energy and therefore on its order of emission. Indeed, each time DICEBOX simulates a 7-photon event, it can be seen that the first photon presents the spectrum with the largest energy range, which corresponds to the fact that it has the largest available energy. As photons are emitted, the available energy decreases and the energy range for photon emission decreases accordingly. The form of the spectra of the first photons corresponds to that of particles being emitted by a highly energetic system, and as photons are successively emitted, it can be observed that the maximum of the curve also decreases in energy. The last photons (notably the 5^{th} in purple, the 6^{th} in brown and the 7^{th} in black) come mostly from the successive tran-

sitions of the known excited states that ultimately bring the nucleus to its ground state, which explains the peaks standing out from the continuous shape in the case of the 5^{th} photon spectrum. For the 7^{th} photon it can be said that it overwhelmingly represents the transition of the first excited state at 0.778 MeV to the ground state, and at much lower frequency, it corresponds to the transitions from states at 1.497 MeV and 1.623 MeV, which also decay directly to the ground state. This implies that in a relatively long decay chain, it is certain to reach the known levels, corroborated by the amount of peaks of the 6^{th} photon spectrum, indicating that prior to the 7^{th} decay, the ENSDF decay scheme is already been followed by the simulation.

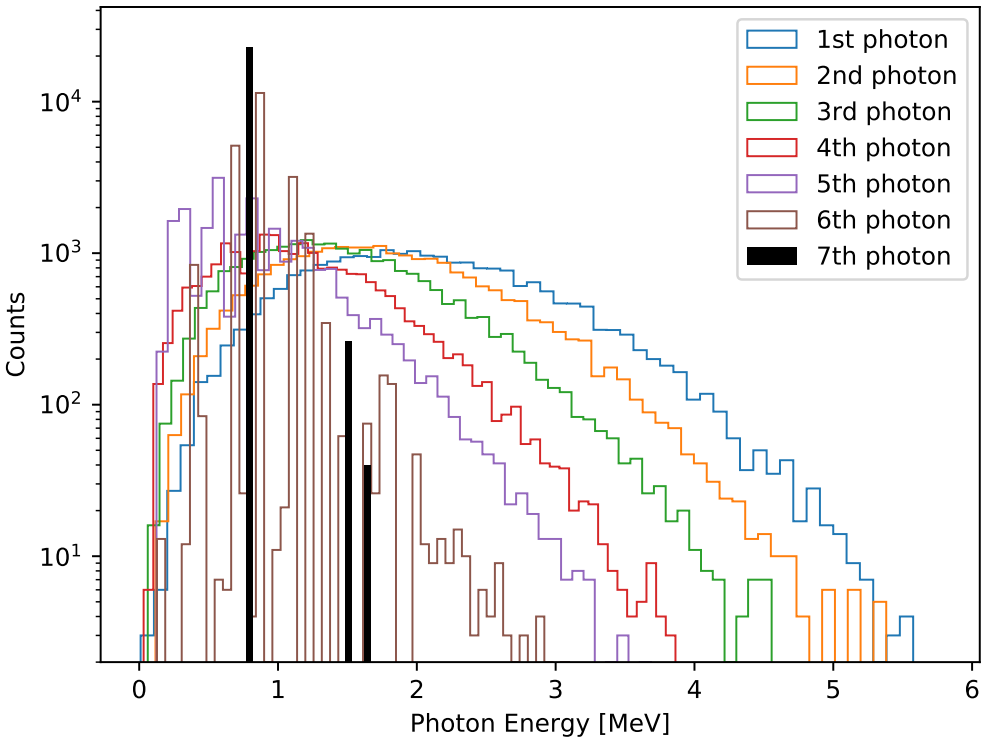

Figure 4.4: Energy distribution of photons in 7-photon DICEBOX events of ^{95}Mo(n,γ) by order of emission.

Another aspect that stands out from the simulation analysis is the influence of the multiplicity of the event on the energy of the photon knowing its order of emission. For example, if the focus is on the third emitted photon, its spectrum is expected to be very different between 3-photon events compared to 7-photon events. This is illustrated by the emission densities according to the gamma multiplicity of the event shown in Figure 4.5: in blue is shown the third photon in 3-photon events, suggesting the two possibilities for the emission of this last gamma emission are either to carry all the available energy following two photon emissions from the quasi-continuum, (this corresponds to the continuous spectrum at higher energies) or to bring the nucleus to the ground state through a well known transition, exactly like what was explained for the 7^{th} photon in the previous paragraph concerning the states at 0.778, 1.497 and 1.623 MeV, and it suggests the second photon which preceded it, was already taken from ENSDF data. In red, purple and brown it can be seen that the spectrum of the third photon of 6-, 7- and 8-photon events is a continuous spectrum, which suggests that well defined excited states have not been reached yet at the

third emission. The intermediary situation is the case of 4-photon events, where at high energies the shape of the spectrum is continuous, whereas at low energies emission peaks can be observed and should correspond to the well known transitions. It should also be noted that all the maxima of the continuous spectra align at the same energy due to the photon strength functions that foster photons of approximately 1 MeV.

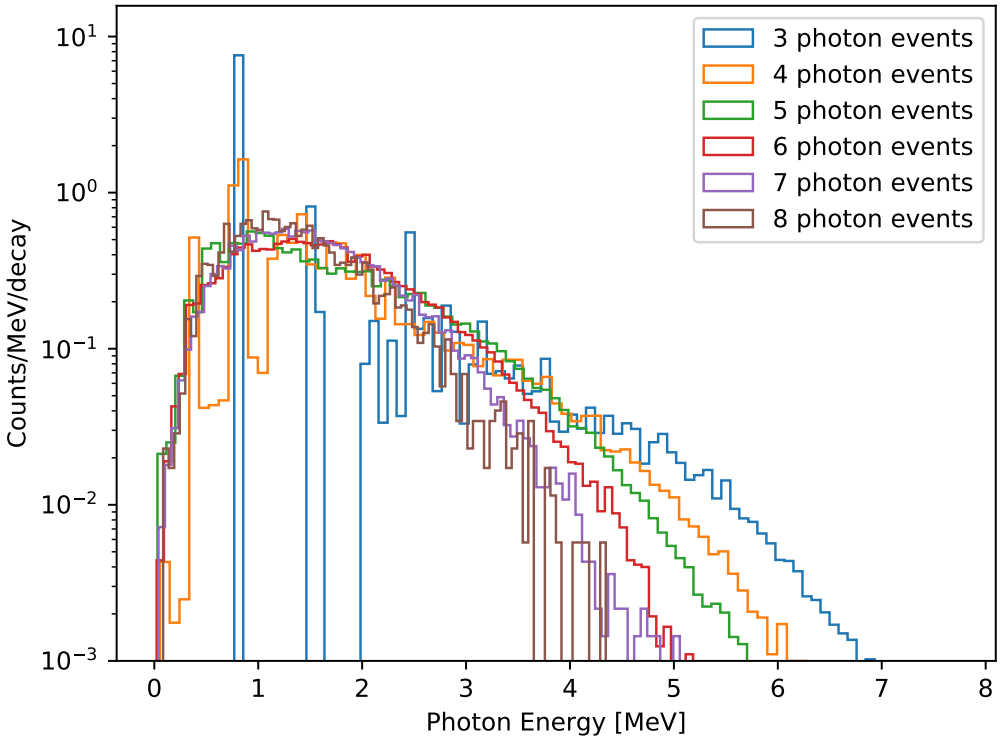

Figure 4.5: Energy distributions produced by DICEBOX for the third photon in variable multiplicity of the ^{96}Mo after neutron capture on ^{95}Mo.

Moreover, if one investigates the simulation outcome of the last photons emitted per neutron capture event, it can be concluded that for the longest decay chains (6-, 7- and 8-photon events) the last emitted photon comes mostly from the well defined levels, as it can be observed on Figure 4.6 where the emission densities of the last emitted photon are plotted according to the multiplicity of the event. For the shorter decay chains (2-, 3- and 4-photon events), a significant number of photon emissions correspond to a decay that carries the available energy post neutron capture. Additionally, it can be noticed that the critical energy between the quasi-continuum and the well-known states becomes clearly visible. Above this critical energy, photons are emitted with the available energy left. The gap between the continuous spectrum and the discrete peaks of about 1 MeV can be reduced if the critical energy is set at a lower energy.

4.4.1 Simplified (N,G) Algorithm for analog simulation of gamma cascades from neutron capture

In order to exploit all the existing nuclear data, and avoid analytical models such as the use of NLDs and PSFs, we have implemented an algorithm that reproduces the gamma emission from the quasi-continuum and also simulates the gamma cascades of the known states, based on the Monte Carlo method. For simplicity of notation, the algorithm

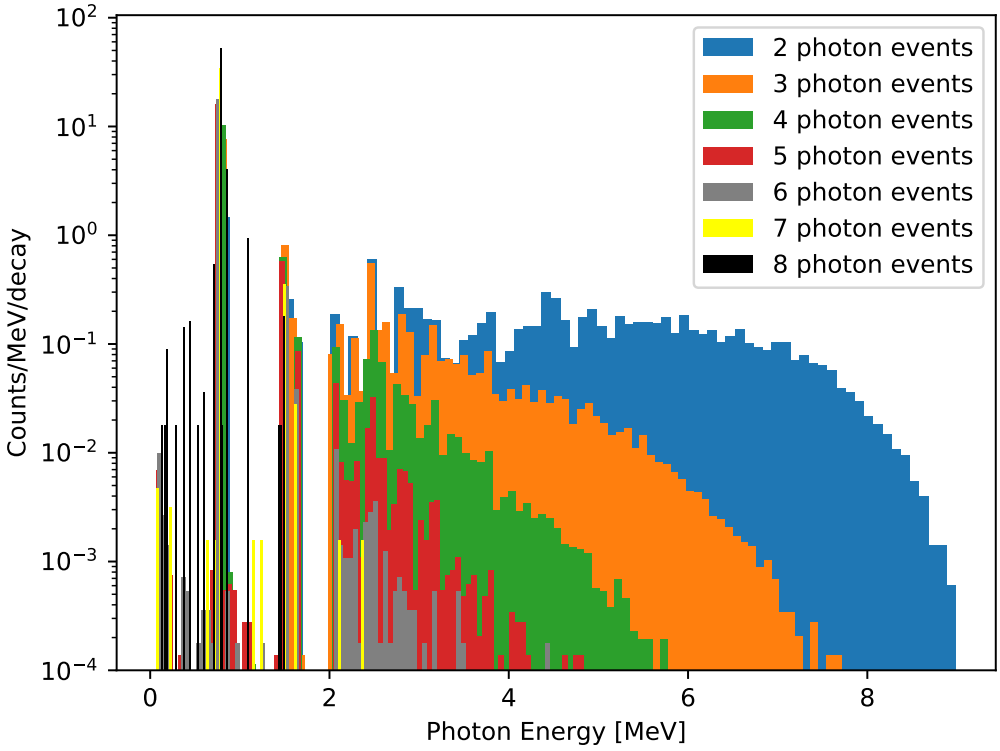

Figure 4.6: Energy distributions for the last photons emitted in variable multiplicity produced by the DICEBOX of ^{95}Mo(n,γ).

is named hereafter SNGA for Simplified (N,G) Algorithm. The SNGA is indeed more elaborate than what one typically finds in the reactor transport codes, but less elaborate than DICEBOX. This algorithm requires as input data:

1. the incoming energy of the neutron
2. the evaluated nuclear data of the target isotope for the quasi-continuum distribution (MF=6, MT=102)
3. the structure data specific to thermal capture which gives the observed primary γ intensities

The SNGA proposed here to generate (n,γ) analog events, where all particles are simulated one by one, is made with the expectation that this method reproduces the physical behavior of the neutron capture reaction. Mainly, it produces the spectrum of photons with the discrete lines of emission, as well as the so-called continuum spectrum. It relies on the structure data found in the RIPL-3 library, to produce realistic cascades from well defined excited states, working alongside the probability distribution defined in the MF=6, MT=102 in the JEFF-3.3 library for photons emitted from the quasi-continuum of states.

The methodology of the SNGA is inspired by an analysis performed to the DICEBOX results. This (n,γ)-specialized Monte Carlo code produces highly realistic events, which means that the order of particles can be retrieved. The most revealing information comes from the first and last photons that are simulated, the characteristics of which are highly related to the multiplicity. Thus, in the SNGA the multiplicity is chosen from a Gaussian

distribution centered around the declared multiplicity found in JEFF-3.3. The chosen multiplicity *guides* the simulated (n,γ) event towards a decay channel. For example, a 2 photon event has few options. Either the first photon is considered as discrete because a relatively low energy discrete state is reached and a second photon brings the nucleus to the ground state from an identified excited state, or, it is considered a photon from the quasi-continuum that does not bring the nucleus to a discrete state in which case the available energy is allocated completely to the second photon.

Some assumptions have to be made for choosing the possible decay channels. First, the multiplicity is chosen from the Gaussian distribution (this was chosen for simplicity but in reality the multiplicity distribution is not Gaussian). The first photon can either bring the excited nucleus to the ground state, or bring it to a discrete state, or it can be a so-called continuous gamma, and the excited nucleus remains in the quasi-continuum after the emission. It was estimated from DICEBOX results that around 1% of the (n,γ) events consisted of a single photon with the maximum available energy. The ENSDF (n,γ) E=TH library suggests that 14% of the first photon in (n,γ) events brings the excited nucleus to a known state, for the example of ^{95}Mo (this percentage depends on the isotope), thus it was assumed that after the emission of a continuous gamma, the probability of re-emitting a continuous gamma is 85%=100%-1%-14%. As soon as the nucleus reaches a known state, the possible cascades from the reached state determine the ensuing photons. If no known states are reached, if the last photon of the chosen multiplicity is reached, this last photon must carry all the available energy. The flow chart that summarizes the (n, γ) algorithm is shown in Figure 4.7.

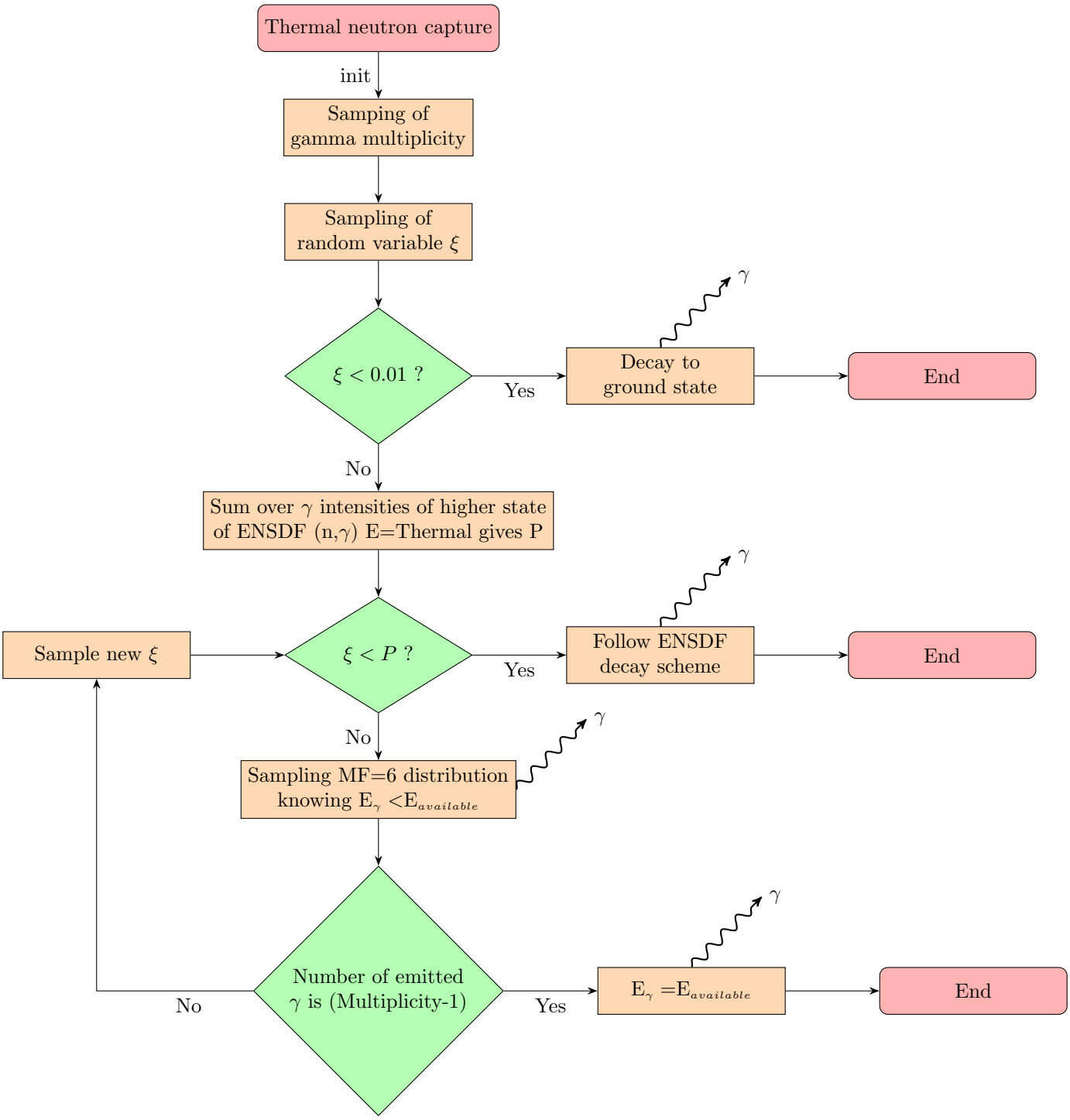

Figure 4.7: Flow chart describing the (n, γ) simulation algorithm.

4.4.2 Coherence of the implementation for gamma spectra and multiplicity

The clues obtained by analyzing the DICEBOX simulations allowed the construction of an algorithm intended to reproduce the expected outcomes of the (n,γ) reaction, particularly the multiplicity and the shape of the spectrum. The control case of ^{95}Mo was tested with the SNGA and the resulting spectrum can be seen in Figure 4.8. By construction, the rightmost hand side peak represents the photon that brings the excited nucleus to its ground state, in this case it is a photon of 9.154 MeV, equal to the reaction Q-value. The emission peaks that stand out from the continuous shape correspond to the photons that either bring the nucleus in its quasi-continuum of states (at higher energies) to well-known states, or (at lower energies) to the photons emitted in the decay cascade. The continuous shape results from the sampling of the distributions found in MF=6, MT=102, which explains the step-like features associated to the energy ranges declared in the data.

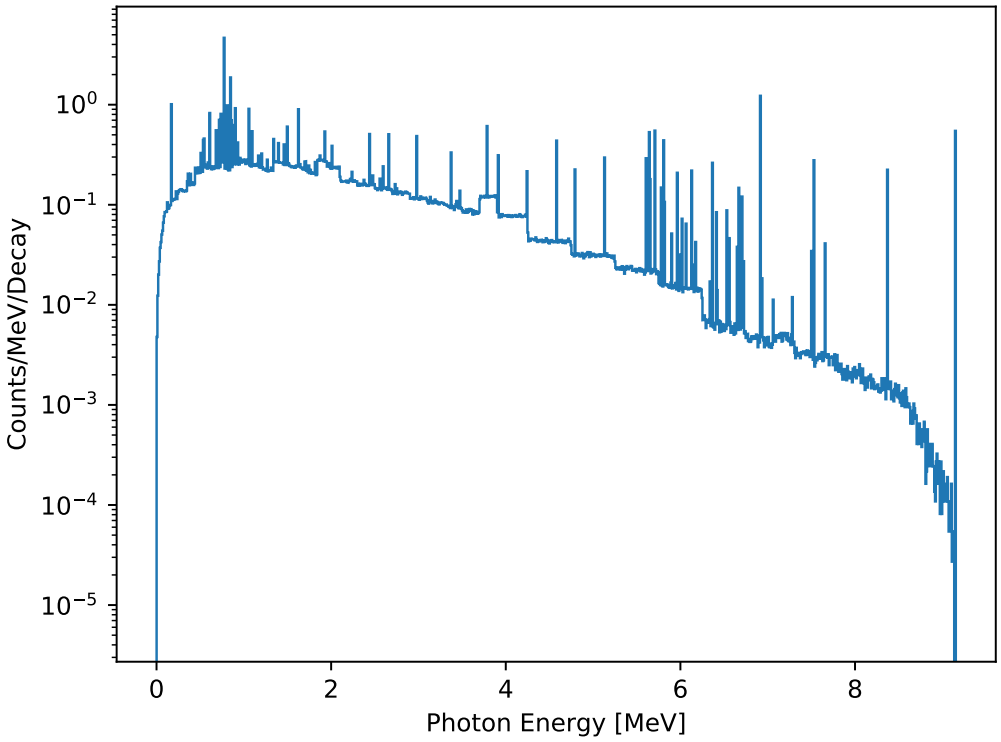

Figure 4.8: Photon production spectrum from the SNGA for ^{95}Mo(n,γ).

The motivation for the SNGA is to rely solely on nuclear data to take into consideration the three main sources of gamma emission of the neutron capture reaction; these being the photon transitions that maintain the excited nucleus in its quasi-continuum of states, the photon transitions that bring the nucleus from its quasi-continuum of states to the discrete states, and the photon transitions associated to the known decay cascades. The SNGA uses the data found in MF=6 MT=102 for the first transitions, then the ENSDF data provides the probabilities for reaching the discrete states, and finally RIPL-3 is followed to simulate the gamma cascades of the discrete states to reach the ground state. The algorithm produces a gamma multiplicity compatible to that of the DICEBOX simulation, as shown on Figure 4.9 for 10^6 neutron capture events.

The obtained gamma multiplicity distribution on Figure 4.9 is not exactly representative of the individual multiplicity given to the Monte Carlo algorithm in the beginning of each neutron story. At each initialization, the decay algorithm is given a value of the number of photons that should be produced. This number is sampled from a Gaussian distribution centered around the declared multiplicity of MF=6 MT=102. Once the cascade begins, it is possible that the sampled multiplicity is not respected. For example, if 4 is sampled, it is possible to reach a discrete state in one step, and the ground state in the next step, which makes a decay of 2 photons. However, if 4 is sampled, and 3 photons have been sampled from the continuous spectrum of MF=6 MT=102, the fourth one will carry the remaining available energy. In all cases, energy is conserved, either by following the transition probabilities, or by respecting the assigned multiplicity. It can be noted that 1-photon events are more frequent than 1%, and 7-photon events are less frequent than in DICEBOX, and that 8- and 9-photon events are nonexistent, due to how the data and the algorithm are constructed. The distribution shown on Figure 4.9 is thus called effective as it depends more on the implemented constraints during the decay process more than the initial value fed to the simulation, which explains the fact that it is not a Gaussian distribution.

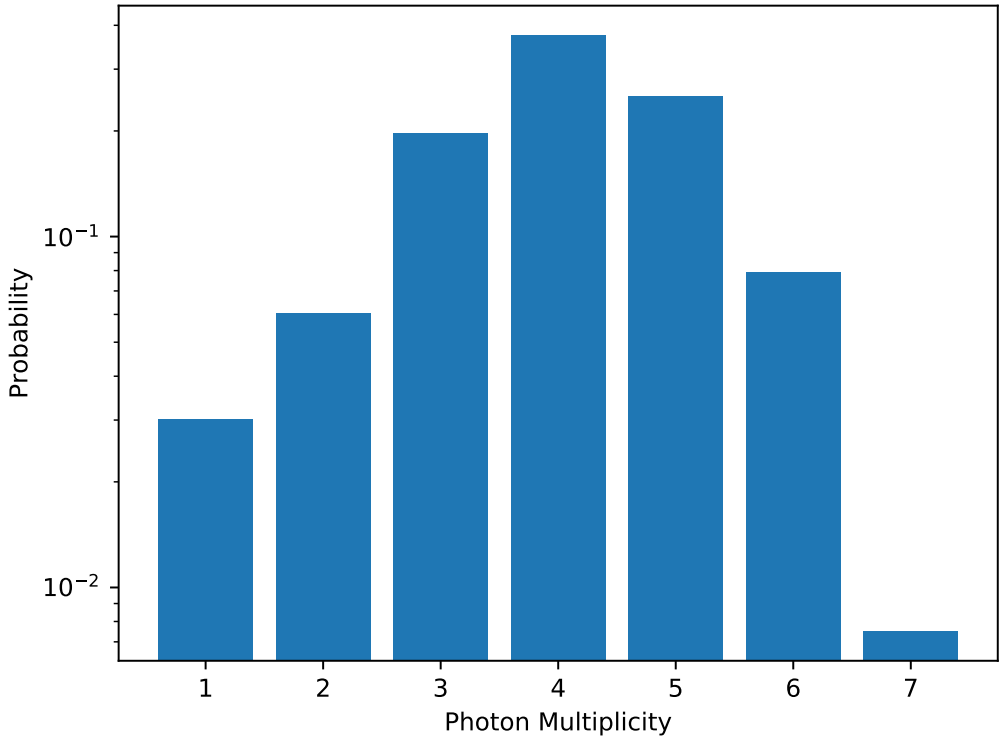

Figure 4.9: Effective gamma multiplicity produced with the SNGA for ^{95}Mo(n,γ) simulation.

A parallel analysis to that of the DICEBOX results was performed for the SNGA in terms of energy spectrum according to the order of emission, as it can be observed on Figure 4.10. One of the instructions for the Monte Carlo simulation is, at each gamma emission, to decrease accordingly the energy range to sample from in the continuous spectrum. This allows to artificially copy the expected shape of the continuous spectra, in that the first photons are more likely to carry higher energies, with the exception of the last one, because

of the instruction to carry all the remaining available energy if the last photon has to be simulated. Another remarkable aspect is the presence of peaks standing out from the continuous shape, which correspond to transitions towards discrete states, and the peaks are mostly present at high energies in the case of the first and the fifth photons, and at low energies in the third, fourth and fifth photons, as expected when RIPL-3 data is followed.

If one compares the last photons emitted in the 5-photon events of DICEBOX (shown in red on Figure 4.6) to the last photons in the 5-photon events of the SNGA (shown in purple on Figure 4.10) it can be noticed that the latter case produces a continuous spectrum whereas the former shows a clear cut that separates a continuous spectrum at higher energies, and discrete peaks at lower energies. This is due to the absence of a critical energy in the SNGA and also to the instruction to emit a photon that carries all the remaining available energy if the last photon of the sampled multiplicity for the capture event is reached.

Another aspect that is not reproduced, compared to the DICEBOX simulation, is the maximum energy of a given photon: in the DICEBOX results shown on Figure 4.4 the maximum energy of the fourth photon in 7-photon events, is noticeably lower than the maximum energy of the first emitted photon. In the case of SNGA, if one emission is of low energy, the energy range from which the next photon is to be sampled is reduced by a small amount and this allows the potential emission of a highly energetic photon. This results in the convergence of the spectra at high energies.

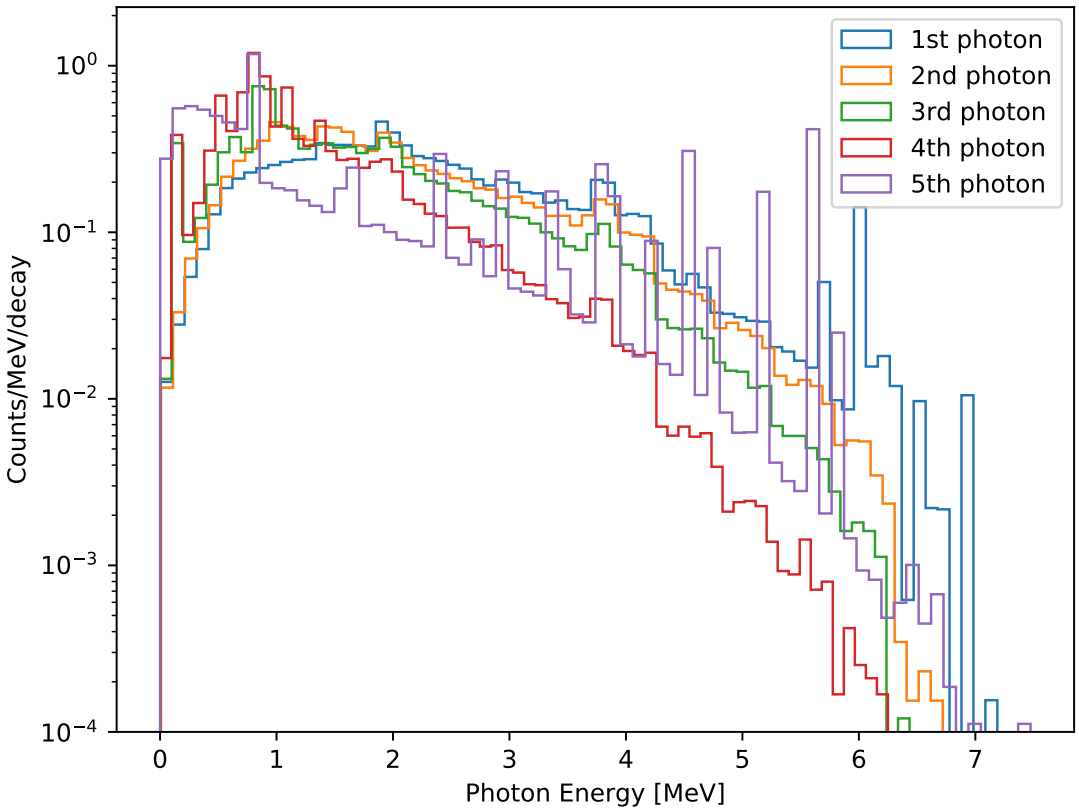

Figure 4.10: Energy distribution of each of the 5 simulated photons in 5-photon events obtained using the SNGA for the ^{95}Mo(n,γ) reaction.

The most significant difference between the simplified algorithm of the (n,γ) reaction with respect to DICEBOX is the imposed constraint of the last emitted photon. In the case of the algorithm, the last photon is the last resort to ensure conservation of total energy whenever the event consists only of photons sampled from the continuous distribution, as can be observed in Figure 4.11. There is also the difference that in the algorithm there is no concept of a critical energy, related by definition to the modelling of the quasi-continuum done by DICEBOX. This can be seen on Figure 4.6 in the sharp edge where on one side there are only peaks, and on the other there is a clear continuous shape, whereas on our algorithm the continuous shape is present for all energies and peaks are found even at high energies.

It can be concluded that in the simplified (n,γ) algorithm, each event conserves the total energy and the resulting multiplicity distribution is coherent with what can be expected from the (n,γ) reaction. However, to rely solely on the available data inevitably leads to simplifications that are not realistic from the phenomenological point of view. In other words, the gamma cascade from the continuum of states towards the ground state is in fact simulated using the analog Monte Carlo method, but the sampled data is insufficient to produced only realistic cascades. This could be addressed in future evaluations by providing parameterized data (nuclear temperature, maximum of emission energy) to generate the different emission spectra needed.

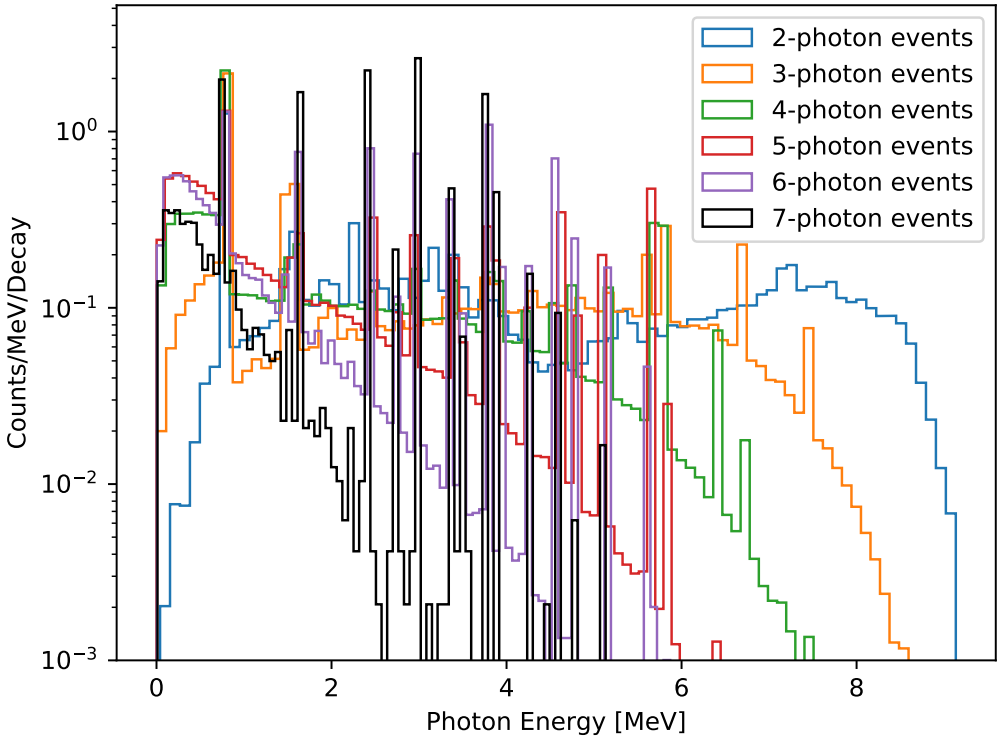

Figure 4.11: Energy distribution of the last photon simulated by the simplified ^{95}Mo(n,γ) simulation.

4.5 ^{155}Gd(n,γ) anomalies

4.5.1 Structure data for thermal capture

Gadolinium is crucial for reactor physics because of its high absorption cross section, especially the odd isotopes, so it was only natural to study the particular aspects of the Gd(n,γ) reaction. In this section the focus is on ^{155}Gd because some unexpected anomalies were found. Firstly, if one compares the different data that characterize the thermal capture of this particular isotope, the first subtleties appear. Indeed, as can be observed in Figure 4.12, there are discrepancies between the three plotted data (ENSDF, CAPGAM, EGAF), in terms of emission intensities and also in terms of existence of photon energies. Secondly, a remarkable aspect is the gap around 4 MeV where no photons have been declared in the case of ENSDF and CAPGAM, whereas EGAF declares a somewhat isolated peak. This type of feature where clearly some photon energies are *forbidden*, usually indicates that there exists an energy region in the excited states that cannot be reached by decaying from higher energies. In the case of ^{156}Gd* - the resulting nucleus of ^{155}Gd(n,γ) - the excited states of about 4.5 MeV present angular momenta of J>10 (this is called a rotational band) and the initial excited state post-reaction at 8.53 MeV presents $J^\pi = 2^-$ according to the ENSDF thermal capture data, which explains the fact of the forbidden transitions as photons cannot carry more than 3 units of angular momentum.

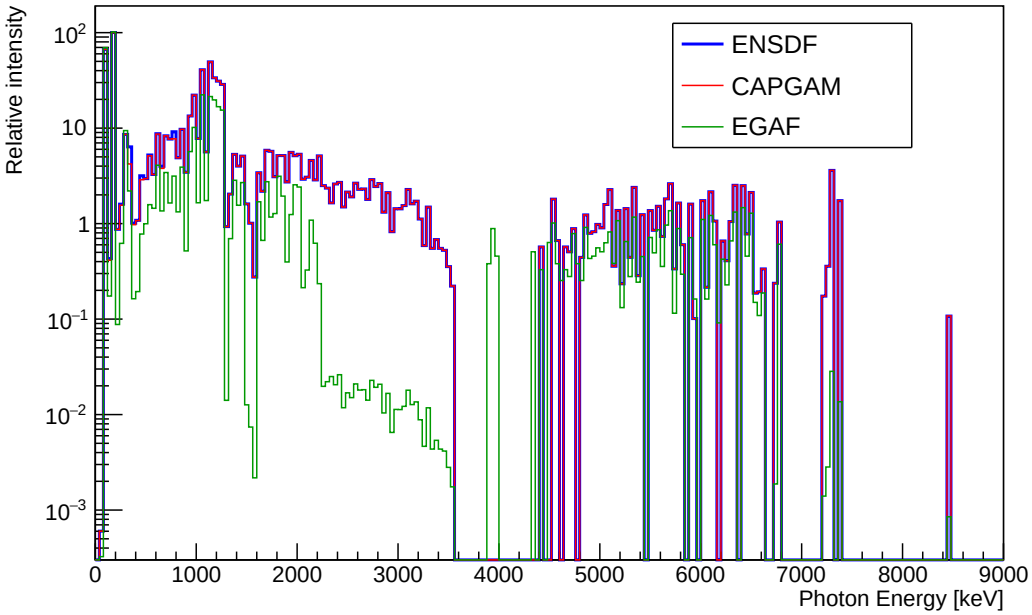

Figure 4.12: Thermal capture data for ^{155}Gd. The data are normalized with respect to the highest emission peak. (Violet-ish tone indicates perfect agreement between ENSDF and CAPGAM).

4.5.2 PHITS simulations

Gamma multiplicity

When simulating thermal neutron capture of ^{155}Gd using PHITS, a few anomalies were found, both in the gamma multiplicity and in the resulting photon production spectrum.

Starting with the gamma multiplicity, two maximum values are obtained in the multiplicity distribution of gammas per cascade, as can be observed on Figure 4.13. What is observed in experiments, not only for gadolinium but most nuclides, is only one peak at around 3 to 5 gammas, approximately. The hypothesis to explain the multiplicity distribution produced by PHITS is that the emitted photon from the initial excited state overfeeds energy states of a rotational band in $^{156}Gd^{*}$ (which is non physical) and the ensuing decay goes through more than seven excited states. The energies of the rotational band (J>10) of ^{156}Gd can be found from around 3.4 MeV to 6.6 MeV, which means that photons from the initial excited state at 8.53 MeV, $J^{\pi} = 2^{-}$, should not decay into states in this range. A first approximation for a correct forbidden energy range would thus be a noticeable tendency of (8.53 - E_{γ}) $\notin$ [3.4 ; 6.6], event though there might be non-rotational states within the range. In a more accurate model for gamma emission, one looks directly at the angular momentum of the target level to know if a transition is allowed.

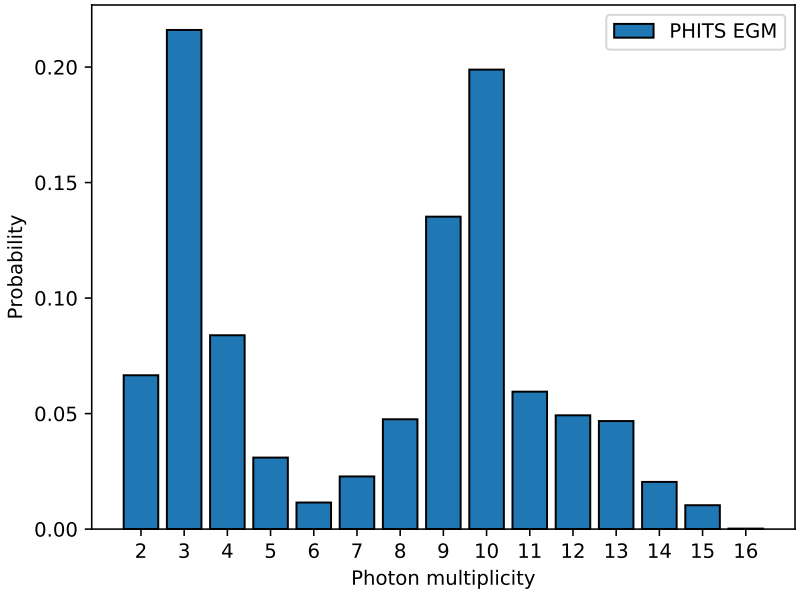

Figure 4.13: Gamma multiplicity in $^{155}Gd(n,\gamma)$ using PHITS.

Figure 4.14 shows the excited states reached from the initial state in EGM PHITS simulation in the first gamma transition. It can be observed that the condition (8.53 - E_{γ}) $\notin$ [3.4 ; 6.6] is not respected, but more importantly, the peak at 4 MeV indicates that there is indeed an error, because the excited state declared in ENSDF at 3.995 MeV of ^{156}Gd indicates J=16, so the most frequently simulated first transition is actually forbidden.

Once it is known that the 3.995 MeV excited state is the most frequently reached in the EGM PHITS simulation, one can analyse the decay scheme stored in the PHITS source code, which mirrors the ENSDF data, and determine its possible gamma cascades towards the ground state. The methodology used for implementing such an analysis is to create a C++ code, hereafter called PCA for PHITS Cascade Algorithm, to read the PHITS data, and simulate the cascades using the Monte Carlo method to estimate the average number of states that are reached (thus the gamma multiplicity associated to this particular

excited state) in the decay process starting from the 3.995 MeV state. As expected from the anomaly, the overwhelming majority of cascades produce 9 photons, which matches perfectly with multiplicity peak of 10 photons, if the transition from the initial state at 8.53 MeV is counted.

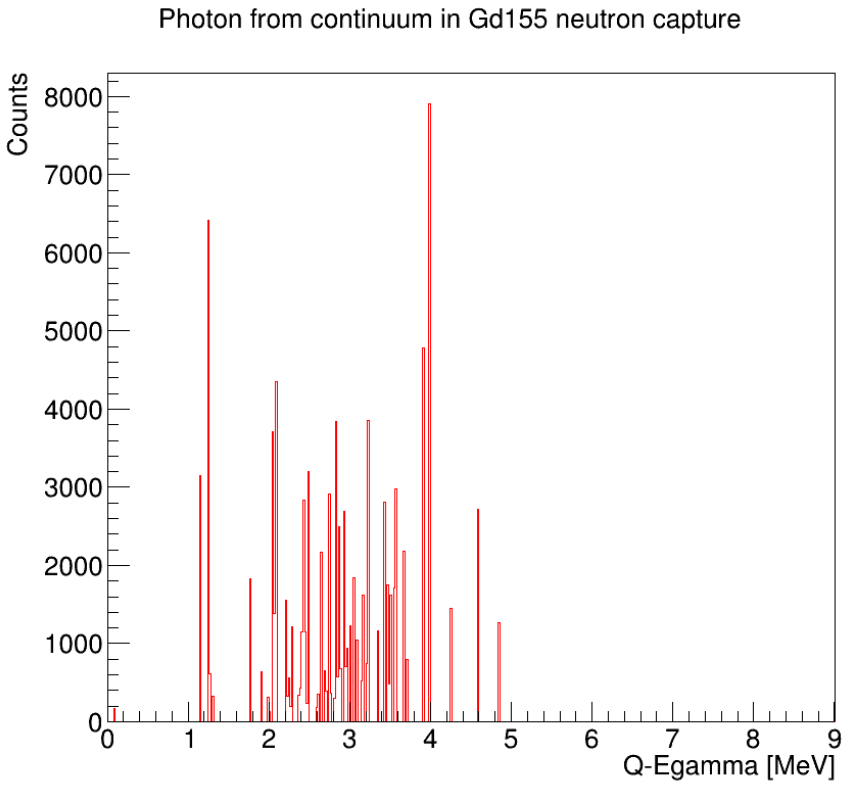

Figure 4.14: Excited states reached at first photon emission in ^{155}Gd(n,γ) PHITS simulation.

However, if one randomly selects an initial excited state using the PCA, the double hump in the multiplicity distribution disappears, as shown in Figure 4.15 (this case is called No spin considerations), which is expected because the declared transition probabilities (those found in ENSDF) already exclude the forbidden transitions, as they reproduce the expected physical outcomes. If one does not allow transitions with a difference in angular momenta of more than three units (the case called Spin considerations in Figure 4.15), the multiplicity distribution found is also valid. It is unclear though, why cascades of about ten gammas are more frequent in the case of the Spin considerations. Potentially, this comes from the fact that there are data artifacts within the PHITS data such as declaring a decay to the state below, whenever ENSDF declares no decay for that particular state, and this could bias the number of emitted photons. It can also be noted that the case of No spin considerations allows cascades of up to 21 photons, which suggests that declaring transitions towards the immediately lower state can produce an overestimation of the maximum number of emitted gammas.

To conclude on the multiplicity, it can be seen on Table 4.1 that the Spin considerations decreases the average number of emitted gammas with respect to No spin considerations, and both of them produce fewer photons per event compared to the EGM PHITS simula-

tion. Nevertheless, all those values are still significantly higher than what is declared by the JEFF-3.3, ENDF/B-VIII.0 and JENDL-4.0 libraries, in MF=6, MT=102, which indicates that a simple algorithm that would only follow the transitions declared in ENSDF is insufficient to produce realistic (n,γ) reactions, with regards to the photon multiplicity.

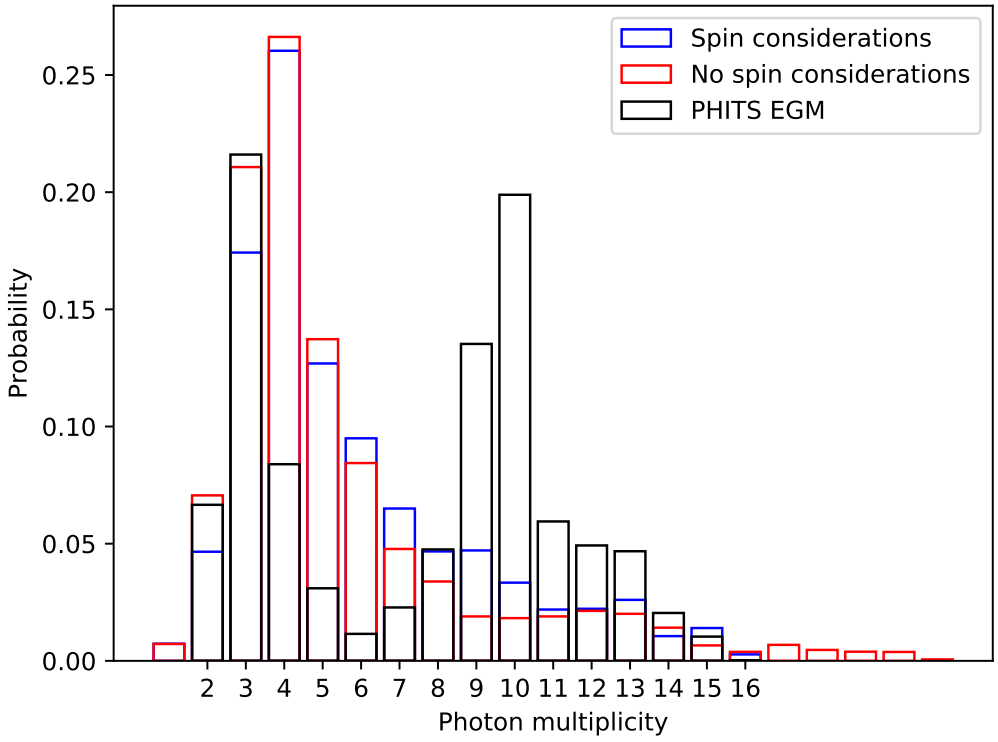

Figure 4.15: Multiplicity obtained when following ENSDF decay scheme of ^{156}Gd found in PHITS source code. Spin considerations disallow transitions of $|\Delta J|>3$.

Gamma spectrum from ENSDF decay scheme

The photon spectra of ^{155}Gd(n,γ) with and without the spin considerations shown on Figure 4.16 confirms the importance of considering the difference in angular momentum of the gamma transitions. Indeed, the energy range associated to the rotational band is without photons in the case of Spin considerations, whereas the case No spin considerations still produces photons. Another noticeable aspect is the relatively flat profile of the higher energy photons, which can be explained by the uniform sampling of the destination states. The deviation from the flat profile is explained by the fact that in every event the cascade is simulated as suggested by the ENSDF decay scheme, which accounts for the significantly higher emission of lower energy photons.

The creation of the algorithm that reads the PHITS data and produces the game of chance to simulate the gamma cascades evolved in parallel ways: it was attempted to consider the gamma decay scheme from the graph theory point of view, in which a recursion algorithm determines all the possible paths to reach the ground state. This

Source	γ multiplicity at 10^{-5} eV
JEFF-3.3	3.99
ENDF/B-VIII.0	3.92
JENDL-4.0	4.05
Spin considerations	5.87
No spin considerations	6.40
PHITS EGM	7.38

Table 4.1: Comparison of the average number of emitted photons in the ^{155}Gd(n,γ) reaction

formalism allows to easily determine the paths of a given length or that go through a specific excited state. It also inspired the aforementioned algorithm that is described in Figure 4.7.

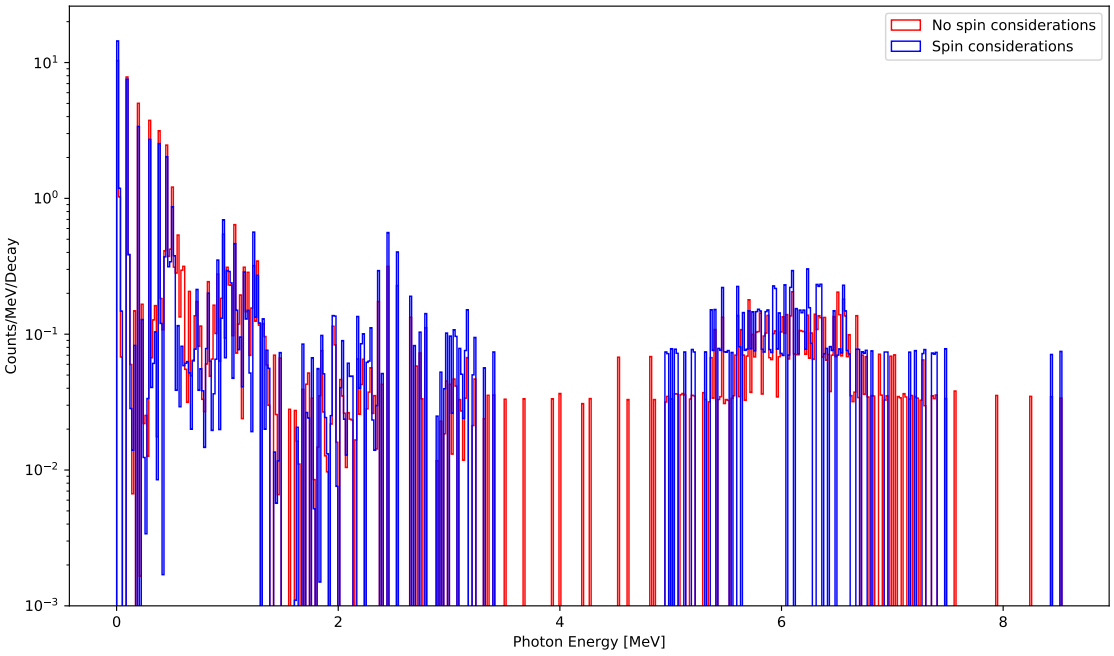

Figure 4.16: Photon spectrum obtained when following ENSDF decay scheme of ^{156}Gd found in PHITS source code. Spin considerations impede transitions of $|\Delta J|>3$.

^{198}Hg anomaly

Once the case of gadolinium had been sufficiently understood, the full library of nuclides within the PHITS data was tested, by means of implementing EGM simulations and checking weather the produced gamma multiplicity presented two maxima. It was found that the gamma multiplicity distribution of ^{198}Hg(n,γ) presents two maxima, and indeed the ^{199}Hg ENSDF data suggests the existence of a rotational band. However, as can be observed in Figure 4.17, the Spin considerations algorithm does not produce a multiplicity

distribution clearly fostering the 4.4 average gamma multiplicity that is declared in JEFF-3.3 for thermal capture in MF=6, MT=102. This might be due to the way the PHITS data is constructed, where the information gaps of the adopted levels of ENSDF are filled by declaring decays to the closest lower energy state. It is possible however, to condense this data artifacts by detecting the schemes of the type N→N-1→N-2→...→M, and replacing them by N→M. This was attempted by introducing another constraint in the algorithm which resulted in a slight improvement but it is not necessarily realistic from the phenomenological point of view.

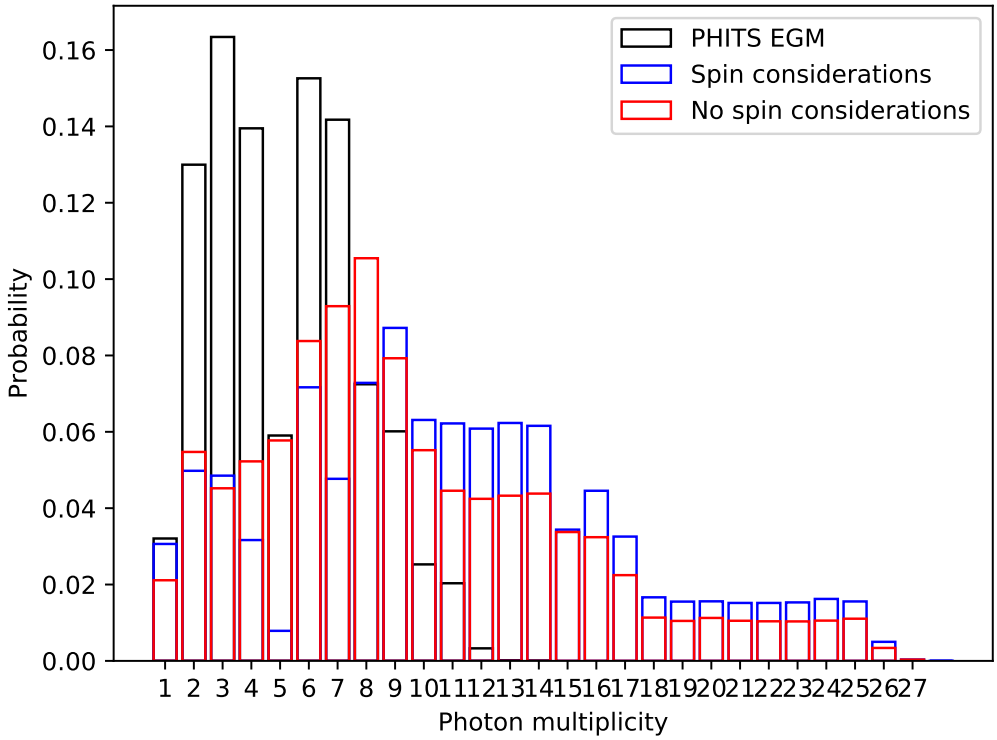

Figure 4.17: ^{198}Hg(n,γ) also yields a double hump distribution but the spin considerations do not produce a more realistic multiplicity distribution.

4.6 Case of ^{40}Ca(n,γ)

In the context of oil exploration, the reaction ^{40}Ca(n,γ) is used to detect porous formations by means of neutron irradiation and gamma ray detection. The modelling of this detection setup has been studied by M.L. Mauborgne *et al.* in ref. [31], showing that the major obstacles found may be caused by missing or inaccurate cross sections, one of them being the absence of the primary gamma of 6.42 MeV coming from ^{40}Ca(n,γ) (not crucial for reactor simulations). Indeed, as can be observed in Figure 4.18, the sought after peak at 6.42 MeV, which serves as a signature for the presence of calcium, is not declared in ENDF/B-VIII.0, nor in TENDL21, and both declare discrete emission peaks at low energies, up to 3.20 MeV and 2.96 MeV respectively, in addition to the continuous spectrum

Source	γ multiplicity at 10^{-5} eV
JEFF-3.3 MF=6	4.44
ENDF/B-VIII.0 MF=12	3.54
JENDL-5 MF=6	2.63
Spin considerations	5.87
No spin considerations	6.40
PHITS EGM	7.38

Table 4.2: Comparison between the photon yields for the ^{198}Hg(n,γ) reaction declared in MT=102, and PHITS and PCA simulations

expected from the decays from the quasi-continuum. The case of ENDF/B-VI.4 does not present a continuous spectrum but declares emission peaks that match exactly to those of the EGAF library. In this situation, the oil exploration team concludes that the modelling of the porous formations yields better coherence with what is physically expected when older data is used. It should be noted that the data in ENDF/B-VI.4 describes natural calcium (Ca-nat), whereas EGAF, ENDF/B-VIII.0 and TENDL21 describe the nucleus of ^{40}Ca, present at 97% in Ca-nat.

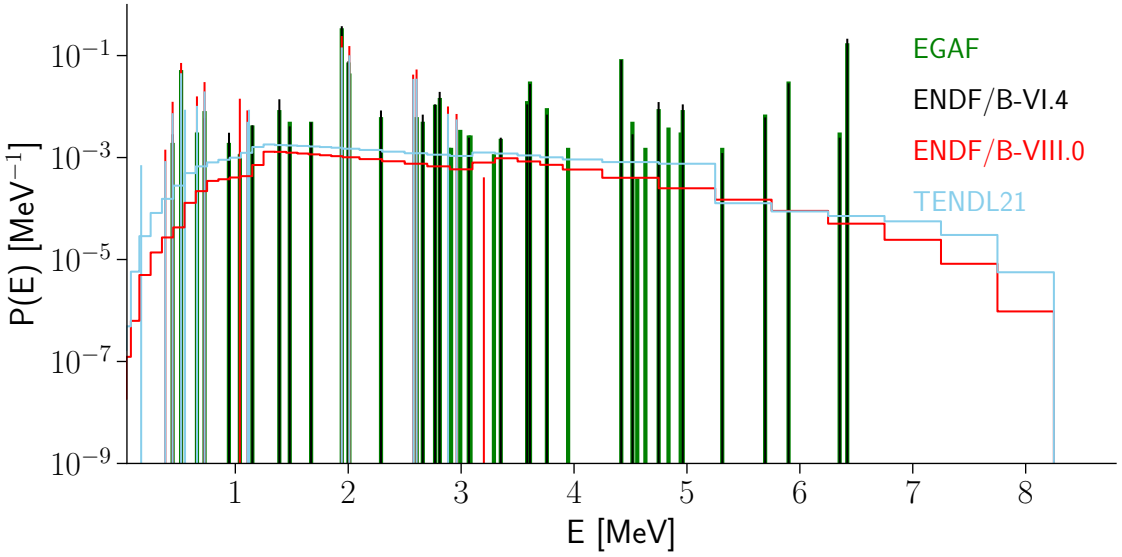

Figure 4.18: Spectra of gamma production from ^{40}Ca(n,γ) according to different nuclear data sources. High energy peaks are only present in ENDF/B-VI.4 and EGAF.

The obstacle presented here falls within the scope of this PhD thesis as there is a need of extending the nuclear data for more precise modelling. The SNGA was used to test the ^{40}Ca(n,γ) reaction, by means of exploiting the structure data found in the ENSDF (N,G) E=TH dataset of ^{41}Ca. The 6.42 MeV gamma is declared in ENSDF as the highest intensity decay from the initial state post neutron capture at 8.36 MeV with spin-parity $J^\pi = 1/2^+$. The level reached with the emission of the 6.42 MeV gamma is at 1.94 MeV with spin-parity $J^\pi = 3/2^-$, and decays to the ground state of spin-parity $J^\pi = 7/2^-$.

The spin-parity values indicate that one-photon events are highly unlikely as $|J_i - J_f| =$

3. This shows the limits of the SNGA because one of its instructions is to produce one-photon events 1% of the time as can be seen in Figure 4.19 with the presence of the peak at 8.36 MeV. Another bias of the SNGA is the conditional probability of sampling from MF=6 after having sampled previously from MF=6, for the gamma emissions from the quasi-continuum. As can be observed in Figure 4.19, the discrete emission peaks are the dominant decay mode with respect to the continuous spectrum. This is because the cumulative probability found in ENSDF of gamma emission that brings the initially excited nucleus ^{41}Ca* to one of its well defined excited states is 85%, which means that the continuous shape of the spectrum can be underestimated because of how the SNGA is constructed. Nevertheless, the emission peak at 6.42 MeV is well represented, and the intensity of the peak at 1.94 MeV suggests the correlation between the two photons. It is expected that the intensity of the latter is higher than that of the former as other decays bring the nucleus to the 1.94 MeV level.

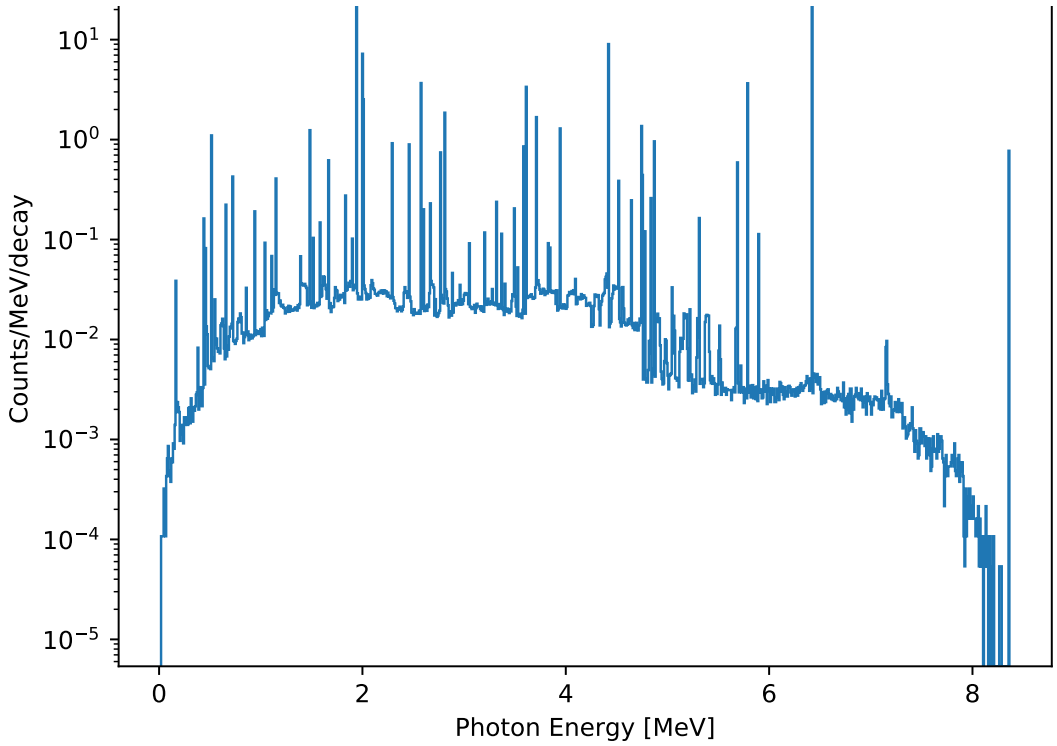

Figure 4.19: Spectrum of gamma production from ^{40}Ca(n,γ) produced by the SNGA.

The biases found with the test of ^{40}Ca(n,γ) using the SNGA suggest that mass considerations, as well as spin considerations, are needed for more realistic spectra. The mass of the absorbing nucleus has an indirect correlation with the energy of the excited states, which implies that the primary gammas bringing the nucleus to its well defined states become the main decay mode for light nuclei. Additionally, the one-photon decay should only be allowed if $|J_i - J_f| < 3$.

4.7 Discussion and perspectives on the analog simulation of (n,γ)

In this chapter, the study of the neutron capture reaction is done from the theoretical point of view, by considering the aspects of the quasi-continuum of states and the well known excited states, and from the empirical point of view, by analysing the outcomes of the reference Monte Carlo code for (n,γ) reactions, DICEBOX. It can be concluded that the existence of the quasi-continuum of states, in particular for heavy nuclei, and the influence of the incident neutron energy on the resonances for primary gamma emissions post neutron capture, are two characteristics of the (n,γ) reaction that generate a probability space that is unpractical to store as raw data. A solution for this is to create an analytical model to generate the states of the quasi continuum according to the incident neutron energy, as is done by DICEBOX. The example of ^{95}Mo(n,γ) simulated by DICEBOX is shown on Figure 4.20 where the gamma spectra are plotted according to the multiplicity of the event and the order of emission. It can be observed clearly that the spectra have a continuous component accompanied with discrete emission peaks, corresponding respectively to the emissions that maintain the nucleus in its quasi-continuum of states post gamma emission, and to gamma emissions that bring the nucleus to one of its excited states.

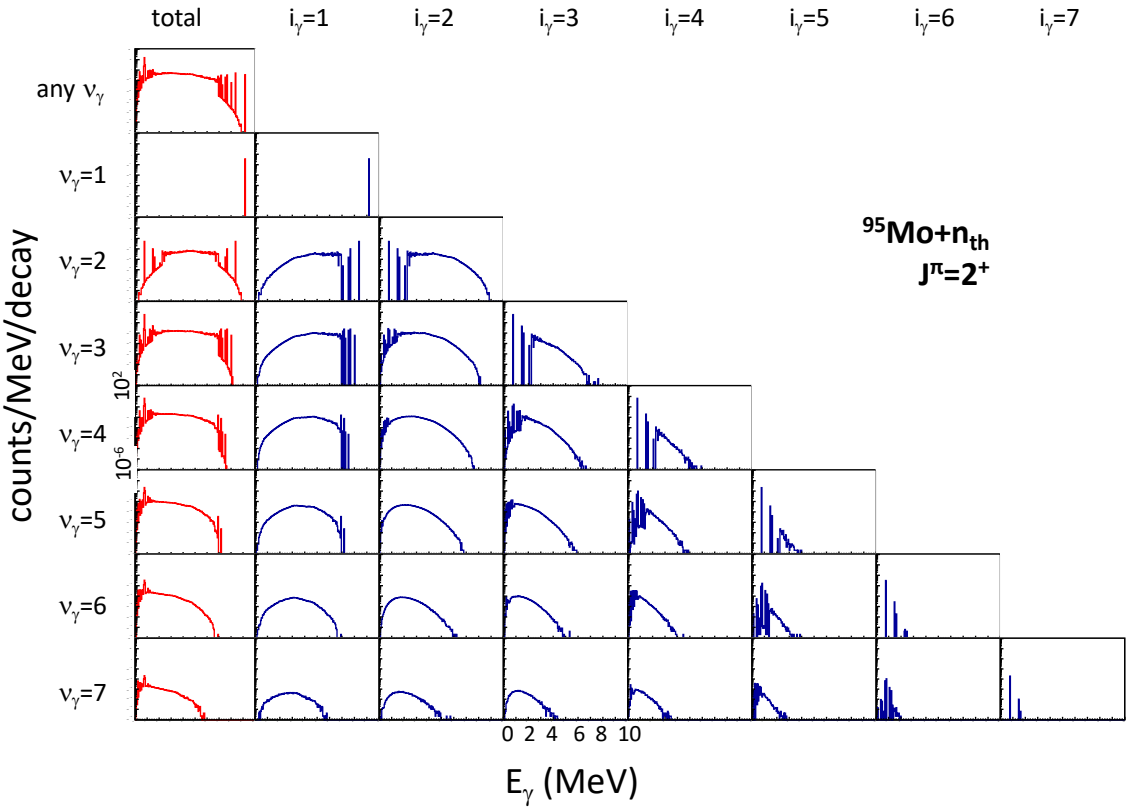

Figure 4.20: Gamma spectra of ^{95}Mo(n,γ) simulated by DICEBOX according to gamma multiplicity and order of emission.

The sampling of the continuous spectra stored in the nuclear evaluations, in MF=6 MT=102, was attempted in order to skip the generation of states. The averaged spectra found in MF=6 MT=102, are listed according to the neutron incident energy and are intended to reproduce the expected gamma emissions from the quasi-continuum of states. In this sense, both obstacles (generation of states and influence of incident energy) can be addressed by relying on the available nuclear data. In order to implement such an

algorithm, several aspects must be taken into account, mainly the criteria to stop sampling from the distributions and start simulating the gamma cascades with the structure data of the ENSDF or RIPL-3 libraries, as well as defining the rules for conserving total energy during the distribution sampling.

The Simplified (N,G) Algorithm (SNGA) was developed during this PhD thesis to implement analog Monte Carlo simulations of the gamma cascades of the (n,γ) reaction by means of random sampling of the MF=6 MT=102 distributions to account for the gamma emissions from the quasi-continuum, and also by following the decay schemes stored in the RIPL-3 structure data. The SNGA has yielded photon production spectra and gamma multiplicities with general agreement to those of DICEBOX, in addition to the fact that all events conserve total energy. However, the SNGA relies on somewhat arbitrary parameters that are not adapted to all nuclei, and the absence of a critical energy to separate the states of the quasi-continuum from the well known excited states results in unwanted biases. It can be concluded that the spectra shown on Figure 4.20 cannot be reproduced by the SNGA, as analytical models are need.

In terms of nuclear data, when the ENDF-6 format is replaced by GNDS, it will be possible to store the parameters that characterize best this reaction. For instance, the critical energy can be set so that continuous distributions are properly generated by analytical methods (these distributions also need a set of parameters to be generated). It was also found during this study that so-called rotational bands bias the gamma multiplicity, so the states that belong to the band could be flagged to be avoided, or spin considerations can be included in the algorithms, provided the spin are declared in the data.

5 - Proposal for analog simulation of (n,2n) reactions

5.1 Brief description of the (n,2n) reaction and its associated nuclear data

The objective of this chapter is to apply the lessons learned from the neutron-induced inelastic scattering and the neutron capture reactions previously explained to create a methodology for implementing an analog Monte Carlo simulation of the ^{A}X(n,2n)$^{A-1}$X reaction. This is a threshold reaction that requires a significant amount of input energy, on the order of tens of MeV for light nuclei, which generally implies that there are several possibilities for the attribution of the available energy to the outgoing particles; these are two neutrons, one residual nucleus, and a gamma cascade can occur in one or more of the steps of the decay process towards the final state of $^{A-1}$X. For the attribution of energies one needs to determine which reaction mechanism takes place during the neutron interaction, and here 3 processes are briefly presented.

A first possibility for the (n,2n) mechanism is to consider it as a stripping reaction, where the incoming neutron strips one neutron from the target nucleus, in which case the kinematical approach is that of a two-body reaction in the outgoing channel: the stripped residual nucleus and a di-neutron (a neutron pair). One can expect that the direct reaction of the stripping process shows clear anisotropies in the di-neutron emission and results in a flat spectrum for the separation of the di-neutron into two neutrons. In the center of mass of the di-neutron, both neutrons should be emitted with the same energies, but in the laboratory frame the Lorentz boost should be measurable. The reaction Q-value of such a process, considering null binding energy of the di-neutron, would correspond to the neutron separation energy S_n as follows

$$\begin{aligned} Q &= M_n + M(^{A}X) - [2M_n + M(^{A-1}X)] \\ &= M(^{A}X) - M_n - M(^{A-1}X) \\ &= S_n(^{A}X) \end{aligned} \tag{5.1}$$

Another possibility is to consider that the neutron is absorbed by the target nucleus ^{A}X, forming a compound nucleus of high excitation energy $^{A+1}$X*, and one could expect the two neutrons to be emitted isotropically in a so-called evaporation spectrum. The multi-step process would be the following

$$n + {}^{A}X \rightarrow {}^{A+1}X^* \rightarrow {}^{A}X^* + n' \rightarrow {}^{A-1}X^* + n' + n'' \tag{5.2}$$

where n' is emitted by $^{A+1}X^*$, and n'' is emitted by $^{A}X^*$, which justifies that one can consider two-body kinematics in the outgoing channel for the successive neutron emissions. The relevant reaction Q-values would depend on the excitation energy E_{exc} as follows

$$\begin{aligned} Q_1 &= M(^{A+1}X) + E_{exc}(^{A+1}X) - [M(^{A}X) + E_{exc}(^{A}X) + M_n] \\ Q_2 &= M(^{A}X) + E_{exc}(^{A}X) - [M(^{A-1}X) + E_{exc}(^{A-1}X) + M_n] \end{aligned} \tag{5.3}$$

A variant of the compound nucleus hypothesis is to regard the (n,2n) reaction as an inelastic reaction that brings ^{A}X to an excited state higher than its neutron separation

energy S_n, and the decay proceeds by the emission of a neutron and a gamma cascade of $^{A-1}$X*. Considering the inelastic process at high energies, it can be expected for the scattered neutron to exhibit anisotropies of emission and a flat spectrum, whereas for the second neutron it can be expected to have isotropic emission from an evaporation spectrum. It is important to note that the three processes described here can be treated with two-body kinematics. In particular, the inelastic hypothesis would yield the following steps

$$n + {}^{A}X \rightarrow {}^{A}X^* + n' \rightarrow {}^{A-1}X^* + n' + n'' \tag{5.4}$$

where n' is the scattered neutron and n'' is emitted by $^{A}X^*$. The reaction Q-value associated to this inelastic hypothesis can be written as Q_2 of equation 5.3, with different values for the excitation energies. The difference between the scenarii is thus observed in the outcome spectra and emission angles of the neutrons.

The potential gamma cascades can occur at any given step regardless of the mechanism, so for the sake of simplicity and knowing the interactions are extremely fast, here the gamma decays will be used to account for the remaining available energy after the emission of the two neutrons and the attribution of the kinetic energy of the emitting nucleus. That is to say, only the gamma cascades associated to $^{A-1}$X will be considered.

The focus in this chapter is on the ^{19}F(n,2n)^{18}F reaction because ^{19}F is the only nuclide in the JEFF-3.3 library that contains in its evaluation file four different probability distributions functions (pdf) for the outgoing particles. In other words, one can find in file MF=6 section MT=16 two different pdf for the emission of the two neutrons, as well as the pdf of the residual nucleus ^{18}F and of the photons emitted by ^{18}F*. The spectrum of the first neutron has a flattened bell profile, which corresponds to the spectrum of a scattered neutron. The second neutron is attributed an evaporation spectrum, which reaffirms the inelastic scattering hypothesis in the particular case of this nuclide.

In terms of the analog Monte Carlo implementation of the (n,2n) reaction, one can sample the energies of each neutron and of ^{18}F from the pdfs of MF=6, followed by a gamma cascade simulation based on the algorithms previously developed for the inelastic or capture reactions. The procedure will be to first sample without constraints to show the non-conservation of total energy, then the order of sampling will be tested to asses the impact on the kinematics in order to conclude on the most adapted method according to the available data.

5.2 Monte Carlo simulations of the (n,2n) reaction

In this section the focus is on ^{19}F(n,2n)^{18}F and on the gamma cascade that can be produced from the (^{18}F*) system. The nuclear data used here for this reaction is found in MF=6, MT=16 of JEFF-3.3, and was tested from the perspectives of the analog and non-analog Monte Carlo simulations using an incident kinetic energy T_n = 20 MeV (the highest energy of MT=16 for which there are associated distributions for the outgoing particles). The distributions at 20 MeV correspond, in order, to the first emitted neutron n', the second emitted neutron n'', the ^{18}F nucleus and the photons. In the non-analog case the distributions were randomly sampled, meaning that no correlations are expected between the energies of the outgoing particles. Also, only one photon energy is sampled from its distribution. In the analog case the distributions were sampled with the objective

of creating a correlation between the sampled energies so that total energy is conserved. In addition, the gamma cascades were simulated by following the ENSDF decay schemes of the residual nucleus. In both analog and non-analog cases, the number of simulated (n,2n) events is 10^6.

5.2.1 Non-analog case

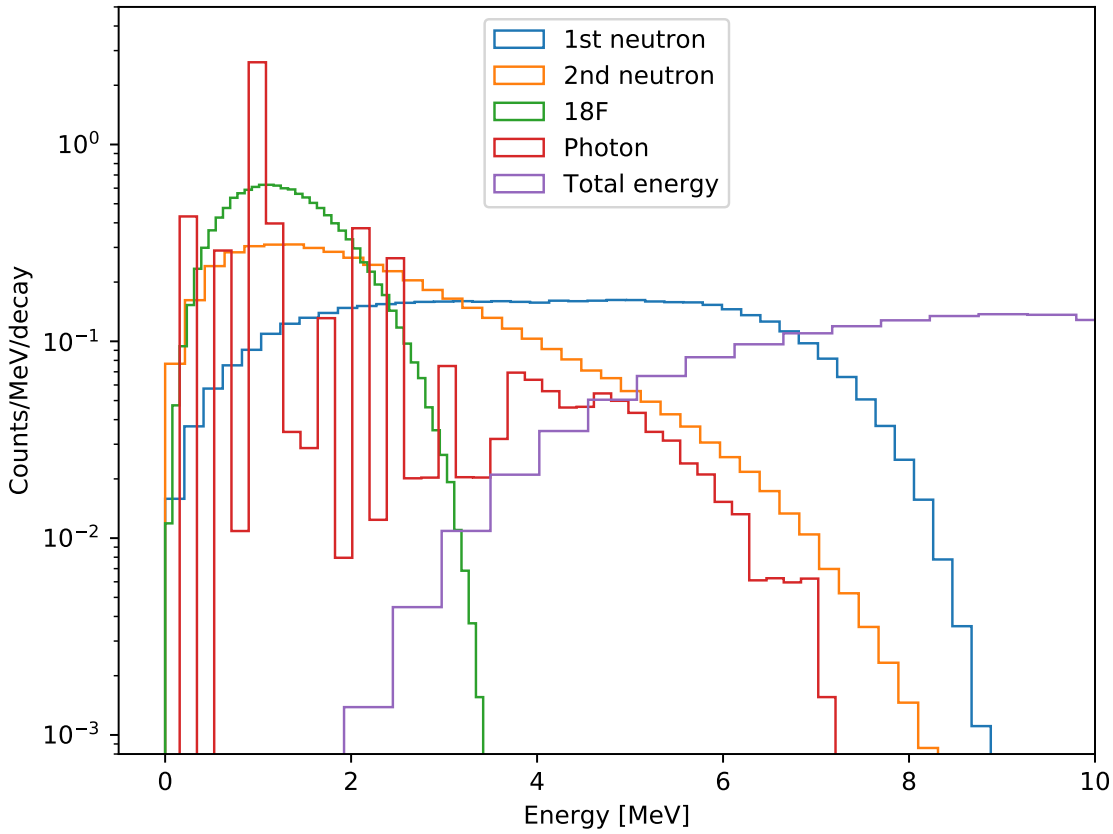

Figure 5.1: Total energy per (n,2n) event is not conserved when MF=6 MT=16 distributions are sampled randomly. This is the case of no instructions given, for 10^6 events.

When no instructions are given, *i.e.* the sampling of the distributions is done randomly, it means that the shape of the MF=6 distributions should appear if the iterations are sufficient and if the energy bins are the same as in the distribution. As can be observed on Figure 5.1, when the distributions are sampled randomly, the sum of the four sampled energies $E_{n'}$, $E_{n''}$, E_F and E_γ has a significant component under and above the available energy of the reaction which is unexpected as this is a threshold reaction. The maximum of the curve called Total Energy corresponds roughly to the available energy, which suggests that the average energy of the reaction is a good approximation of the available energy. Nevertheless, there is a significant amount of events with over- and underestimations of total energy. One can also notice that the photon spectrum is continuous with the additional presence of emission peaks. This shape is intended to reproduce the continuous aspect of the highly energetic gammas, and the discrete aspect of the expected gamma emissions from the state transitions.

The shape of the spectra shown on Figure 5.1 indicate that the (n,2n) mechanism for the case of ^{19}F corresponds best to the inelastic hypothesis, mentioned in the introduction of this chapter. Indeed, the flat profile of the first neutron suggests that the neutron is scattered post interaction, and the evaporation spectrum of the second neutron is coherent with the hypothesis that the inelastic scattering excites ^{19}F to an energy higher than the neutron separation energy S_n. This justifies the order of sampling chosen for the analog simulation, discussed in the next subsection, as the order of sampling needs to replicate the physical process, that is to say, first there is a scattered neutron, then there is another neutron evaporated from the excited recoil, and finally the gamma cascade takes place considering the decrease in available energy due to the kinetic energy of n', n'' and ^{18}F*.

5.2.2 Analog case

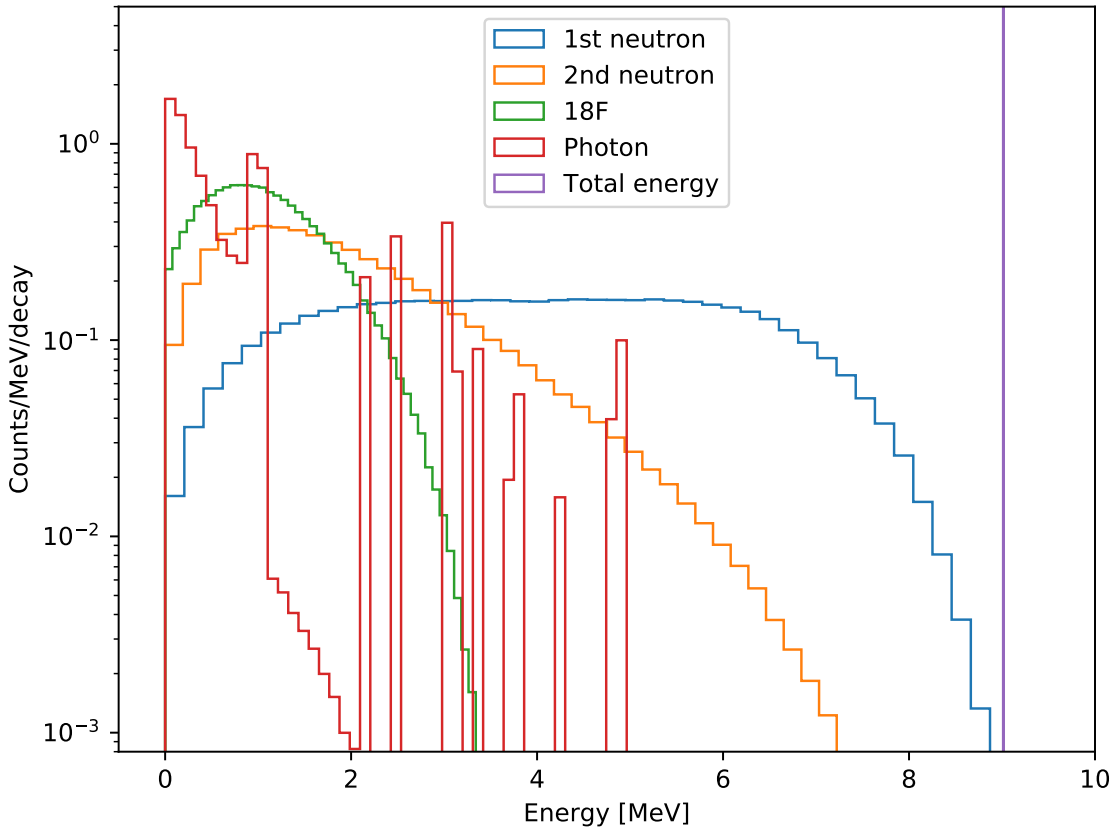

Figure 5.2: Total energy is conserved when the sampling of MF=6 MT=16 is done considering a decrease in available energy at each sampling for the ^{19}F(n,2n) reaction.

Taking into account the lessons learned from the neutron-induced inelastic and capture reactions, the algorithm hereafter called N2NA for (N,2N) Algorithm, was created with the objective of implementing an analog Monte Carlo simulation of the ^{19}F(n,2n) reaction where each (n,2n) event conserves total energy. The N2NA produces the spectra shown on Figure 5.2, and a complete flow chart of the algorithm is provided at the end of this chapter. A brief summary of the instructions of the algorithm is listed below

1. Sample the energy $E_{n'}$ from the n' MF=6 distribution

2. Decrease by $E_{n'}$ the available energy ($E_{av} = T_n + \frac{1+AWR}{AWR}Q - E_{n'}$)
3. Sample the energy $E_{n''} < E_{av}$ from the n'' MF=6 distribution
4. $E_{av} = E_{av} - E_{n''}$
5. Sample the energy $E_F < E_{av}$ from the ^{18}F MF=6 distribution
6. $E_{av} = E_{av} - E_F$
7. Find the excited state of ^{18}F with the highest energy lower than E_{av} and emit photon to reach the level
8. Simulate the gamma cascade using the ENSDF decay scheme starting from the level found in the previous step if the level is not the ground state

It can be observed in Figure 5.2 that the total energy per (n,2n) event is concentrated on the energy bin just above 9 MeV. This is the expected result by construction of the N2NA. Indeed, according to MF=3, MT=16 of JEFF-3.3, the Q-value of this particular reaction is $Q = -10.431$ MeV and the mass of ^{19}F in units of neutron mass is AWR=18.835. The available energy in the LAB frame for an incident neutron energy of $T_n = 20$ MeV is

$$E_{av} = 20 + \frac{1 + 18.835}{18.835}(-10.431) = 9.015 \text{ MeV} \tag{5.5}$$

It should be noted that the shape of the spectra of n', n'' and ^{18}F are in very good agreement with those shown in the non-analog case. The most noticeable difference regarding these spectra is the maximum energy of the second neutron: in the non-analog case there are neutrons evaporated with a maximum energy of more than 9 MeV, whereas in the analog case the maximum energy is less than 9 MeV, due to the decrease in available energy after the sampling of the first neutron set within the N2NA.

Regarding the gamma spectrum, the maximum declared energy is more than 8 MeV in the non-analog case and less than 5 MeV in the analog case. The structure data used for the simulation of gamma cascades in the N2NA is taken from the source data of PHITS, where the highest gamma transition energy declared is 5.6 MeV, corresponding to a direct decay to the ground state from the 5.6 MeV excited state. However, ENSDF and RIPL-3 declare gamma transition energies for ^{18}F of up to 7.6 MeV, which is still less than the maximum energy of 8 MeV of the MF=6 gamma spectrum.

The extreme case of $E_{av} = 9.015 - E_{n'} - E_{n''} - E_{^{18}F} > 5.6$ MeV can yield events with total energy lower than 9.015 MeV because the gamma transitions cannot account for more than 5.6 MeV. It can be seen in Figure 5.2 from the Total Energy distribution that there are no events where total energy is under its expected value, in addition to the fact that there are no gamma transitions of 5.6 MeV. This is to say that the extreme case of $E_{av} > 5.6$ MeV before the simulation of the gamma cascade is highly unlikely. In terms of gamma multiplicity, at 20 MeV, the dedicated section for gammas declares a photon yield of 1.2118 and the N2NA produces on average 2.06 photons per (n,2n) event.

5.3 Comparison with the PHITS analog simulation

The nuclear evaluations of ^{19}F in the JENDL-4.0 and JENDL-5 libraries, store one distribution with a neutron multiplicity of 2 in file MF=6, section MT=16, regarding the

(n,2n) product energy-angle distributions. That is to say that the data used by PHITS will result in the same spectrum for both neutrons, as can be observed in Figure 5.3, where the maximum energy of the neutrons is less than the previously calculated available energy $E_{av} = 9.015$ MeV. The $5{\times}10^5$ neutron histories simulated using the Event Generator Mode of PHITS produced (n,2n) events where the emitted particles are correlated in the sense that total energy is conserved, and the gamma cascade is realistic as it follows the ENSDF decay scheme.

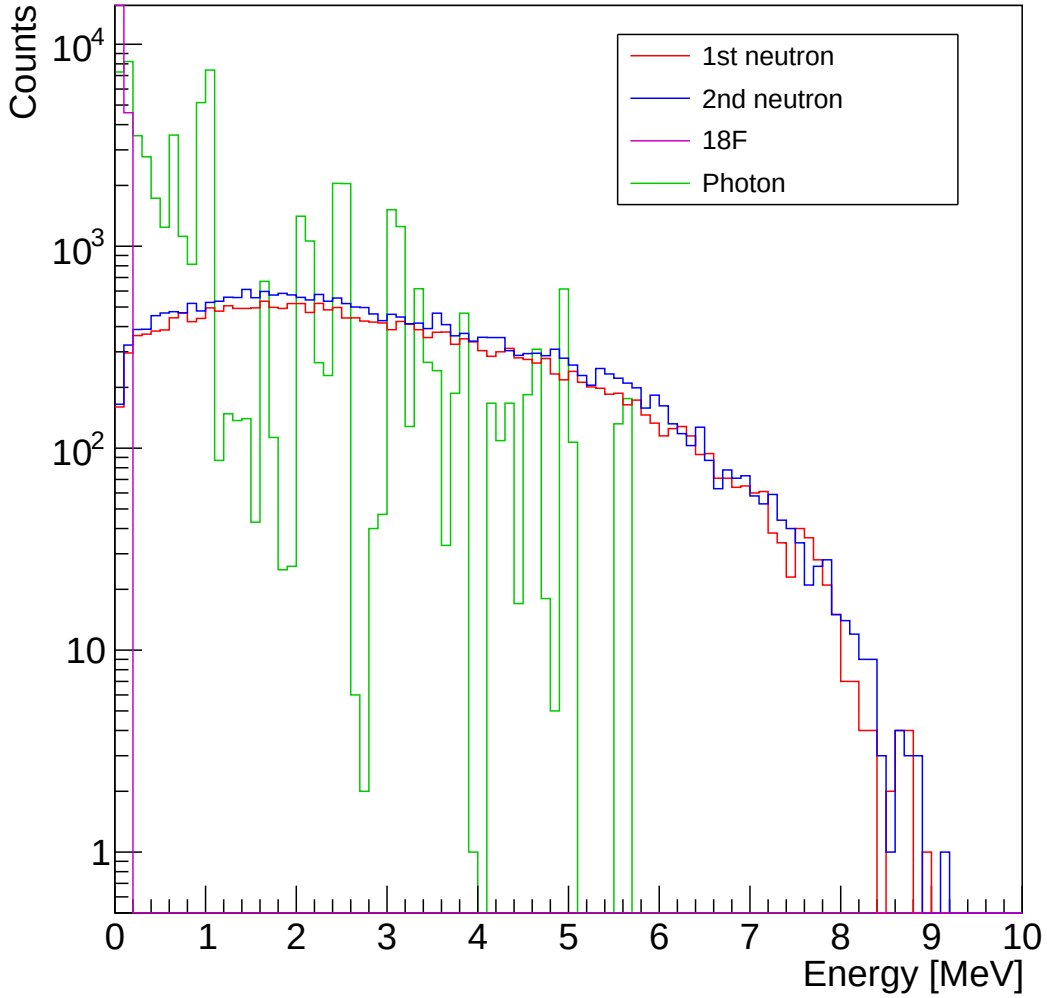

Figure 5.3: PHITS simulation of ^{19}F(n,2n) with Event Generator Mode on for $5{\times}10^5$ neutron histories.

It can also be noticed that the gamma spectrum of Figure 5.3 is in good agreement with the one produced by the N2NA, with the exception of the existence of the 5.6 MeV transitions towards the ground state in the PHITS simulation. The last significant difference with the previously shown spectra is the case of the energy distribution obtained for the residual nucleus ^{18}F. In the PHITS simulation, the kinetic energies of ^{18}F are all concentrated in the lowest energy bins, and indeed when one looks at the real values in the output file, the energies are on the order of tens and hundreds of keV. These values are significantly low with respect to what is declared in the JEFF-3.3 distributions, where the maximum kinetic energy of ^{18}F is 3.5 MeV. This difference might be at the origin of the

presence of the 5.6 MeV photon, because the order of emission in PHITS is the same as in the N2NA: first neutron, second neutron, residual nucleus, gamma cascade, and the residual nucleus does not decrease significantly the available energy in the case of the PHITS simulation.

The PHITS simulation, in particular the spectrum related to ^{18}F, raises the question on the validity of the distribution stored for the residual nucleus ^{18}F in MF=6, MT=16 of the JEFF-3.3 library. Indeed, a quick kinematical calculation considering classical theory and assuming the scattered neutron n' and the recoil ^{19}F share the same momentum yields the relation:

$$T_F = \frac{M_n}{M_F} T_{n'} = \frac{1}{18.835} \times 9 = 0.478 \text{ MeV}. \tag{5.6}$$

This comes from the expected correlation between the scattered neutron and the recoil, within the scope of the inelastic hypothesis. If the scattered neutron has a kinetic energy of 9 MeV, the maximum energy allowed for an incident neutron energy of 20 MeV, then the recoil ^{19}F should have a maximum kinetic energy of 478 keV. Considering that the second neutron is evaporated from the highly energetic ^{19}F*, it can be expected that the emission of the second neutron can give a boost to the residual ^{18}F. If the second neutron is emitted in the opposite orientation as that of $\vec{P_F}$, the kinetic energy of 478 keV of ^{19}F is again divided by 18. This suggests that the energy range given by the JEFF-3.3 library goes to higher energies than it should be possible.

These kinematical considerations can have an impact on the decision of the order of the sampling in the N2NA, because of the necessary correlation between the scattered neutron and the recoil ^{19}F in the scope of the inelastic hypothesis. In the N2NA, the energy of the residual is sampled after having emitted the second neutron, which does not account for the first correlation.

In any case, the objective of this part of the PhD was to explore all the available data for the simulation of the (n,2n) reaction, while also finding the limitations and the possibilities for improvement. However, it can be said that the stored spectrum for the residual ^{18}F and for the the gammas are not what is expected in terms of energy range, as the maximum energies seem to be higher than expected.

5.4 PATMOS simulation

PATMOS is a Monte Carlo neutron transport prototype (or mini-app) under development at CEA [32]. It was possible, during the course of this PhD, to have the opportunity to be in contact with the developing team and to have access to testable and executable files of PATMOS. The test consisted in choosing the target nucleus, an incident neutron energy and the produced particles, and verifying the correct spectrum is obtained. The challenge was to tell the executable that 2 samplings should be done, for the case of ^{19}F(n,2n), and the spectra for the two neutrons can be seen on Figure 5.4. Unfortunately, PATMOS can only transport neutrons for the moment so the residual and the photons cannot be simulated yet. The spectra obtained from the PATMOS simulation are in coherence with the non-analog case, which is as expected, because PATMOS implements a sampling from the two neutron distributions, the same as what was done in the non-analog scenario, where correlations are not taken into consideration.

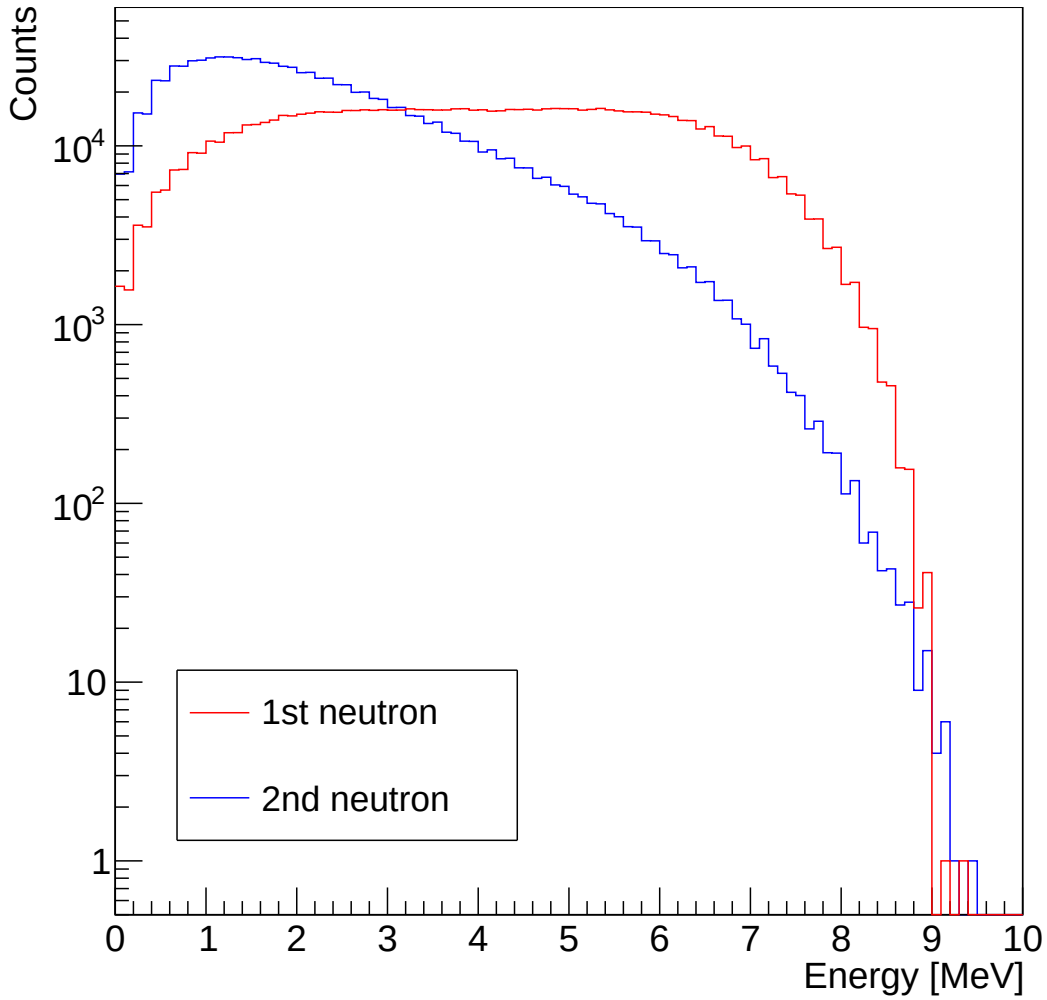

Figure 5.4: PATMOS simulation of ^{19}F(n,2n).

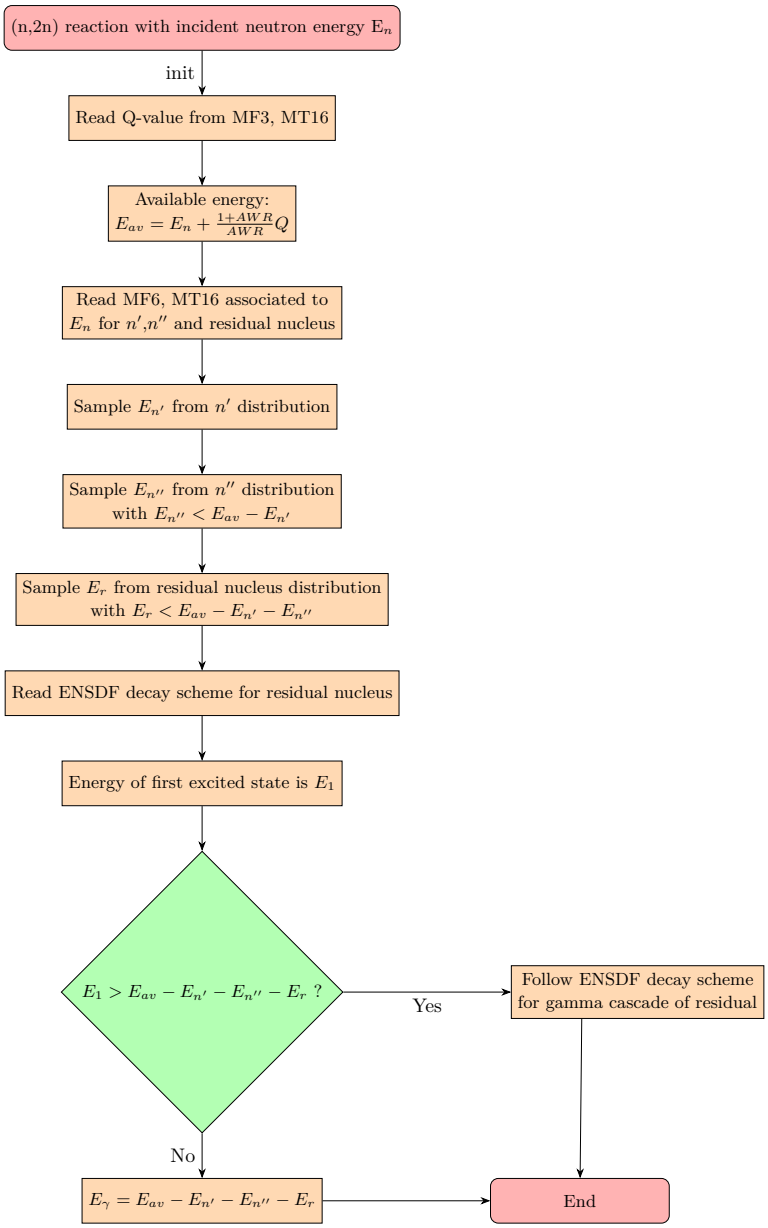

Figure 5.5: Flow chart for the N2NA.

6 - Conclusion and perspectives

The analog simulation of nuclear reactions that produce more than two particles requires specialized data to describe the different modes of particle production, and a specialized algorithm adapted to the available nuclear data for reproducing the expected reaction outcomes. There are reaction outcomes that the nuclear data can reproduce by means of sampling a probability distribution function, in which case the algorithm has few tasks to implement. There are reaction outcomes that require the implementation of analytical models and/or creating games of chance so that the Monte Carlo method can reproduce the reaction outcomes. With this in mind, the neutron-induced inelastic and capture reactions, as well as the (n,2n) reaction, were studied from the perspective of the analog Monte Carlo simulation by means of exploring the existing evaluated nuclear data, and also by implementing simulations using TRIPOLI-4® developed at the Commissariat à l'Énérgie Atomique, PHITS developed at the Japanese Atomic Energy Agency, DICEBOX distributed by the International Atomic Energy Agency, as wells as simplified algorithms that were developed in the framework of this PhD for very specific tasks: these are the Simplified (N,G) Algorithm (SNGA) and the (N,2N) Algorithm (N2NA).

This PhD takes its origins from the possibilities that were opened by the FIFRELIN and FREYA projects. FIFRELIN is used in the form of external files containing neutron and photon production data that result from a fission event, so that there is no need of online sampling which would be too time-consuming. For FREYA, the process is online for the sampling of neutrons. The objective of the projects was to include the possibility of having an analog implementation of the fission reaction in TRIPOLI-4®. In the fission reaction, there is a variable number of neutrons and photons that are emitted during the scission process, and also by the fission fragments. The idea with FIFRELIN and FREYA is to produce a library of individual and realistic fission events, from which a Monte Carlo transport code such as TRIPOLI-4® can sample events and use them as new neutron sources in the geometry. The events of the library are produced from fission models capable of generating a variable number of photons and neutrons with conservation of total energy and momentum. Also, the events contain the nature of the fission fragments and the neutrons and photons emitted by them, so that every particle is correlated.

There have been improvements in the ENDF-6 nuclear data format with regards to the analog simulation capabilities, particularly for fission reactions in the ENDF/B-VIII.0 versions of the ^{235}U, ^{238}U and ^{239}Pu evaluations. The newest versions have, for example, a neutron spectrum associated to each of the defined neutron multiplicities. In other words, if the fission event sets a neutron multiplicity of 1, the declared spectrum corresponds to the possible energies that can be attributed to that of one neutron. In case the sampled number of neutrons is more than one, there is one neutron spectrum associated to all the neutrons to be emitted. Still, when multiple neutrons share the same spectrum, a simulation based on this data cannot be considered fully analog. This is to say that the amount of data grows in the sense of ever more demanding simulations, where averaged quantities are not sufficient, and this is particularly the case in an analog simulation, which is much more time-consuming than its non-analog counterpart.

The case of fission requires analytical modelling and intricate kinematical calculations, as there are several stages of the process and particles are emitted all along. In the

case of neutron-induced inelastic scattering, the process is more straightforward, as the kinematics of the scattered neutron is completely known once the angle in the center of mass is sampled, and the ensuing gamma cascade can be simulated if the structure data is provided to the Monte Carlo code for the de-excitation via discrete states.

In the framework of this PhD, the inelastic scattering was studied by implementing analog and non-analog TRIPOLI-4® simulations. The analog simulation consists in reproducing the gamma cascades associated to a nucleus that has been brought to one of its excited states by inelastic scattering, after which it decays by gamma radiation emitted during the transition between excited states. The non-analog version consists in emitting one gamma that is counted by the code as more than one using weights. In the beginning of the analysis, the focus was on ^{27}Al, as one of the differences between its JEFF-3.2 and its JEFF-3.3 evaluated files, is the presence of MF=6 (photon production energy and angle distributions) in the former and MF=12 (gamma transition energies and probabilities) in the latter.

When the Monte Carlo neutron transport code reads MF=6, it will sample one photon from the photon production energy distribution found in MF=6 and it will attribute a given particle weight, also declared within the MF=6 file, so that after a sufficient number of iterations, the total energy is conserved. This is the non-analog simulation of the gamma cascades associated to neutron-induced inelastic scattering. When the Monte Carlo neutron transport code reads the presence of MF=12, it can simulate the gamma cascade starting from the state reached by the aluminium nucleus after neutron interaction.

The first comparison that can be done is simulating many neutrons per batch, as any usual reactor simulation, and the photon production spectrum should be the same regardless of the usage of MF=6 or MF=12, as they are both supposed to produce the same averaged results. This was tested and indeed the spectra are in good agreement in terms of total and average energy. However there are differences in the height and width of the emission peaks. This is due to the fact that photons in MF=6 are defined in the center of mass reference frame (CM), so TRIPOLI-4® can calculate the Lorentz boost that increases the measured photon energy in the laboratory frame of reference (LAB), if the photon is emitted in the same orientation as the recoil nucleus. Since in MF=12 the photons are solely defined in the LAB, no calculations are implemented and the photon is simulated with the energy of the transition without kinematical corrections.

It was found that the maximum and minimum energies that can be expected from the Lorentz boost do not coincide with those of TRIPOLI-4®, the reason being that the CM from which the photons are emitted is not updated to the excited aluminium system (^{27}Al*), but rather is kept to the scattered neutron and excited aluminium ($n'+^{27}$Al*) system.

The same nuclear system was simulated using PHITS, which is specialized in nuclear reaction simulations, and its Event Generator Mode (EGM) allows analog simulations. It must be said that the precision of this Monte Carlo code is outstanding in terms of kinematics. The limits of the Lorentz boost spread match perfectly between theory and simulation results, and this calculation is done throughout the whole cascade.

The TRIPOLI-4® and PHITS simulations are the primary verification method to compare analog and non-analog simulations of the inelastic reaction. The requirements for this comparison are having both an evaluation file that contains MF=6, and another that contains MF=12. During this PhD it was possible to detect 22 evaluation files of the JEFF-3.3

library that had incomplete MF=12 (incomplete in the sense that the neutron cross section data declared more excited states than those of MF=12) and is was possible to create an additional 50 MF=12 for the nuclides that still have MF=6. There has been an evolution towards changing MF=6 by MF=12 in recent years, as MF=12 can be used to create an MF=6 but not the other way around.

The RIPL-3 library was chosen as the source for transcribing the structure data into the MF=12 data format, as it was initially attempted to use ENSDF data, and it proved to be too challenging. Indeed, it can be said that the ENSDF data is too vast in the sense that all the adopted levels are stored. This means that it is a library that gathers all the approved experimental results, which in turn means that there might be levels with different energies, with a very small difference in energy, but it is possible that they are the same level, but the transitions declared are different. The RIPL-3 library is maintained by the IAEA and is more compatible with the levels already stored in the JEFF library (in MF=3, MT=51...90), compared to ENSDF.

In the case of inelastic scattering simulation, the structure data (the excited states and the transition probabilities) are sufficient to simulate the gamma cascade, as the target nucleus does not change. When the target nucleus changes, for example in neutron capture, one cannot refer to only one evaluation file. Also, in the ENDF-6 format, the allowed number of excited states is limited to 40 plus a so-called continuum where decays from higher energy levels can be stored.

In the case of neutron capture, the excitation energy of the absorbing target reaches several MeV and for the high mass nuclei, this is already the domain of the quasi-continuum of states. It is called so because at high excitation energies the density of levels becomes very high, and the spacing between levels (states) becomes comparable to the width of the states. If there are several states to decay to, each branching has its own partial radiation width. This is the same as a branching ratio. So the states are still discrete, and every emitted photon will be discrete, but the overlap of states results in continuous spectra.

The full analog simulation of the (n,γ) reaction can be done using only nuclear data, provided that the quasi-continuum of states is not reached. This applies mostly to light nuclei. When the quasi-continuum is reached, there is an impact of the neutron incident energy on the primary gamma intensities, which means that some transitions will be fostered more than others by varying a small amount the incident energy. This is why in this PhD, the (n,γ) simulations concerned only the lowest possible energy neutrons.

The reference Monte Carlo code for the simulation of the capture reaction used in this PhD is DICEBOX, capable of generating by analytical models the excited states of the quasi-continuum that start from a given critical energy below which the excited states are known and do not overlap. The case of ^{95}Mo(n,γ) was thoroughly studied in order to create the algorithm SNGA with the objective of relying solely on the nuclear data found in JEFF-3.3 for reproducing the continuous spectrum, and in RIPL-3 for the gamma cascade of the known levels.

The SNGA reads the ENSDF data for the primary gammas, which account for the high energy peaks, reads the MF=6 MT=102 data to sample photon energies from the distribution, which accounts for the continuous shape of the spectrum, and reads the RIPL-3 data to simulate the cascade of the known levels, which accounts for the emission peaks of lower energy. The photon spectra produced by the SNGA can thus be considered an analog simulation of the capture reaction as every photon is simulated with the expected

correlations, and every capture event conserves total energy.

The improvements that can envisaged to the SNGA are the inclusion of the critical energy, as the instructions to go from the quasi-continuum to the discrete states is somewhat arbitrary. Also, it was designed mostly for heavy nuclei, where the contribution of the quasi-continuum is more significant, so mass considerations should be explored.

The specific part of the SNGA that simulates the gamma cascade of the known levels based on the structure data of RIPL-3 is a continuation of the previously developed algorithm that reads the PHITS source code data, which is a copy of the ENSDF data. The algorithm to read the PHITS data was created to test the decay schemes declared for ^{156}Gd. It was found when implementing EGM PHITS simulations of the ^{155}Gd(n,γ) reaction that the obtained gamma multiplicity has two maxima at 3 and 10, whereas the expected distribution is one maximum around 3 or 4. This unexpected gamma multiplicity can be explained by the fact that a level belonging to the ^{156}Gd rotational band is overfed in the PHITS simulation and the ensuing cascade is of 9 photons.

The rotational band is a certain range of energy where the levels have high angular momenta, generally $J > 10$, and gamma transitions between two levels that have $\Delta J > 3$ are highly unlikely. This is not the case in the PHITS simulation, where the initial state post capture by the gadolinium is at 8.54 MeV of excitation energy and with spin-parity $J^\pi = 2^-$ and a significant number of events decay to the level at 4 MeV with spin-parity $J^\pi = 16^-$. This transition is highly unlikely, yet the most frequent primary gamma of the PHITS simulation is precisely this one.

The algorithm to test the decay data stored in the PHITS source code was given the instruction to follow the decay scheme with and without considering the difference in angular momentum between the departure and arrival states. The case without spin considerations follows the decay scheme based on the probabilities of transition and the resulting gamma multiplicity has only one maximum, as expected because the transition probabilities already include the fact that $\Delta J > 3$ transitions are highly unlikely. The case with spin considerations also results in a one-maximum gamma multiplicity distribution, with the additional advantage that the expected energy gap within the rotational band is not reached, whereas the case without the spin considerations does not respect this expected tendency.

The signature of the two maxima for the rotational band was used for detecting other potential anomalies: simulations were implemented for the entire PHITS library and it was found that ^{199}Hg is in the same situation as ^{156}Gd, with the double maxima in the gamma multiplicity distribution due to the rotational band. The algorithm to simulate the gamma cascade did not produce the expected gamma multiplicity distribution as most events consist in long decay chains, potentially because of the way the ENSDF data is treated by the PHITS team, artificially declaring gamma transitions to the closest energy level when the transition is absent in the ENSDF data.

The lessons learned from the neutron-induced inelastic and capture reactions can be applied to other reactions, and in particular in this PhD, the (n,2n) reaction. In terms of an analog simulation of this reaction, the case of ^{19}F(n,2n) was chosen as it is the only nuclide that has a probability distribution function for each of the particles in the outgoing reaction channels. These are the first and second neutrons, the residual nucleus ^{18}F and the gammas that can be emitted from ^{18}F*.

The shape of the spectra suggest that the reaction mechanism is an inelastic scattering

by the incoming neutron that brings ^{19}F to an excitation energy higher than the neutron separation energy S_n. The spectrum is mostly flat, as expected from neutron scattering. The second neutron is then emitted with an evaporation spectrum. These are the clues that indicate that for this nucleus in particular the reaction mechanism is like the inelastic scattering.

The ^{19}F(n,2n) reaction was simulated using PATMOS, an in-house developed prototype neutron transport code based on the Monte Carlo method, with the objective of discovering the code. Unfortunately, it does not have photon transport yet, so the aforementioned algorithms could not be tested. The reaction was also simulated using PHITS, and the obtained spectra pointed to the possibility that the spectrum associated to the residual nucleus ^{18}F might be too large. In the MF=6, MT=16, associated to the (n,2n) reaction, in the JEFF-3.3 library, the distribution of ^{18}F has a maximum energy of 3.5 MeV, which is at least one order of magnitude higher than the maximum energies simulated by PHITS. There are reasons to believe that the declared spectrum overestimates the maximum energies attainable by the residual nucleus, as its mass is more than 18 times that of the neutron and the kinetic energy gained by the scattering is less than 1/18 that of the scattered neutron, which has a maximum declared energy of 9 MeV when the incident neutron energy is 20 MeV.

As future perspectives for the analog simulation, it must be mentioned that the Generalised Nuclear Database Structure (GNDS) offers the possibility to include what has been observed in the course of this PhD. For example, in the case of the inelastic reaction, the GNDS format can include the declaration of the excited states and their transition probabilities, an equivalent format as that of MF=12, with the exception that the photon energy can be modified with regards to the Lorentz boost. Moreover, for the case of the neutron capture reaction, the GNDS format could potentially store parameters such as the critical energy to separate the states of the quasi-continuum from the known levels. Also, instead of generating the levels as it is done by DICEBOX, parameters can be determined and stored in the GNDS format to generate the appropriate probability distribution functions from which to sample photon energies to reproduce the expected spectrum from gamma transitions that keep the excitation state in the quasi-continuum. This is possible because the shape of the spectra is predictable as was observed in the conclusion of the neutron capture chapter. This parametrization can be expanded to other reactions such as (n,2n) according to the reaction mechanism best adapted to each nuclide.

Bibliography

[1] T. Ogawa *et al.* Development of gamma de-excitation model for prediction of prompt gamma-rays and isomer production based on energy-dependent level structure treatment. *Nuclear Instruments and Methods in Physics Research Section B: Beam Interactions with Materials and Atoms*, 325:35–42, 2014.

[2] O. Serot O. Litaize and L. Berge. Fission modelling with fifrelin. *The European Physical Journal A*, 51(12):1–14, 2015.

[3] *et al.* O. Petit. Fifrelin–tripoli-4® coupling for monte carlo simulations with a fission model. application to shielding calculations. In *EPJ Web of Conferences*, volume 153, page 06003. EDP Sciences, 2017.

[4] J. Verbeke *et al.* Stochastic analog neutron transport with tripoli-4 and freya: Bayesian uncertainty quantification for neutron multiplicity counting. *Nuclear Science and Engineering*, 183(2):214–228, 2016.

[5] E. Brun *et al.* Tripoli-4®, cea, edf and areva reference monte carlo code. In *SNA+ MC 2013-Joint International Conference on Supercomputing in Nuclear Applications+ Monte Carlo*, page 06023. EDP Sciences, 2014.

[6] D. Brown *et al.* Endf/b-viii. 0: The 8th major release of the nuclear reaction data library with cielo-project cross sections, new standards and thermal scattering data. *Nuclear Data Sheets*, 148:1–142, 2018.

[7] F. Becvar. Dicebox γ decay simulation tool. *Nucl. Instr. Methods*, 417(434):431–434, 1998.

[8] R. Capote *et al.* Reference input parameter library. *Nuclear Data Sheets*, 110:3107–3214, 2009.

[9] N Allemandou *et al.* The stereo experiment. *Journal of Instrumentation*, 13(07):P07009, 2018.

[10] A. Cucoanes and Nucifer Collaboration. The nucifer experiment. *Nuclear Data Sheets*, 120:157–160, 2014.

[11] T. Tanaka *et al.* Gamma-ray spectra from thermal neutron capture on gadolinium-155 and natural gadolinium. *Progress of Theoretical and Experimental Physics*, 2020(4):043D02, 2020.

[12] T. Sato *et al.* Features of particle and heavy ion transport code system (phits) version 3.02. *Journal of Nuclear Science and Technology*, 55(6):684–690, 2018.

[13] S. Ravaux. *Qualification du calcul de l'échauffement photonique dans les réacteurs nucléaires*. PhD thesis, Université de Grenoble, 2013. https://tel.archives-ouvertes.fr/tel-00961188.

[14] Stankovskiy *et al.* The joint evaluated fission and fusion file (jeff) is an evaluated library. *The European Physical Journal A*, 56(181):1–108, 2020.

[15] J. Pons *et al.* A highly resistive layer within the crust of x-ray pulsars limits their spin periods. *Nature Physics*, 9(7):431–434, 2013.

[16] Prussin and Stanley. *Nuclear physics for applications. A model approach.* Wiley-VCH, 2007.

[17] C. Porter and R. Thomas. Fluctuations of nuclear reaction widths. *Physical Review*, 104(2):483, 1956.

[18] R. Howerton *et al.* Evaluated nuclear data library. Technical report, Lawrence Livermore National Lab., CA (USA), 1981.

[19] V. McLane *et al.* Endf-102 data formats and procedures for the evaluated nuclear data file endf-6. revision november 1995. Technical report, National Nuclear Data Center, 1995.

[20] J. Tuli. Evaluated nuclear structure data file. *Nucl. Instr. Meth.*, A 369, 1996.

[21] T. Burrows. The evaluated nuclear structure data file: Philosophy, content, and uses. *Nuclear Instruments and Methods in Physics Research Section A: Accelerators, Spectrometers, Detectors and Associated Equipment*, 286(3):595–600, 1990.

[22] I. Lux and L. Koblinger. *Monte Carlo Particle Transport Methods: Neutron and Photon Calculations.* CRC Press, 1991.

[23] N. Metropolis and S. Ulam. The monte carlo method. *Journal of the American statistical association*, 44(247):335–341, 1949.

[24] K. Niita *et al.* A new treatment of radiation behaviour beyond one-body observables. In *International Conference on Nuclear Data for Science and Technology*, pages 1167–1169. EDP Sciences, 2007.

[25] R. Firestone *et al.* Egaf: measurement and analysis of gamma-ray cross sections. *Nuclear data sheets*, 119:79–87, 2014.

[26] R. Firestone *et al.* A new gamma-ray spectrum catalog for pgaa. *Journal of Radioanalytical and Nuclear Chemistry*, 244(2):383–389, 2000.

[27] G.L. Molnar*et al.* The new prompt gamma-ray catalogue for pgaa. *Applied Radiation and Isotopes*, 53(4-5):527–533, 2000.

[28] T. Tanaka *et al.* Gamma-ray spectra from thermal neutron capture on gadolinium-155 and natural gadolinium. *Progress of Theoretical and Experimental Physics*, 2020(4):043D02, 2020.

[29] K. Shibata *et al.* Jendl-4.0: a new library for nuclear science and engineering. *Journal of Nuclear Science and Technology*, 48(1), 2011.

[30] T. Kibédi *et al.* Evaluation of theoretical conversion coefficients using bricc, 2008.

[31] ML. Mauborgne *et al.* Designing tools for oil exploration using nuclear modeling. volume 146 of *EPJ Web of Conferences*, 2017.

[32] E. Brun *et al.* Patmos: A prototype monte carlo transport code to test high performance architectures. Proc. M&C, Jeju, Korea, 2017.